AN EXPERIMENTAL STUDY OF PARTICLE SIZE AND CONCENTRATION EFFECTS OF CALCIUM CARBONATE ON RHEOLOGICAL AND FILTRATION PROPERTIES OF DRILL-IN FLUIDS

A THESIS SUBMITTED TO
THE GRADUATE SCHOOL OF NATURAL AND APPLIED SCIENCES
OF
MIDDLE EAST TECHNICAL UNIVERSITY

BY

AYDIN ODABAŞI

IN PARTIAL FULFILLMENT OF THE REQUIREMENTS
FOR
THE DEGREE OF MASTER OF SCIENCE
IN
PETROLEUM AND NATURAL GAS ENGINEERING

MAY 2015

Approval of the thesis:

AN EXPERIMENTAL STUDY OF PARTICLE SIZE AND CONCENTRATION EFFECTS OF CALCIUM CARBONATE ON RHEOLOGICAL AND FILTRATION PROPERTIES OF DRILL-IN FLUIDS

Submitted by **AYDIN ODABASI** in partial fulfillment of the requirements for the degree of **Master of Science in Petroleum and Natural Gas Engineering Department Middle East Technical University** by,

Prof. Dr. Gülbin Dural Ünver ____________________
Dean, Graduate School of **Natural and Applied Sciences**

Prof. Dr. M. Verşan Kök ____________________
Head of Department, **Petroleum and Natural Gas Eng.**

Prof. Dr. M. Verşan Kök ____________________
Supervisor, **Petroleum and Natural Gas Eng.**

Assoc. Prof. Dr. İ. Hakkı Gücüyener ____________________
Co-Supervisor, **GEOS Energy Inc.**

Examining Committee Members:
Prof. Dr. Mahmut Parlaktuna
Petroleum and Natural Gas Engineering Dept., METU ____________________

Prof. Dr. M. Verşan Kök
Petroleum and Natural Gas Engineering Dept., METU ____________________

Associate Prof. Dr. İ. Hakkı Gücüyener
GEOS Energy Inc. ____________________

Assistant Prof. Dr. Çağlar Sinayuc
Petroleum and Natural Gas Engineering Dept., METU ____________________

Osman Gündüz, MS
GEOS Energy Inc. ____________________

Date : ____________________

I hereby declare that all information in this document has been obtained and presented in accordance with academic rules and ethical conduct. I also declare that, as required by these rules and conduct, I have fully cited and referenced all material and results that are not original to this work.

Name, Last name: Aydın Odabaşı

Signature:

ABSTRACT

AN EXPERIMENTAL STUDY OF PARTICLE SIZE AND CONCENTRATION EFFECTS OF CALCIUM CARBONATE ON RHEOLOGICAL AND FILTRATION PROPERTIES OF DRILL-IN FLUIDS

Odabaşı Aydın

M.S., Department of Petroleum and Natural Gas Engineering
Supervisor: Prof. Dr. M. Verşan Kök
Co-Supervisor: Assoc. Prof. Dr. İ. Hakkı Gücüyener

May 2015, 97 pages

Specially designed non-damaging Drill-In Fluids (DIF) are being effectively applied for drilling depleted zones worldwide. Shape, particle size distribution and concentration of materials like calcium carbonate ($CaCO_3$) are key parameters determining the effectiveness of DIF. In this study, 3 different sized and 5 different concentrations $CaCO_3$ are used to examine the effects of these factors on rheology and fluid loss of DIF. Sized calcium carbonates are used as major particles in different concentrations and in different particle size distribution. Rheological behavior of fluid, filter cake quality and filtrate volume are basic parameters to be evaluated in this study. All samples were aged at 120 ºF for 4 hours. After ageing, tests are performed at 75 °F and 100 psi of differential. It is observed that, the DIF showed certain Yield Power Law charcteristics and some parameters (PV,m) was increased with increasing size and concentration whereas other parameters (YP,k) decreased .

Key words: *Drilling, drilling fluid, drilling mud, calcium carbonate.*

ÖZ

KALSİYUM KARBONAT KONSANTRASYONUNUN VE TANE BOYUTUNUN POLİMER ESASLI REZERVUAR SONDAJ SIVILARININ REOLOJİK VE FİLTRASYON ÖZELLİKLERİNE ETKİLERİ ÜSTÜNE DENEYSEL BİR ÇALIŞMA

Odabaşı, Aydın

Yüksek Lisans, Petrol ve Doğal Gaz Mühendisliği Bölümü
Tez Yöneticisi: Prof. Dr. M. Verşan Kök
Ortak-Tez Yöneticisi: Doç. Dr. İ. Hakkı Gücüyener

Mayıs 2015, 97 sayfa

Formasyonu tahrip etmeyen özel olarak tasarlanmış Rezervuar Sondaj Sıvıları (RSS) dünyanın her yerinde basıncı düşmüş alanların delinmesinde etkin bir şekilde kullanılmaktadır. Kalsiyum karbonat($CaCO_3$) malzemelerinin şekli, tane boyutu dağılımı ve konsantrasyonu RSS'nın etkinliğini belirleyen başlıca parametrelerdir. Bu çalışmada, reolojiye ve su kaybına olan etkilerini incelemek adına, 3 farklı boyutta ve 5 farklı konsantrasyonda $CaCO_3$ kullanılmıştır. Değişik boyutta ve konsantrasyondaki boyutlandırılmış kalsiyum karbonat rezervuar sondaj sıvıları etkin malzemeleri olarak değerlendirilecektir. RSS'nın reoloji okumaları, kek kalitesi ve toplam filtrat hacmi bu çalışmada değerlendirilen başlıca parametrelerdir. Hazırlanan örnekler 120 ºF'de 4saat yaşlandırılmıştır. Yaşlandırma çalışmalarından sonra, testler 75 ºF ve 100 psi basınç farkında gerçekleştirilmiştir. Bu deneysel çalımada görüldü ki; RSS kesin olarak "Yield Power Law" akış modeli karakteri göstermiştir ve bazı parametreler(PV,m) artan boyut ve konsantrasyonlarda artış gösterirken bazı parametreler (YP,k) düşüş göstermiştir.

Anahtar kelimeler: *Sondaj, sondaj sıvısı, sondaj çamuru, kalsiyum karbonat.*

To My Family

ACKNOWLEDGEMENTS

I would like to thank my supervisor Prof. Dr. Verşan Kök and co-supervisor Associate Prof. Dr. İ. Hakkı Gücüyener for their guidance, advice, criticism, encouragements and insight throughout the study.

Also Osman Gündüz, Gökhan Bağatır and Hakan Çördük of GEOS Energy Inc., Burak Kayael of TPOFS and Bahri Kutlu are gratefully acknowledged of their help and assistance.

I would also like to thank my whole family for their support and encouragement throughout the study.

TABLE OF CONTENTS

LIST OF FIGURES

FIGURES

LIST OF TABLES

TABLES

CHAPTER 1

INTRODUCTION

While drilling of highly permeable, highly fractured and low pressured zones; partial loss of circulation of fluids because of the migration through formation is known as fluid invasion. Since 1900s, drilling the production zone has brought in great problems to the petroleum industry, high costs for the fluid loss, insufficient techniques and finally side tracks, altering the reservoir depth due to bypassing, new wells to relief the original well and as a result unsatisfactory production rates due to damaging reserves have still be seen in 2000s.

As stated before, lost circulation is one of the most troublesome and costly problem encountered in both petroleum and geothermal drilling industry in Turkey. Classical drilling process for drilling the highly fractured, low pressure and highly permeable formations is not only difficult but also expensive and risky. It has historically been one of the primary contributors to high mud cost. Pilehvari and Nyshadham (2002) has characterized lost circulation by a "*Reduction in the rate of mud returns from the well compared to the rate at which it is pumped downhole during a lost circulation an appreciable part or the entire volume of drilling fluid can be lost into the formation. This may happen while drilling is in progress, due to excessive hydrostatic and annular pressure drop, or during trips, when pressure surges occur due to lowering of drill pipe or casing to the hole.* "

Moreover, lost circulation can be studied in three groups as; seepage loss (1-10 bbl/hr), partial loss (10-500 bbl/hr), and complete loss (over 500 bbl/hr) (Nayberg and Petty, 1986).

There are plenty of studies made for solving the damaging problems during classical drilling. Pumping a mix of lost circulation particles (LCP) may be a solution while drilling the target zone with a seepage, partial or total lost circulation, either by constructing bridges or increasing viscosity of the fluid to limit fluid migration in to the formation but lost circulation materials used in the industry cannot be dissolved in acid and it is highly possible to damage the target zone.

Bridging agents are often used to combat severe fluid loss, and calcium carbonate ($CaCO_3$) is the most common one. It is the most appropriate granular type of material because of its mechanical and chemical properties. $CaCO_3$ is resistant to pressure differentials and swap and surge impacts in the wellbore. Its acid solubility allows using it in production zones. In this work, $CaCO_3$ will be tested as bridging material with different particle sizes.

The range of particle size distribution of $CaCO_3$ used in this study will be based on the range of materials available in market.

The effects of particle size distribution on friction have been explained particularly by Marone and coworkers, who made a series of experiments by varying the particle size, shape, gouge thickness (Anthony & Marone, 2005) and particle size distribution (Mair et al., 2002) as well as humidity, which affects interparticle cohesion (Frye and Marone, 2002). Presence of fault gouge enhances dilation (e.g., Marone et al., 1990) and compaction (e.g., Nakatani, 1998) and changes the friction compared to the case without gouge.

In aforementioned case, while drilling a fractured or permeable target zone, a well-designed drill-in fluid is highly recommended to easily be cleaned after acidizing operations and not to damage to the reservoir. In order to design a good drill-in fluid, the impact of size distribution of particles on rheology and fluid loss must be apprehended well. In this way, rheology acknowledgement may also lead us to the well demonstration of hole cleaning issue. (See Figure 1)

In this study, compositions and rheological parameters are tested depending on particle size, particle concentration difference and also filter loss is controlled by basing upon creating a filter in formation, particle size distribution in the range of the average pore throat size distribution which leads to an optimal filter cake effect of small sized polymers (low molecular weight).

This study is intended to conduct an experimental investigation on determining the methodology to be followed and optimum drill-in fluid rheology design criteria to combat hole cleaning problem anticipated while drilling the highly fractured, low pressure and highly permeable formations.

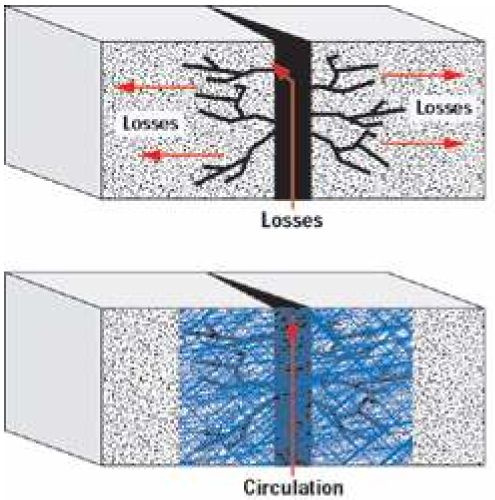

Figure 1 Plugging lost circulation zones with Drill-In Fluid. (MI Drilling Fluids Engineering Manual, Copyright 1998)

CHAPTER 2

LITERATURE REVIEW

2.1. Overview to Loss Circulation

To begin with, it has to be reminded that calculated lost circulation effect on the drilled wells is up to 75%. Lost circulation is an important subject for drilling industry, mainly, because of economic reasons. Not only the increasing economic effects on drilling operations but also the damaging effect of drill-in fluid on the reservoir section of the well is another consideration, as well. While drilling the production zone of the well, it is essential to design a non-damaging lost circulation and reservoir drilling fluids. Moreover, lost circulation has even been believed in minimizing production rates in the well where losses have resulted in failure to secure production tests and samples while the plugging of production zones have to lead to decrease productivity (Bugbee, 1953).

In 1980's, J. F. Gockel and M. Brinemann (1987) illustrated a well-known usual mistaken belief about the chance of the lost circulation is based on the idea that if the drilling fluid weight does not exceed the fracture pressure of a given zone, fluid loss is unlikely to occur. However, for subnormal pressure zones, it is not the best answer for circulation losses. Subnormal pressure zones may occur in natural ways or be the consequence of production depletion of a zone. In both cases the fracture gradient can be normal, but the pore pressure cannot withstand the equal circulating pressure of drilling fluid.

Consideration of granular materials, like $CaCO_3$, particle size distribution influence is presented based on a semi–experimental study (Andreasen and Andrersen, 1930). This particle size distribution effect is latterly revised to calculate the smallest particle size which is called modified Andreasen and Andrersen model (Funk and Digner, 1994). Commonly four types of formation are responsible for lost circulation can be seen on Figure 2

a) High permeability unconsolidated sands and gravel
b) Cavernous or vugular zones in carbonates (limestone or dolomite).
c) Natural fractures, faults and transition zones in carbonates or hard shales
d) Induced fractures from extensive pressure.

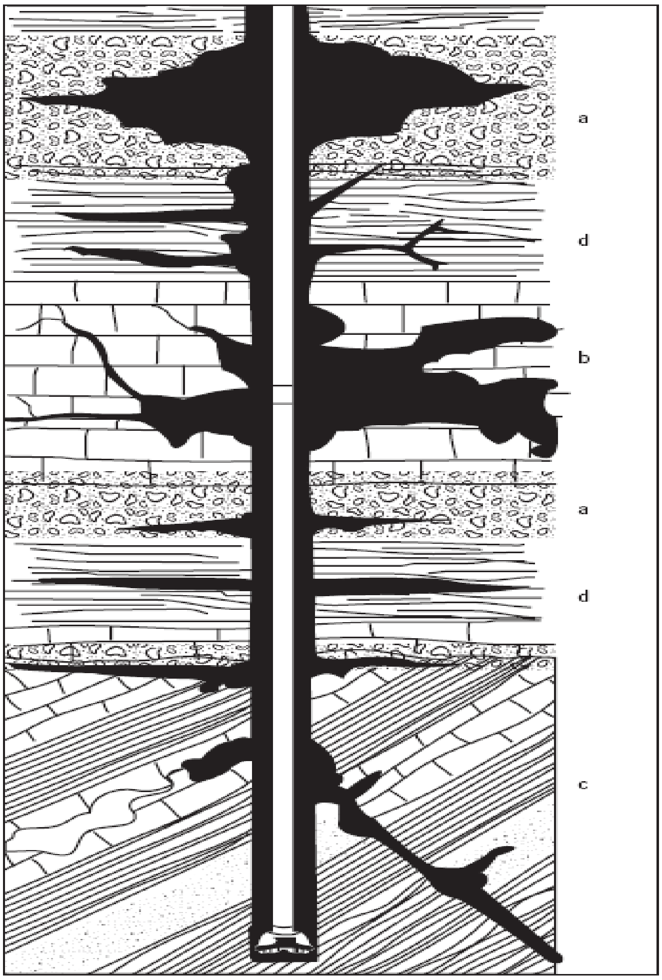

Figure 2 Lost Circulation Sections (MI Drilling Fluids Engineering Manual, Copyright 1998)

Sand formations are not generally consolidated and permeability is quite high in gravels. That is why, whole drilling fluid invasion may occur through the formation. The higher permeability may result in higher lost circulation rates in shallow sands. A cavity occurrence may be seen after lost circulation in this type of formations. These types of fields, especially sands, are the production formations in which subnormal pressure may be observed as to removal of fluids. In such a case, if mud weight is not controlled, mud may invade to the formation. Moreover, low pressure

depleted formation can cause differential stuck if filtration loss of the drill-in fluid is high because of the fluid flow from drilling fluid to formation.

Especially, while drilling in depleted zones, lost circulation is the most probable and fatal problem. Since the greater length of formation is exposed, the narrow operating window between pore pressure and fracture gradient. After fluid loss, well control and stability problems can occur. Furthermore, if it is a productive zone, fluid loss may cause productivity loss.

2.2. Size Selection of Bridging Material

During drilling, drilling fluid is the first foreign fluid contacting with reservoir. If the drilling fluid design is incorrect, many problems can occur such as foreign solid plugging, hydration swelling of reservoir rocks, particle migration, wettability reversal, emulsion plugging, and so on (See Figure 3 and 4). Finally, relative permeability will be decreased and reservoir will be damaged. (Guancheng Jiang; Mutai Bao, 2010).

Figure 3 Wrongly Sized CaCO3 in Drill-In Fluid, (Gücüyener, 2010)

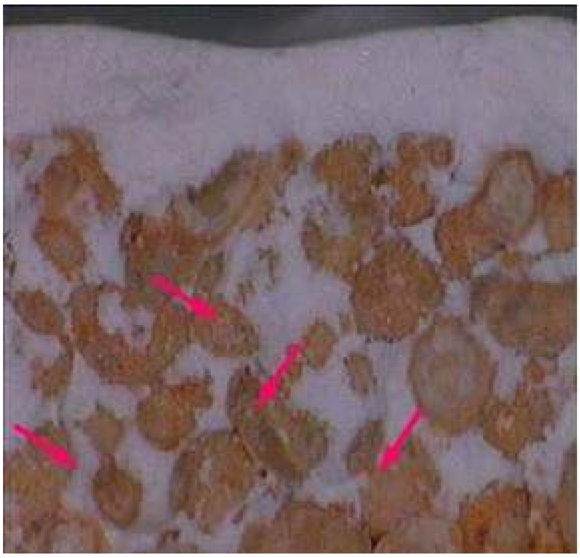

Figure 4 Correctly Sized CaCO3 in Drill-In Fluid, (Gücüyener, 2010)

Thus, here comes an issue of drill-in fluid selection. Selection of the proper drill-in fluid can be a critical factor in obtaining undamaged completions. Choosing the right drill-in fluid to avoid damage is an important part of this process. The drill-in fluid, in addition to performing its functions as a drilling fluid, should satisfy these criteria;

- The fluid should be non-damaging to formation permeability.
- The fluid should be compatible with the completion method that will be used.
- The fluid should be responsive to any stimulation or clean-up techniques. (Stephens,1995)

While selecting the most suitable drill-in fluid in the target zone, another important issue takes part: That is the particle size distribution selection of drill-in fluid. As known generally, when a drill-in fluid is designed, $CaCO_3$ is basically thought to be the most suitable bridging material due to the mechanical properties. Since the calcium carbonate has a strong resistivity to pressure differences causing a differential stuck mostly, primer material for bridging is generally thought as $CaCO_3$. Solubility of $CaCO_3$ in acid is the reason of choice to be the bridging material which provides calcium carbonate a perfect clearance off the porous media after acidizing. Solubility of $CaCO_3$ in 15% HCl is greater than 98% at 76 °F. (GEOS Product Manual, 2015)

As R.D. Cargnel and J. P. Luzardo et al. (1999) stated: Bridging agents are used in Drill-In fluids to prevent problems of massive loss circulation to the formation and formation damage through fine solids migration that invade the hydraulic flow channels of the reservoir rock. Also, thick cake build up that induces a differential sticking problem, as well as torque and drag of the drill string are avoided. (Cargnel, Luzardo, 1999)

Bridging materials are often used in combat of massive lost circulation to the formation and formation damage because of fine solid invasion. Regular mud systems have large quantities of fine solids that invade to the formation causing damage in productive zones. (Marqez 1996).

Physical property control of drilling fluid systems is essential for the improvement of new wells and maintaining well operation. Drilling fluids engineers need to be well equipped and have a good knowledge for drilling operations to access to the routine particle size analysis capabilities. Control of the size distribution and concentration of the particles in the drilling fluid is so important for a mud system that yields good well stability and prevents fluid invasion. In order to form a filter cake that prevents the solids dilled and other mud additives like polymers from entering the formation, the fluid particle size should be small enough to construct a bridge between pores and formation drilled. This prevents fluid loss, keeps the well under pressure, and maintains a stabilization between shale-based formations. On the other hand, the fluid particle size has to be also large enough to ensure that in-depth penetration of the mud into the pore structures does not occur, because this would itself lead to formation damage via pore blockage (Sharma et al., 2004).

2.3. Polymer & Other Additives Selection

A drill-in mud system may contain many components, such as Xhantan Gum Polymer (XCD) to control the mud rheology, $CaCO_3$ mineral as a weighting agent and as a bridging solid, and other additives (starches and alkalinity agents) are added in order to reduce filter loss. While drilling, it is essential to keep the physical properties of the mud under control. Two most important properties to control are the

viscosity and the filtrate loss. "*Viscosity is the internal friction supplied by a fluid when an axial force is applied to cause it to flow. It is also relative to move the cuttings away from the bottom hole of the well , suspending cuttings and weight material in when the circulation is off, remove away cuttings at the surface, reducing to a minimum any adverse effect upon the wellbore, and providing information about formations penetrated*." (M. I. Abdou a & H. El-Sayed Ahmed, 2011).

The other important property of a mud is fluid loss which is the action of controlling the volume of filtrate that passes through a filter medium called filter paper. Control of fluid loss for a mud is ensured by several methods, one of them is addition of fluid-loss-control materials to the mud system and the other is to make the materials already present work better, altering the mud chemistry. ("The Oilfield Glossary: Where the Oil Field Meets the Dictionary", 2014)

During formation of an external filter cake, especially fine solids are forced into the formation, building an internal filter cake. An internal filter cake plugs the near surface pore and reduces the formation permeability. Fine particles penetrate deeper into the pores and are not easily removed by back flushing. Invasion of larger particles is usually localized to near surface. Studies conducted by Bailey et al. (1999) show a strong correlation between invasion and damage. Owing to that, minimizing of internal filter cake and quickly forming of external cake is very important for both fluid loss and formation damage control. A semi permeable slicker external filter cake can significantly reduce the invasion of the solids and the filtrate.

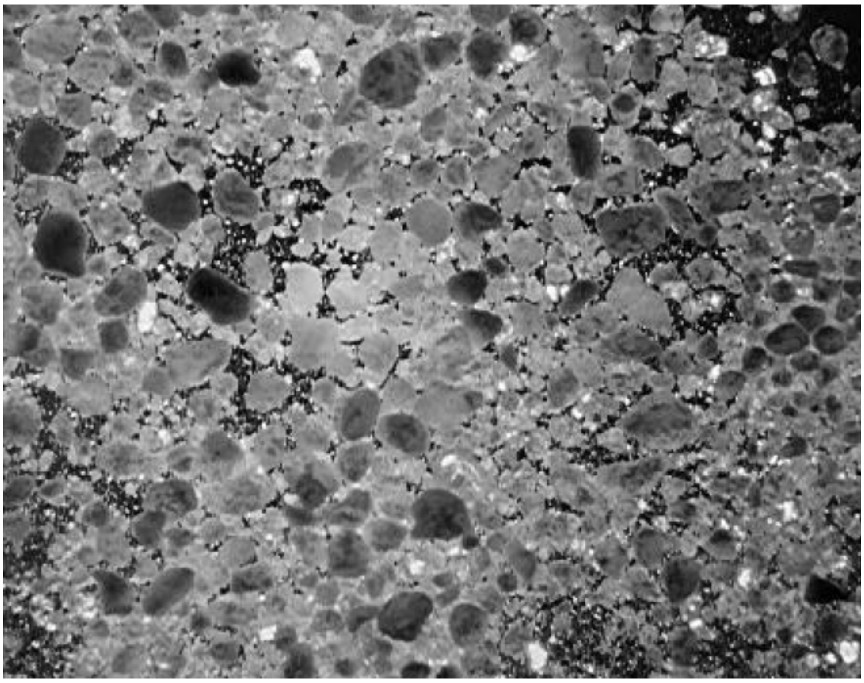

Figure 5 Calcium Carbonate (Verret et al., 2000)

$CaCO_3$ (Figure 5) is the most commonly used, granular type of bridging material. Its mechanical and chemical characteristics are the primer reasons to be used in the production zones. It has a thermal and mechanical resistance making the formed mud cake in the wellbore have mechanical consistency that stands and impact and high-pressure differentials. If $CaCO_3$ particles are not removed and remain in the wellbore or formation, it does only mean a permanently impair the productivity of well unless an acidizing done. Hence, additional treatments like 25% acidizing should be applied to remove these particulates. Chemically, it is acid soluble so that it can be removed from the porous matrix to recover the permeability of the rock by HCl washes.

Salt pills are also granular type of material and they do not need additional treatment like acidizing unlike $CaCO_3$ pills. However, they are less effective in controlling losses and more difficult to design due to solubility issues (Rosato and Supriyono, 2002).

Proper fluid composition, a good bridging material with a good size selection and a correct maintenance of the drilling fluid are the primer parameters to achieve a better productivity. Careful design is required to minimize spurt loss and solid invasion during drilling and completion operations.

2.4. Dimensional Approach to $CaCO_3$

There are many studies with granular particles, especially with $CaCO_3$, conducted to observe the effect on lost circulation. G.E.Loeppke et al. (1990) viewed high-temperature and high-fracture zones. It was stated that dimension of particle must be greater than the fracture if the dimension is normal for single particle bridging. J.C. Rojas et al. (1998) had discussed the effect of particle size and particle concentration of the $CaCO_3$ and concluded that for effective plugging of pores the mud should contain wide range of particles size, and largest particles should be at least as large as the fracture width. They concluded that high concentration provides better plugging (Cargnel and Luzardo, 1999).

There is also a detailed study on the particle size and concentration. This study was based on the study of Abrams' Median Particle-Size Rule (Abrams 1977). They concluded that as the range of particle size is between 1/7 and 1/3 of average pore size, better sealing is performed which yields a small invasion of solids into the porous media and particle concentration is optimum at 25 lb/bbl for effective plugging. R.D. Cargnel et. al. stated that *"The predominant size of particles in the sample does not keep the geometric relationship to form a matrix that can avoid the filtration invasion. That way, a thicker cake is formed and, with the higher filtrate volume, the amount of particles in the cake is larger."* (1999).

Nowadays, in horizontal wells open hole completions are frequently used. More attention needs to be paid to the cake forming properties of reservoir drilling fluids.

Solid invasion is one of the primary causes of formation damage caused from drilling fluids.

2.5. Rheological Study

Rheology of the drill-in fluid (DIF) is also studied in this work. Although, almost all rheological models were studied to explain the behavior of the fluid, yield power law (YPL) (also known as Hershel Buckley Model), Bingham Plastic and Power Law Model were the most used models.

"As known, Rheology is defined as the study of the deformation and flow of matter. While drilling, the term rheology is also includes the shear stress/shear rate/time relationships of drilling fluids. In order to design a good drilling fluid system, rheological properties are strictly used. It is known that if the mud is not only effected by pressure and temperature but also by velocity, mud behavior becomes non-Newtonian. The velocity of the drilling fluid and its shear rate of a section strongly defines the viscosity of the fluid. That is why, to calculate the hydraulic phenomena of a drilling system, it is vital to know the viscosity in the range of shear rate. In example, flow does not occur when the stress is less than yield point (YP). At low shear rates there is a typical non-linear relationship between shear stress and shear rate, which tends to be attenuated with the increase of shear rate." ("Rheology of Drilling Muds", n. d.)

Measurements of rheology on drilling sites are made by a viscometer at two different speeds of 600 and 300 rotation per minute (rpm). High shear rate region of the flow is represented by these two speeds. Since there are very different shear rates for drilling fluids, from very small velocities in the mud pits to very high velocities through bit nozzles, the rheological parameters on two measurements will cause significant discrepancies such as yield point overestimation. Generally, the viscometer used on the oilfield allows measurements at 3, 6, 100, 200, 300 and 600 rpm.

As a result, rheological models are useful tools to describe mathematically the relationship between shear stress and shear rate of a given fluid. Conventionally, oil and gas industry uses the Bingham and Power Law models to illustrate drilling fluid behavior. Also, standard American Petroleum Institute (API) methods for drilling hydraulics makes an assumption of either a Power Law or a Bingham Plastic model.

Actually, most drilling fluids intersect mostly close to the Modified Power Law or Herschel-Buckley rheological model. This is important for annular geometries of normal drilling conditions where shear rates are usually low. Here comes a situation which is, while the Power Law Model underestimates the frictional pressure drop, Bingham Plastic Model overestimates.

2.5.1. Basic Rheological Definitions

2.5.1.1. Shear Rate

When fluid flow is laminar, fluid layers near the wall flow at a slower rate than those further from the wall flow. The layers near the center of the flow channel have the highest velocity. The velocity of a layer relative to the layers next to it is called the shear rate and designated by the symbol γ. (Gücüyener, 2010).

2.5.1.2. Shear Stress

In laminar flow, there occurs a resistance to flow between fluid layers, because of the shear rate. This resistivity to flow is called the shear stress and designated by the symbol τ.

2.5.1.3. Viscosity

Viscosity is defined as the ratio of the shear stress to the shear rate, and has a symbol μ. The relationship is given as,

$$\mu = \tau / \gamma \tag{2.1}$$

The unit of viscosity is centipoise (cP) or millipascal × second (mPa× s).

2.5.1.4. Newtonian Fluids

Are the fluids like water, gasses and high gravity oils.

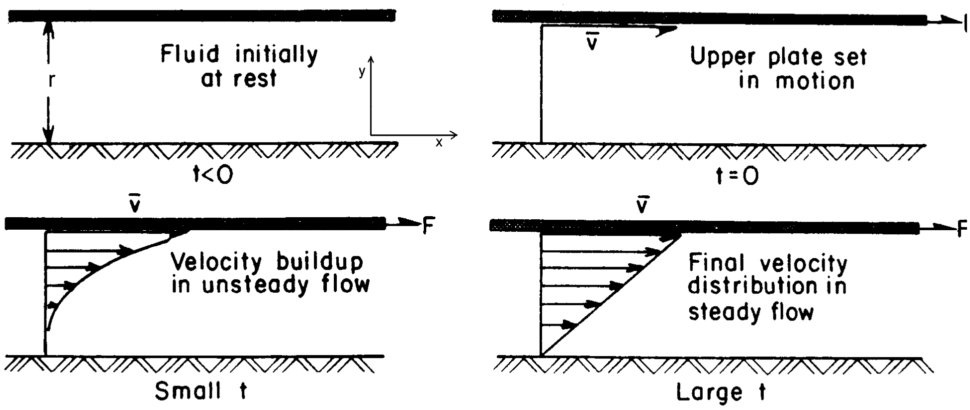

Figure 6 Laminar Flow of Newtonian Fluid ("Rheology of Drilling Muds", n. d.)

As seen in Figure 6, for Newtonian fluids shear stress, shear rate and viscosity equation has explained in a manner of an area "A", distinct by a distance "r", fluid flow in a direction with a constant velocity "v" under a constant force "F". (Gücüyener, 2010).

$$\frac{F}{A} = \mu \frac{v}{r} \tag{2.2}$$

Shear stress: Is the stress exerted on the fluid and defined by;

$$\tau = \frac{F}{A} \tag{2.3}$$

Shear Rate: Is the velocity gradient between velocity "v" and distance "r"

$$\gamma = \frac{v}{r} = \frac{dv}{dr} \tag{2.4}$$

From the equations above, Newtonian Models represent a direct proportionality between shear stress τ to the shear rate γ. Giving the following equation;

$$\tau = \mu \gamma \tag{2.5}$$

Where μ is a constant of proportionality and is the viscosity of the fluid. A graphical view of shear stress and shear rate for a Newtonian fluid can be seen in Figure 7. (Gücüyener, 2010).

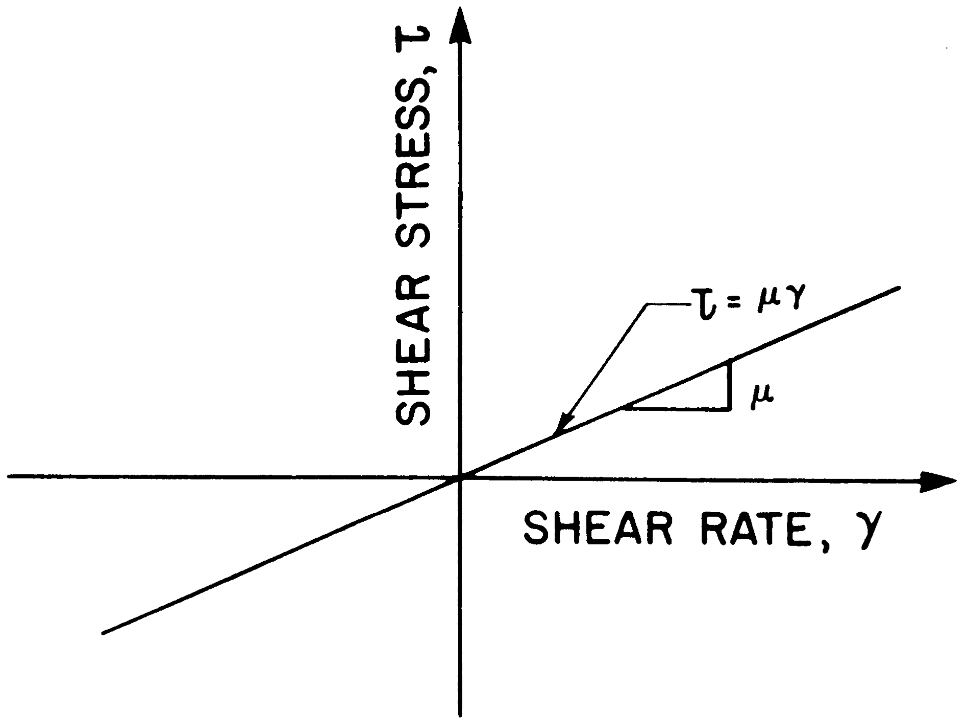

Figure 7 Shear stress Vs Shear rate for a Newtonian fluid. ("Rheology of Drilling Muds", n. d.)

2.5.1.5. Non-Newtonian Fluids

They are the fluids that does not represent a direct proportionality between shear rate and shear stress. It is studied in three main models which are Bingham Plastic Model, Power Law Model and Herschel-Buckley Model. (Gücüyener, 2010).

2.5.1.5.1. Bingham Plastic (BP) Fluids

Are fluids which does represent a Newtonian behavior with an initial yield stress called yield point (YP). Mathematical demonstration is as below:

$$\tau = YP + PV\gamma \tag{2.6}$$

Where PV is Plastic Viscosity.
As the shear rate of a Bingham Plastic Fluid increases, the AV of it decreases. That is why, Bingham Plastic Fluids represent a shear thinning behavior. (Gücüyener I.H., Drilling Hydraulics, 2010).

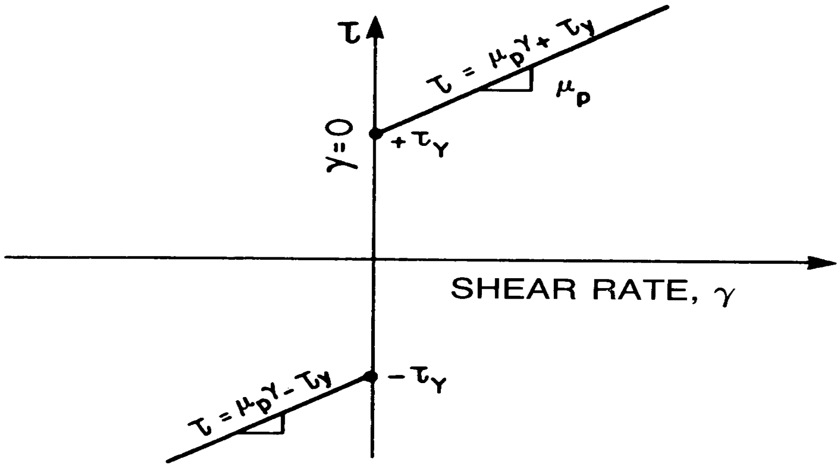

Figure 8 Shear Rate Vs Shear Stress for a Bingham plastic fluid. ("Rheology of Drilling Muds", n. d.)

2.5.1.5.2. Power Law (PL) Model

Power law model is the model in which API uses and it generally exhibits a pseudo plastic behavior of drilling fluids. (Bourgoyne, 2003). This model mainly has two parameters which are consistency index (K) and flow behavior index (m). As shown in Figure 8, when m equals to 1, the below equation becomes a Newtonian model. Power Law model explains the situations where m<1 and m>1 (Chowdhury, 2009).

$$\tau = K\gamma^n \tag{2.7}$$

Where K is consistency index and n is flow behavior index.

2.5.1.5.3. Yield Power Law (YPL) Model (Herschel Buckley Model)

Yield Power Law is the model known as the combination of the Power Law and Bingham Plastic models. (Islam, 2008). While Herschel Buckley includes YP in its calculations, Power Law does not. Mathematical demonstration of the model is;

$$\tau = \tau_y + k\gamma^m \tag{2.8}$$

The Herschel-Bulkley behaves like Power law model when $\tau_y = 0$ and behaves like Bingham plastic model when m = 1. (Islam A, 2008).

A general summary of flow behaviors of fluids can be seen in Figure 9.

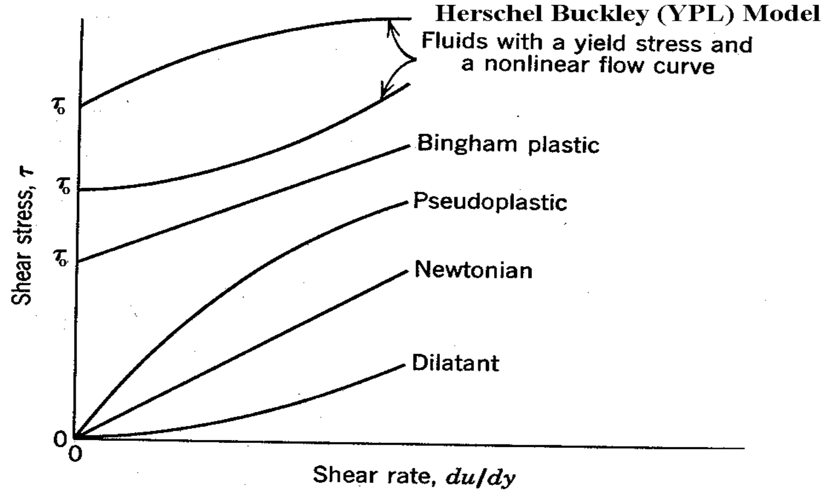

Figure 9 Flow curves for various types of time independent fluids. ("Rheology of Drilling Muds", n. d.)

CHAPTER 3

STATEMENT OF PROBLEM

Drill-In Fluid (DIF) is one of the primary issue while drilling target zone of a well due to reservoir damage and hole cleaning problems. The design of DIF is determined as non-damaging DIF to eliminate the damaging problem. Considering the hole cleaning problem, size distribution effect on drill-in fluid's rheology and fluid loss for most suitable drill-fluid design is studied in this part. Using calcium carbonate ($CaCO_3$) is the most popular way for constructing a bridge between drilling fluid and wellbore because of simplicity of usage, economic reasons and mechanical durability. It is important to determine the particle size and concentration, the rheology and fluid loss of the fluid successfully.

The aim of this work is to investigate effect of concentration and particle size of $CaCO_3$ on the rheological and filtration properties of drill-in fluids. During the study, some contributing polymers, caustic soda, distilled water and $CaCO_3$ at different particle sizes at different concentrations have been used. Ageing process has been done to provide the well conditions and then tests have been run at room temperature.

CHAPTER 4

EXPERIMENTAL SET-UP AND PROCEDURE

4.1. Determination of Particle Size Distribution

The experimental procedure started first with determining the size distribution of $CaCO_3$ samples.

Non-sized sample of $CaCO_3$ was obtained from Nidaş Mining A.Ş. (See Table 4.2. for the specifications of non-sized sample.) The samples were prepared by using Circular Vibratory Screen, EFL2 MK3, 300mm Dia (See Figure 13) dry standard sieves of different sizes respectively; No:60 = 60 mesh = 250 mμ, No:80 = 80 mesh = 180 mμ, No:100 = 100 mesh = 150 mμ, No:120 = 115 mesh = 125 mμ, No:160 = 160 mesh = 90 mμ, No:200 = 200 mesh = 75 mμ, No:325 = 325 mesh = 45 mμ. A particle size under the size of 75 μm represents a fine sample and a particle size above 75 μm represents coarse samples. The preparation of drilling fluids and its requirements of materials are suited to the world specifications of American Petroleum Institute (2003, 1997) (American Petroleum Institute, 1997) (See Figures 10,11,12.)

The samples of the calcium carbonate were prepared from the Nidaş Carbonates AŞ. and collected from the sieving of grain sizes. Then, samples of water-based mud were prepared by adding calcium carbonate of different sizes and different concentrations of 5, 15,30,45,60 lb/bbl. respectively.

Table 1 Sieves Standard no. Mesh sizes and Standard sieves designations. (Dhanlal De Lloyd, 2000)

Mesh Size in microns	TYLER	ASTM-E11	BS-410	DIN-4188
µm	Mesh	NO.	Mesh	mm
500	32	35	30	0.500
425	35	40	36	
250	60	60	60	0.250
180	80	80	85	0.180
150	100	100	100	
125	115	120	120	0.125
90	160	160	160	0.090
75	200	200	200	
45	325	325	350	0.045

As seen in Table 1, designation of standard sieves and mesh sizes are shown. As De Lloyd et. al. (2000) noted, larger sieve openings, 1 inch to ¼ inch, have been specified by "mesh" size which means the size of the opening in inches. As the sieve gets smaller, the mesh sizes of 3 ½ to 400 are specified by the number of openings per linear inch in the sieve. The other procedure is used to specify particle size by mesh designation, particles are retained by the sieve is stated by a "+" before the sieve mesh; the particles pass through the sieve is stated by a "-" before the sieve mesh; conventionally more than 90% of the particles will pass through the specified opening. (Sigma-Aldrich, 2012)

Figure 10 ASTM-E11 numbers of sieves and their mesh sizes in microns

Figure 11 ASTM-E11 numbers of sieves and their mesh sizes in microns. [ASTM E175-82(1995) Standard Terminology of Microscopy, American Society for Testing and Materials, West Conshohocken, PA (1995)]

Figure 12 ASTM-E11 numbers of sieves and their mesh sizes. [ASTM E175-82(1995) Standard Terminology of Microscopy, American Society for Testing and Materials, West Conshohocken, PA (1995)]

Figure 13 Circular Vibratory Screen, Endecotts, EFL2 MK3, 300mm Dia

Table 2 Non-sized CaCO3 (Nidaş A.Ş. Product Sheet, Copyright © 2010)

RAW MATERIALS	NİDAŞ A.Ş. NİĞDE / TÜRKİYE	
PRODUCT SPECIFICATIONS	High purity and whiteness, very finely ground natural, micronized calcium carbonate, low-oil absorption	
MAIN APPLICATIONS	PAPER,PAINT,PLASTIC,PVC GRANULE,CABLE,CHEMICALS ETC.	
CHEMICAL PROPERTIES	$CaCO_3$	>99,6 %
	MgO	<0,20 %
	Fe_2O_3	<0,01 %
	SiO_2	<0,01 %
	AI_2O_3	<0,02 %
	HCl insoluble content	<0,01 %
PHYSICAL PROPERTIES	DENSTIY (ISO 787-10)	2,7 gr/cm³
	HARDNES	3 MOHS
	REFRACTIVE INDEX	1,59
GENARAL PROPERTIES	PACKET BULK DENSITY	0,9 g/ml
	pH	9
	OIL ABSORPTION	13 g /100 g
	DOP ABSORPTION	23 g /100 g
	MOISTURE-EX WORKS	0.3%
	Whiteness' (ASTM E-313)	97%
	Moisture-Ex Works	94%
PACKING	Bulk in Big bag 25kg craft bags or pp bags in sling bags or palletized	
SYMPATEC HELOS PARTICLE SIZE ANALYSIS PARTICLE SIZE DISTRIBUTIONS	d 50 Mean particle size	12,00 - 18,00 µm
	d 97 Particle size	60,00 - 70,00 µm
	Under 2µm Particles	9 - 12 %
	RESIDUE ON 45µm SIEVE	10,00

4.2. Determination of Rheological Properties

The rheological properties of the mud samples used in this study that were measured include apparent viscosity (AP), plastic viscosity (PV), yield point (YP), and filter loss. The control mud samples were prepared from XCD polymer, starch and different sized calcium carbonates with distilled water to obtain water-based mud of different grain sizes at different concentrations. Distilled water was used in order not to be effected from the hardness of the fresh water while studying the rheological behavior of the water based mud (WBM). The particle size of $CaCO_3$ and its effect on the rheological behavior were studied, as well.

To read rheological properties, FANN 35 Viscometer was used which is known as an Industry Standard for measurements of mud rheology. Being able to produce a wide spectrum of a true coaxial cylinder rotational readings, Model 35 Viscometer is the most commonly used Fann viscometer. *(See Figure 14)*

Figure 14 FANN 35A Model Rotational Viscometer (Fann Instrument Company, Model 35 Viscometer Instruction Manual, 2015)

Procedure required for determining PV and YP, is listed below: (Fann Instrument Company, Model 35 Viscometer Instruction Manual, 2015)

1. Collect the drilling fluid sample.
2. Place the sample in a thermostatically controlled viscometer cup.
3. Immerse the viscometer rotor sleeve exactly to the scribed line.
4. Heat the sample to the selected temperature. (in this study, 25 ^{0}C)
5. Rotate the viscometer sleeve at 600 rpm until a steady dial reading is obtained. Record the dial reading (θ_{600}).
6. Rotate the viscometer sleeve at 300 rpm until a steady dial reading is obtained. Record the dial reading (θ_{300}).
7. Rotate the viscometer sleeve at 200 rpm until a steady dial reading is obtained. Record the dial reading (θ_{200}).
8. Rotate the viscometer sleeve at 100 rpm until a steady dial reading is obtained. Record the dial reading (θ_{100}).
9. Rotate the viscometer sleeve at 6 rpm until a steady dial reading is obtained. Record the dial reading (θ_{6}).
10. Rotate the viscometer sleeve at 3 rpm until a steady dial reading is obtained. Record the dial reading (θ_{3}).

4.2.1. Approximate Methods for Determining the Rheological Parameters

Approximate the plastic viscosity PV (cp) and yield point YP (lb/100ft^2) using the θ_{600} and θ_{300} viscometer dial readings.

$$PV = \theta_{600} - \theta_{300} \tag{4.1}$$

$$YP = 2\theta_{300} - \theta_{600} = \theta_{300} - PV \tag{4.2}$$

Approximate the flow behavior index n_p (-) and the consistency index K_p (lb-s^n/100ft^2) for pipe flow using the θ_{600} and θ_{300} viscometer dial readings.

$$n_p = 3.32\log(\theta_{600} / \theta_{300}) \tag{4.3}$$

$$K_p = \theta_{300} / 511^{n_p} \tag{4.4}$$

Approximate the flow behavior index n_a (-) and the consistency index K_a (lb-s^n/100ft^2) for annular flow using the θ_{100} and θ_3 viscometer dial readings.

$$n_a = 0.657\log(\theta_{100} / \theta_3) \tag{4.5}$$

$$K_a = \theta_{100} / 170.3^{n_a} \tag{4.6}$$

Approximate the Herschel-Bulkley model parameters; the low shear rate yield point τ_y (lb/100ft^2), flow behavior index m (-) and consistency index k (lb-s^n/100ft^2) using the θ_{600}, θ_{300}, θ_6 and θ_3 viscometer dial readings.

$$\tau_y = 2\theta_3 - \theta_6 \tag{4.7}$$

$$m = 3.32\log[(\theta_{600} - \tau_y) / (\theta_{300} - \tau_y)] \tag{4.8}$$

$$k = (\theta_{300} - \tau_y) / 511^{n_p} \tag{4.9}$$

4.2.2. Numerical Methods for Determining the Rheological Parameters

$$A = \exp\left[\frac{\sum_{i=1}^{N} y_i \sum_{i=1}^{N} x_i^2 - \sum_{i=1}^{N} y_i x_i \sum_{i=1}^{N} x_i}{N\sum_{i=1}^{N} x_i^2 - \left(\sum_{i=1}^{N} x_i\right)^2}\right] \tag{4.10}$$

$$B = \frac{N\sum_{i=1}^{N} y_i x_i - \sum_{i=1}^{N} x_i \sum_{i=1}^{N} y_i}{N\sum_{i=1}^{N} x_i^2 - \left(\sum_{i=1}^{N} x_i\right)^2} \tag{4.11}$$

These formulas can be applied to Bingham Plastic, Power Law and Yield Power Law rheologic models. Referring parameters are as below:

Bingham Plastic Model: Where the parameters refer to:

$$x_i = \gamma_i \quad y_i = \tau_i \quad A = YP \quad B = PV$$

Power Law Model: Where the parameters refer to:

$$x_i = \ln \gamma_i \quad y_i = \ln \tau_i \quad A = K \quad B = n$$

Herschel-BulkleyModel: Where the parameters refer to:

$$x_i = \ln \gamma_i \quad y_i = \ln(\tau_i - \tau_y) \quad \tau_y = 2\theta_3 - \theta_6 \quad A = k \quad B = m$$

4.3. Measurement of Fluid Loss

In this study, the American Petroleum Institute (API) API filter press is used to measure the fluid loss at a differential of 100 psi.

The OFITE low pressure low temperature filtration press is used in this study which helps to determine filtration and filter cake properties of drilling fluids. The filter press design features, a steel body called cell to hold the fluid sample, an inlet pressure, and a cap with screen and filter paper. OFITE low pressure filter press can be seen in Figure 15 To obtain reasonable results, a proper 9-cm filter paper must be used. In this study, Whitman No. 50 Filter Paper is used. (OFITE Instruments, 2009)

Figure 15 Overview of OFITE Low Pressure Filter Press (OFITE Instruments, 2009)

Procedure for determining the filtration can be observed step by step below (OFITE Instruments, 2009):

1. Collect the mud sample.
2. Assemble the cell with the filter paper in place.
3. Pour the sample into the cell to within ½ inch from the top.
4. Set the cell into the frame; place and tighten the top on the cell.
5. Place a dry, graduated cylinder under the drain tube.
6. Close the relief valve and adjust the regulator so a pressure of 100 ± 5 psi
7. Maintain the pressure at 100 ± 5 psi (690 ± 35 kPa) for 30 minutes.
8. Report the spurt loss at the very beginning of process if exists.
9. Shut off the flow through the pressure regulator and open the relief valve carefully.
10. Report the volume of filtrate in the graduated cylinder to the nearest mL.
11. Release the pressure, verify that all pressure has been relieved, and remove the cell from the frame.
12. Disassemble the cell and discard the mud.

4.4. Mixing and Ageing

To mix the drilling fluid, Sterling Multimixer Model is used. Sterling Multimixer Model can be seen in Figure 16 (Sterling, 2003). Additives are added in order, after adding the additives, samples are mixed in Srerling Multimixer for 30 minutes. (Gueven et al., 1988).

After this procedure, mud is filled up to stainless steel aging cells and cells are put into a stabilized temperature of 120 ºF roller oven for 4 hours to simulate the fluid in well conditions. After 4 hours, the cells are taken hot from oven (Figure 17) and mixed for 30 minutes in Sterling Multimixer and added $CaCO_3$ after cooling the sample to room conditions.

Figure 16 The Sterling Multi Mixer (Sterling, Multimixer Instruction Manual, 2003)

Figure 17 GEOS Aging Unit

4.5. Additives

In order to prepare a drill-in fluid; XCD polymer, starch and NaOH are mixed as base fluid. As bridging material, $CaCO_3$ different sized samples were sieved and used. Distilled water was used in this study not to be effected from the hardness of the fresh water. Composition of base fluid is shown in Table 4.3.

Table 3Composition of Base Fluid

Additives	**Amount**
XCD, lb/bbl	1.5
Starch, lb/bbl	6
NaOH, lb/bbl	0.75

4.5.1. XCD Polymer

It is a high molecular weight Xanthan Gum biopolymer. It is used to viscosity water based drilling and completion fluids. It is known as the primer viscosity modifier which is used for this study in concentration of 1,5 lb/bbl.

4.5.2. Starch

Starch is a filter loss agent in fresh drilling fluids water based. It is an anionic polymer which is cellulose based. In this study, it is used in concentration of 6 lb/bbl.

4.5.3. Caustic Soda (NaOH)

NaOH is used the increase the pH of the water-based drilling fluids.

4.5.4. $CaCO_3$

Different sizes of $CaCO_3$ are used. These commercially available $CaCO_3$s' named regarding to their micron sizes after being sieved. The specifications of $CaCO_3$ s are given in Table 4.2. Specific gravity of $CaCO_3$ s are taken as 2.7. The most leading an differenting part of the experiment is the $CaCO_3$ s.

4.6. Formulation

To make the final volume of mud samples 350 cc, the volume increasing factor of $CaCO_3$ was taken into account. After ageing all of the distilled water-polymer mixtures were collected in a jar and then divided into 5 different volumes as seen below. Thus, as the concentration of the $CaCO_3$ increased, the volume of distilled water-polymer mixture decreased according to volume increasing the calculation of $CaCO_3$. Volume increases per 100 bbl of mud due to adding $CaCO_3$; (Lapeyrouse, 2002)

$$V_{inc} = 100 \text{ x } (W_2 - W_1) \div (22.5 - W_2) \quad (4.5)$$

Where;

W_1 = current mud weight in ppg

W_2 = new mud weight in ppg

1. 5 lb/bbl $CaCO_3$ (348,1 ml distilled water + 1,5 lb/bbl XCD + 6 lb/bbl starch)
2. 15 lb/bbl $CaCO_3$ (344,4 ml distilled water + 1,5 lb/bbl XCD + 6 lb/bbl starch)
3. 30 lb/bbl $CaCO_3$ (338,9 ml distilled water + 1,5 lb/bbl XCD + 6 lb/bbl starch)
4. 45 lb/bbl $CaCO_3$ (333,3 ml distilled water + 1,5 lb/bbl XCD + 6 lb/bbl starch)
5. 60 lb/bbl $CaCO_3$ (327,8 ml distilled water + 1,5 lb/bbl XCD + 6 lb/bbl starch)

CHAPTER 5

RESULTS AND DISCUSSION

Based on the data from several tests of drill-in fluids with different sized $CaCO_3$ samples with different concentrations, both the size distribution and concentration effects on both rheology and fluid loss are evaluated. The shear stress versus shear rate curves for the different samples of drill-in fluids under constant temperature and pressure are presented. The results are compared with three different rheological models namely Bingham plastic, power law and Herschel Buckley (Yield Power Law). Effects of $CaCO_3$ concentration and particle size on fluid loss of the fluids under consideration are also evaluated in this section.

5.1 Effect of Concentration of $CaCO_3$ on Rheological Behavior of Drill-In Fluids.

Rheological behavior of DIFs is evaluated as a function of sized $CaCO_3$ at five different concentrations and the results are illustrated through Figures 18 to 32 As apparently seen from these figures, the DIFs under consideration are well characterized with a non-linear flow curve above the yield stress. In other words, these fluids exhibit yield-pseudoplastic behavior significantly deviating from the Bingham plastic and pseudoplastic rheology. The Herschel-Bulkley (Yield Power Law) model accurately describes the relationship between the shear stress and the shear rate for these fluids at any $CaCO_3$ concentration and particle size distribution. The numerical data of the flow curves can be seen at Appendices.

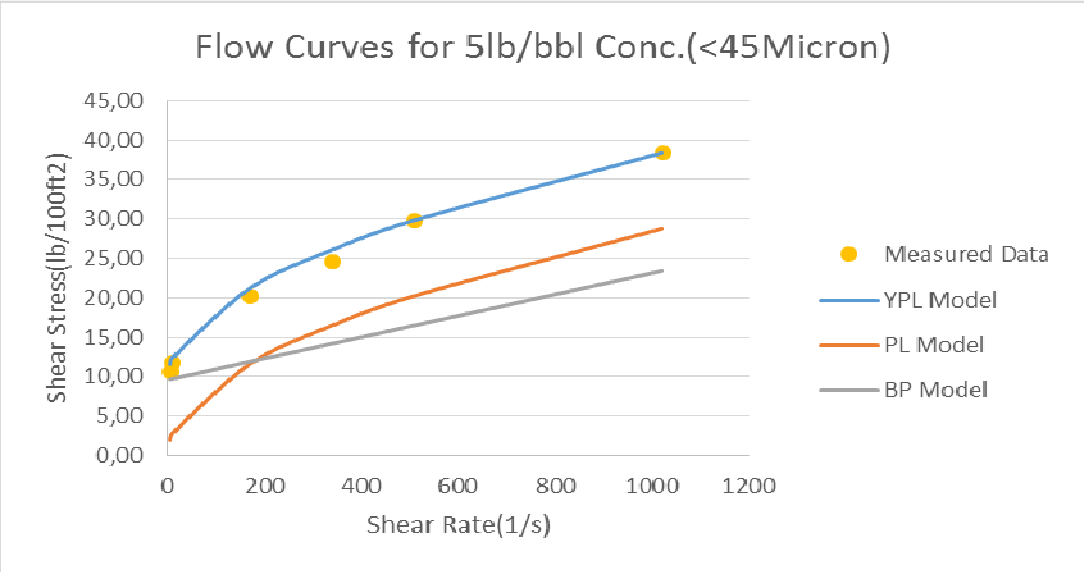

Figure 18 Flow Curves for BP, PL and YPL Models (CaCO3<45µm, 5lb/bbl)

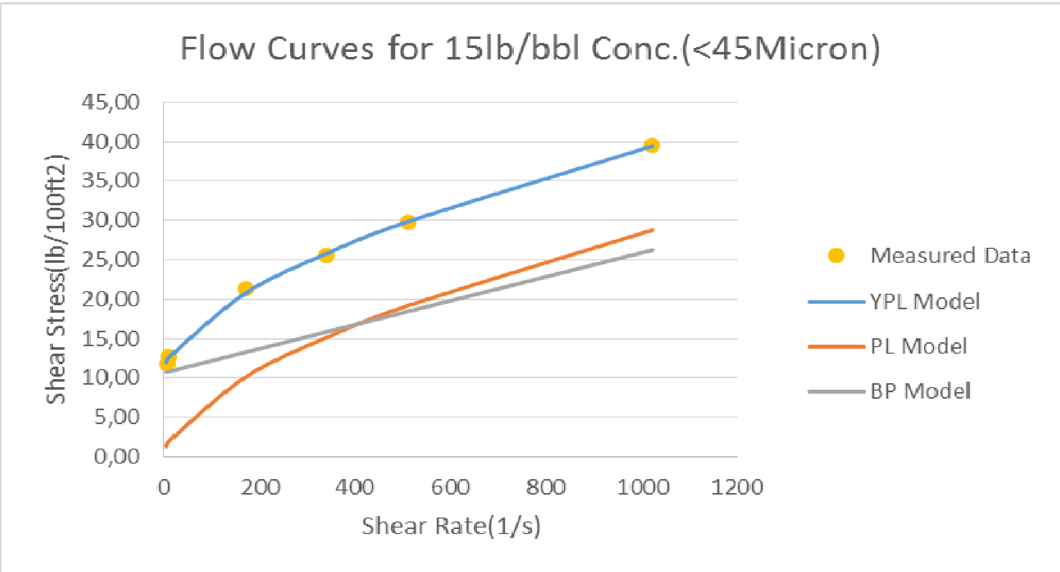

Figure 19 Flow Curves for BP, PL and YPL Models (CaCO3<45µm, 15lb/bbl)

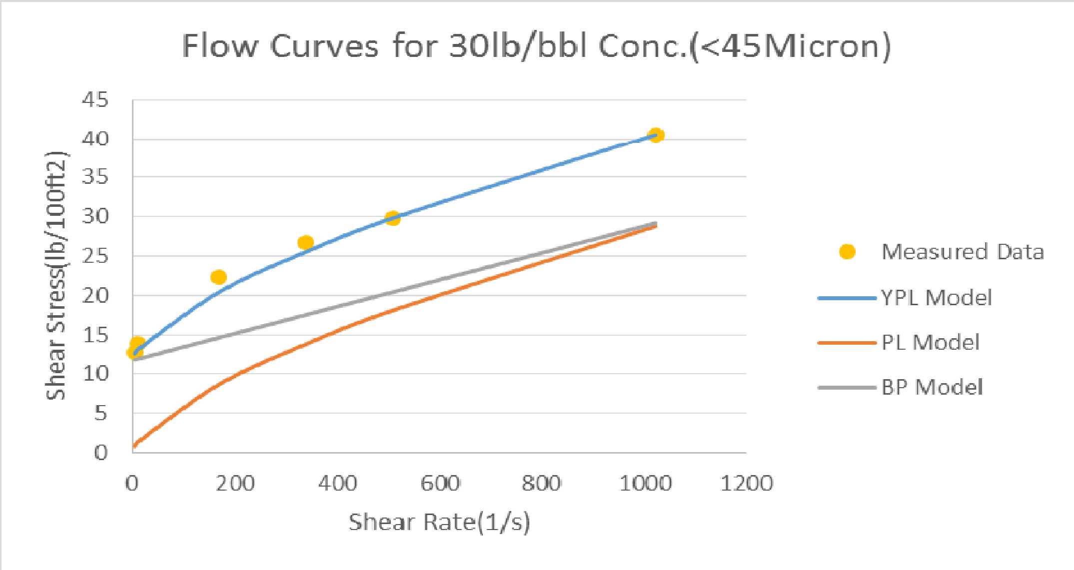

Figure 20 Flow Curves for BP, PL and YPL Models (CaCO3<45µm, 30lb/bbl)

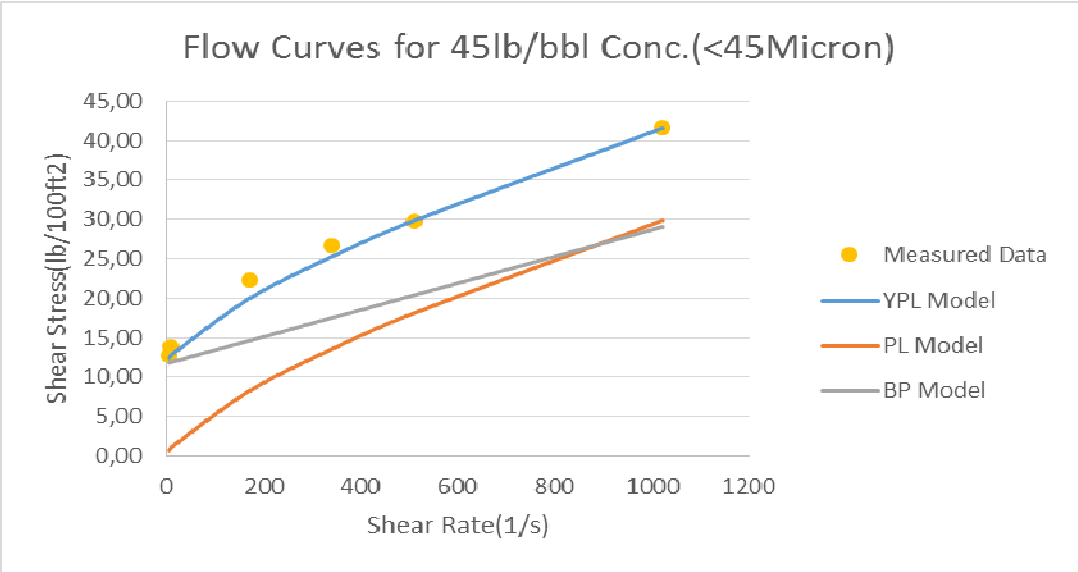

Figure 21 Flow Curves for BP, PL and YPL Models (CaCO3<45µm, 45lb/bbl)

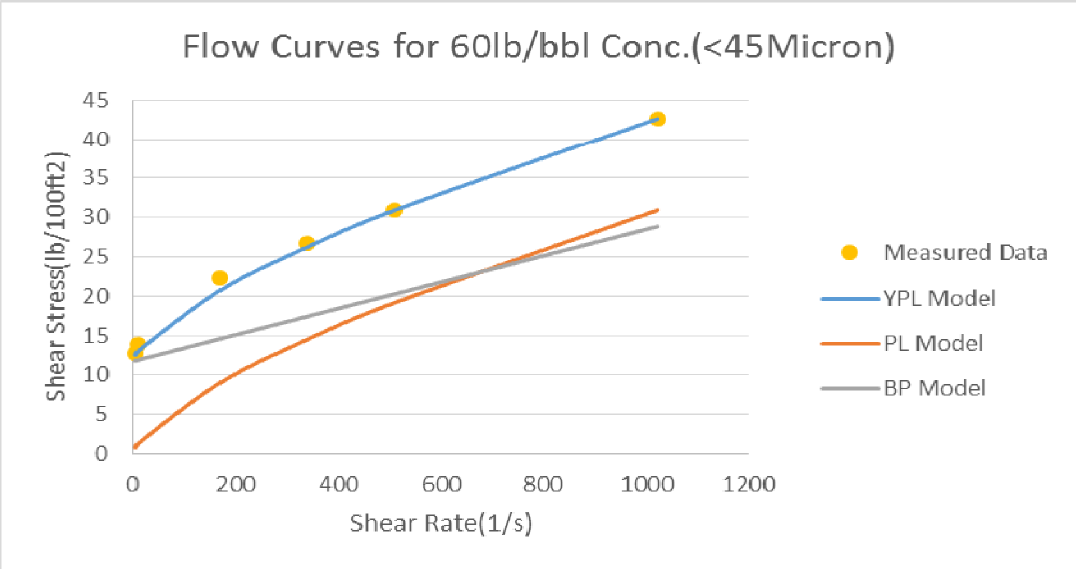

Figure 22 Flow Curves for BP, PL and YPL Models (CaCO3<45µm, 60lb/bbl)

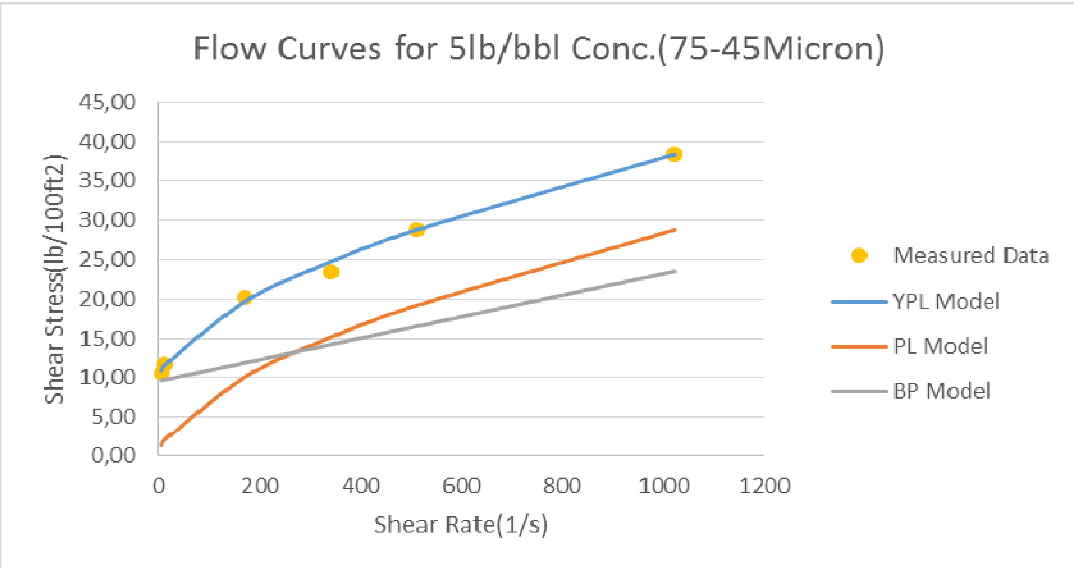

Figure 23 Flow Curves for BP, PL and YPL Models (CaCO3 75-45µm, 5lb/bbl)

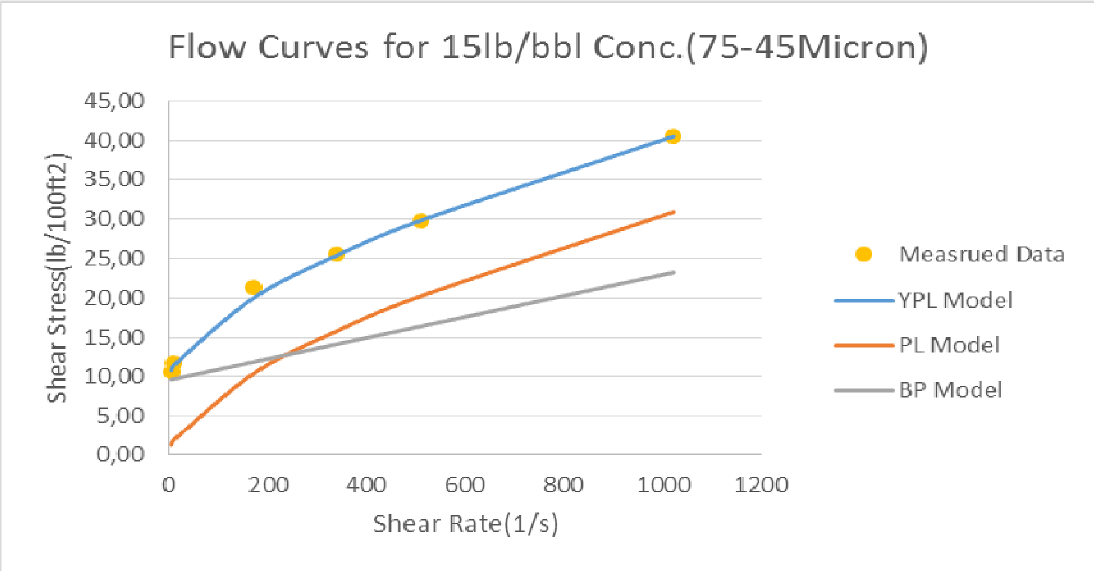

Figure 24 Flow Curves for BP, PL and YPL Models (CaCO3 75-45µm, 15lb/bbl)

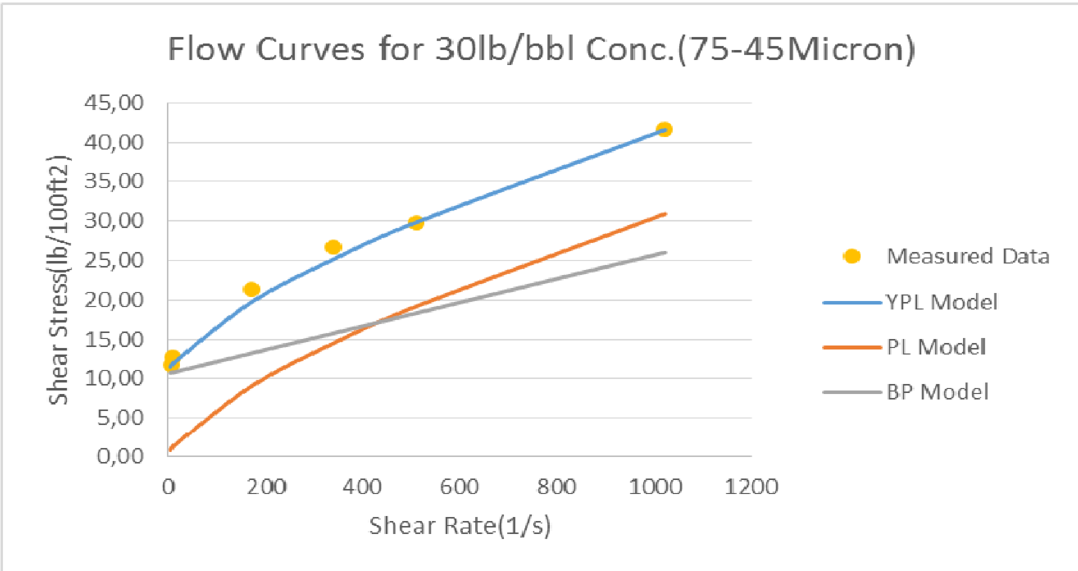

Figure 25 Flow Curves for BP, PL and YPL Models (CaCO3 75-45µm, 30lb/bbl)

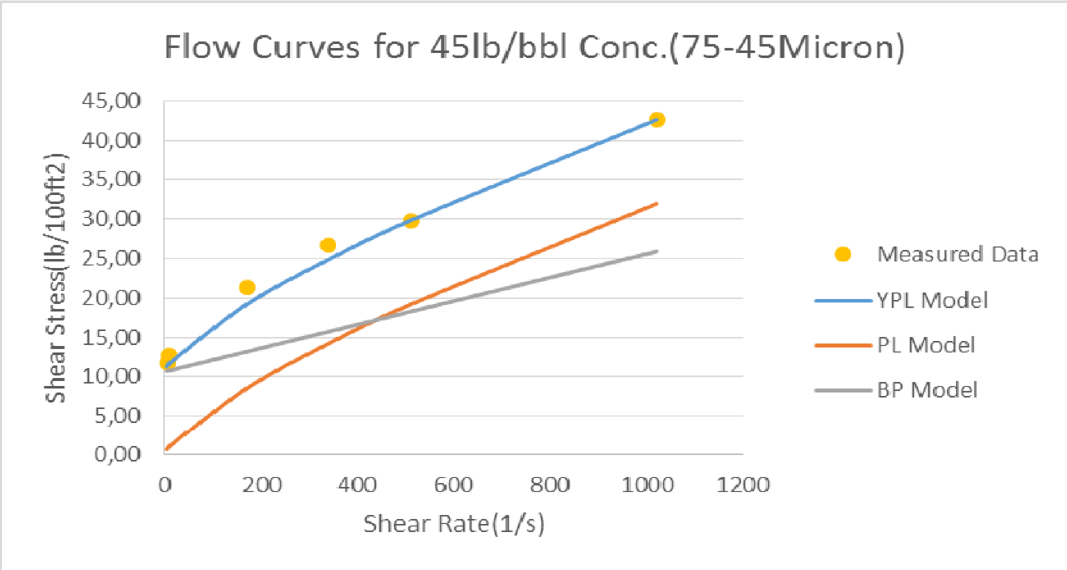

Figure 26 Flow Curves for BP, PL and YPL Models (CaCO3 75-45µm, 45lb/bbl)

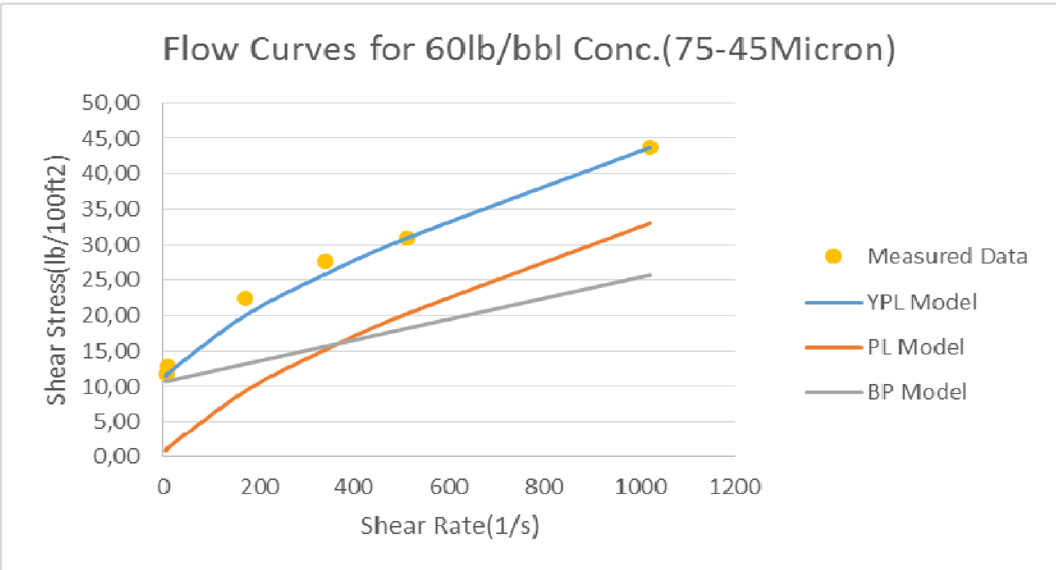

Figure 27 Flow Curves for BP, PL and YPL Models (CaCO3 75-45µm, 60lb/bbl)

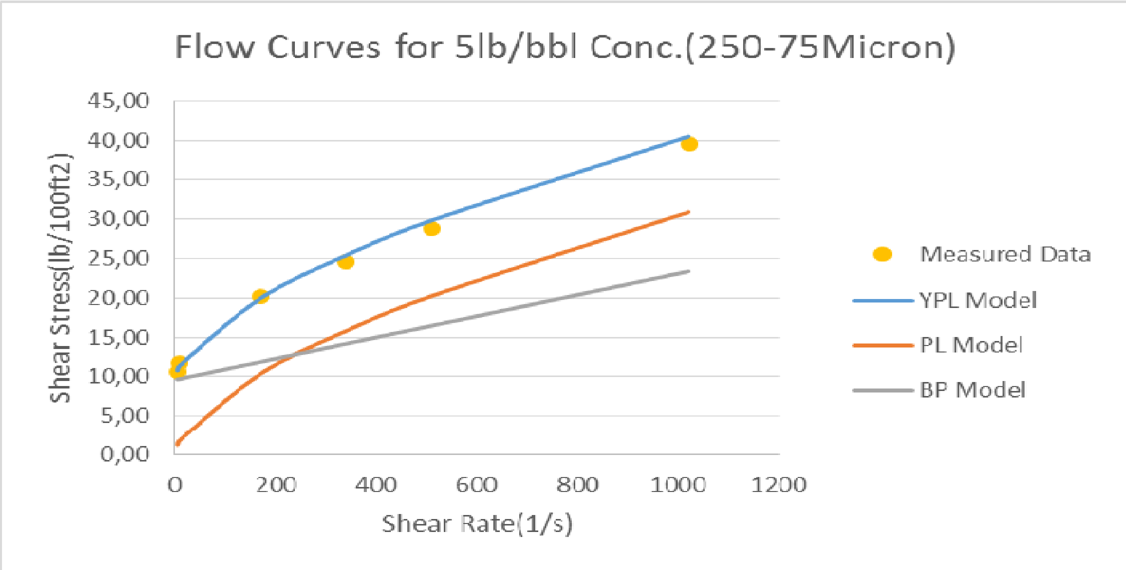

Figure 28 Flow Curves for BP, PL and YPL Models (CaCO3 250-75µm, 5lb/bbl)

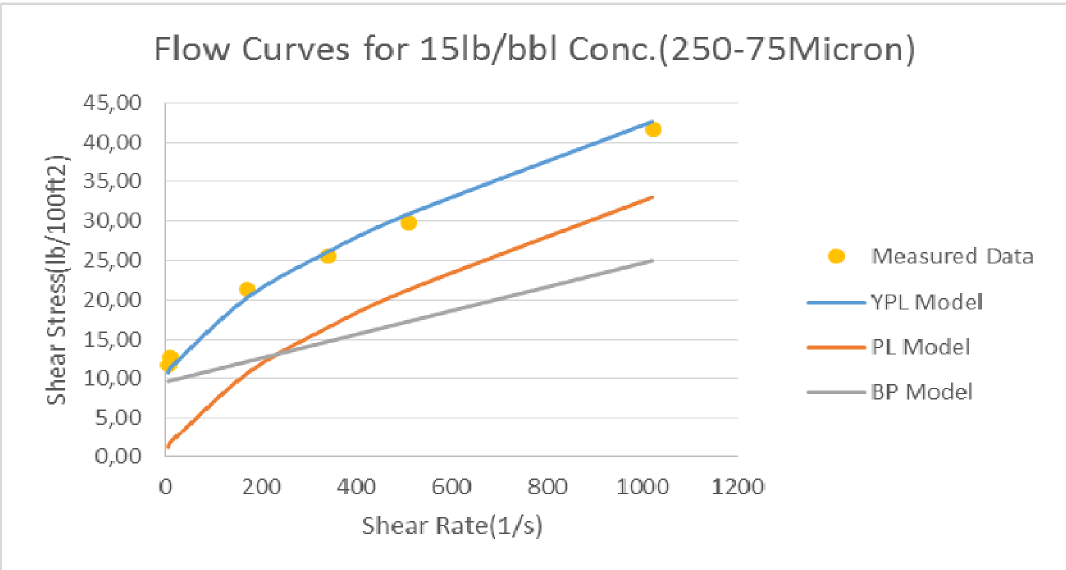

Figure 29 Flow Curves for BP, PL and YPL Models (CaCO3 250-75µm, 15lb/bbl)

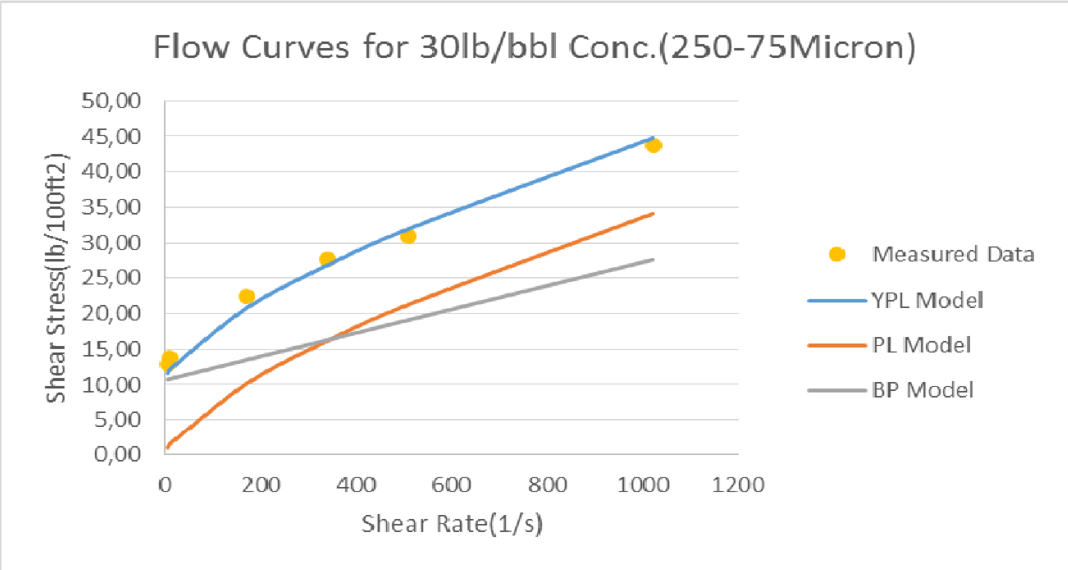

Figure 30 Flow Curves for BP, PL and YPL Models (CaCO3 250-75µm, 30 lb/bbl)

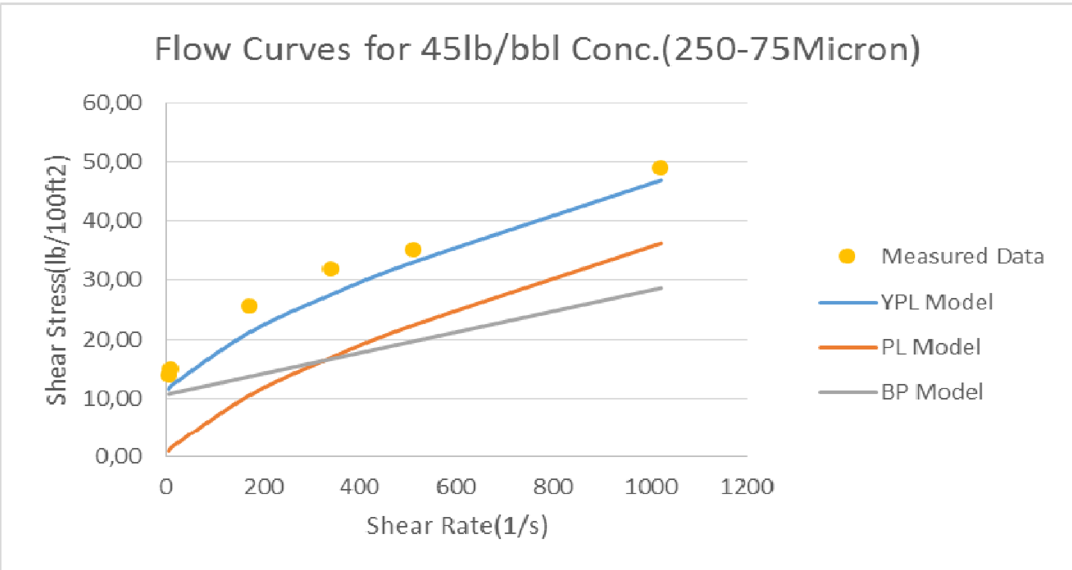

Figure 31 Flow Curves for BP, PL and YPL Models (CaCO3 250-75µm, 45 lb/bbl)

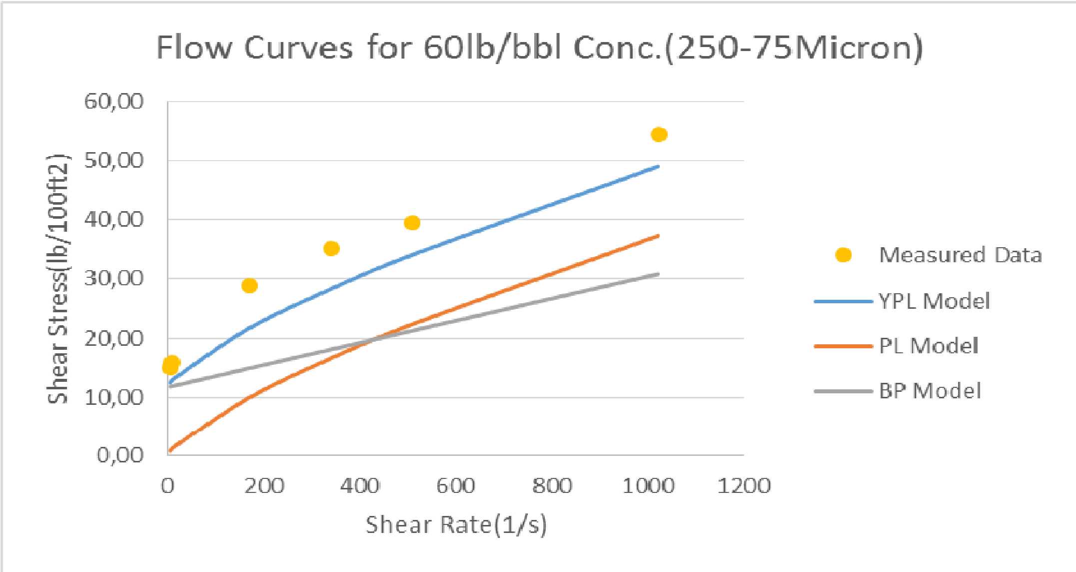

Figure 32 Flow Curves for BP, PL and YPL Models (CaCO3 250-75µm, 60 lb/bbl)

5.2. Effect of Concentration and Particle Size of $CaCO_3$ on Rheological Properties

Effect of sized $CaCO_3$ at different concentrations on rheological parameters of the Bingham plastic, power law and yield-power law model are evaluated in this section.

5.2.1. Effect of Concentration and Particle Size of $CaCO_3$ on PV and YP

As shown from Figures 33 to 35 plastic viscosity (PV) of DIFs increases proportionally with concentration for all sizes of $CaCO_3$. Increase in plastic viscosity is largely due to increasing mechanical friction between solid particles as a function $CaCO_3$ concentration in DIFs.

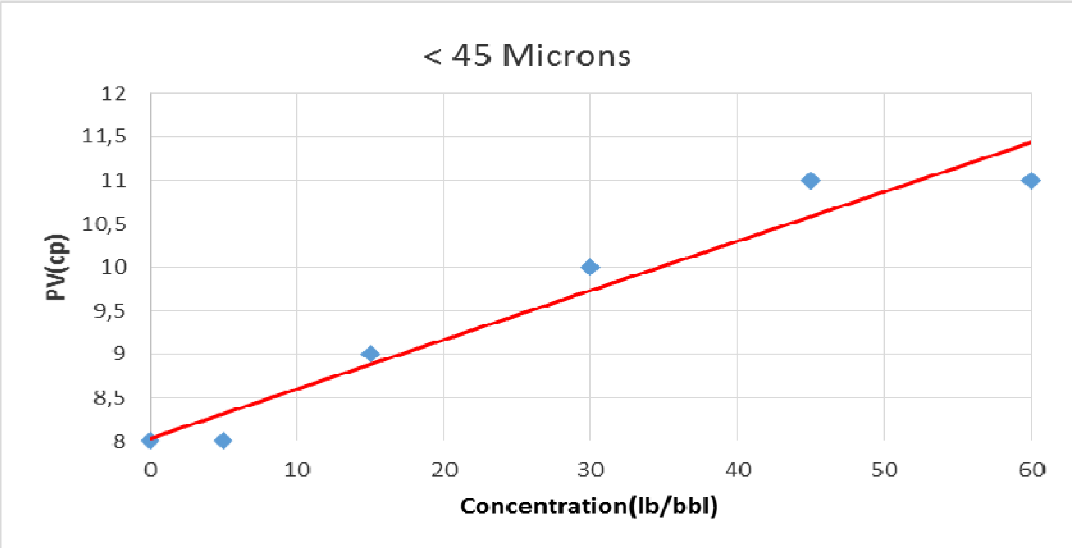

Figure 33 Effect of CaCO3 Concentration on PV (<45 µm)

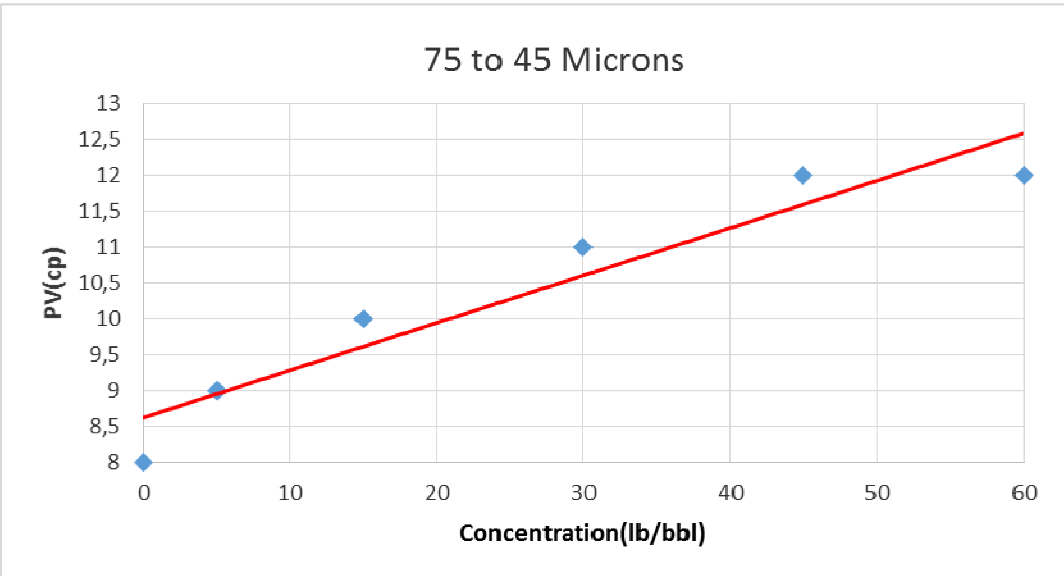

Figure 34 . Effect of CaCO3 Concentration on PV (75-45 µm)

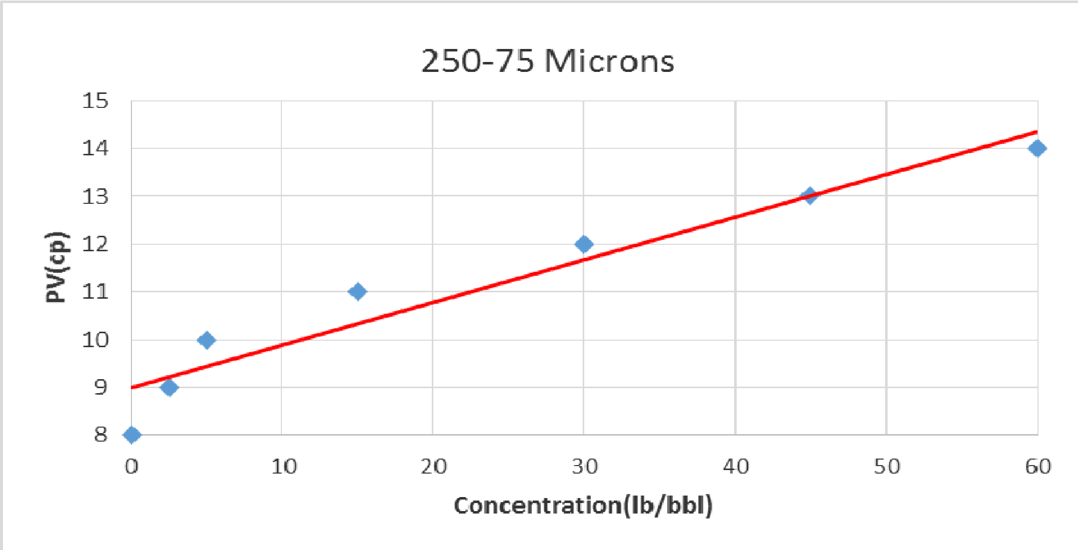

Figure 35 Effect of CaCO3 Concentration on PV (250-75 µm)

As shown from Figure 36, PV increases with increasing particle size of $CaCO_3$. This is an unexpected result which is opposing the general principle of PV increase with decreasing particle size.

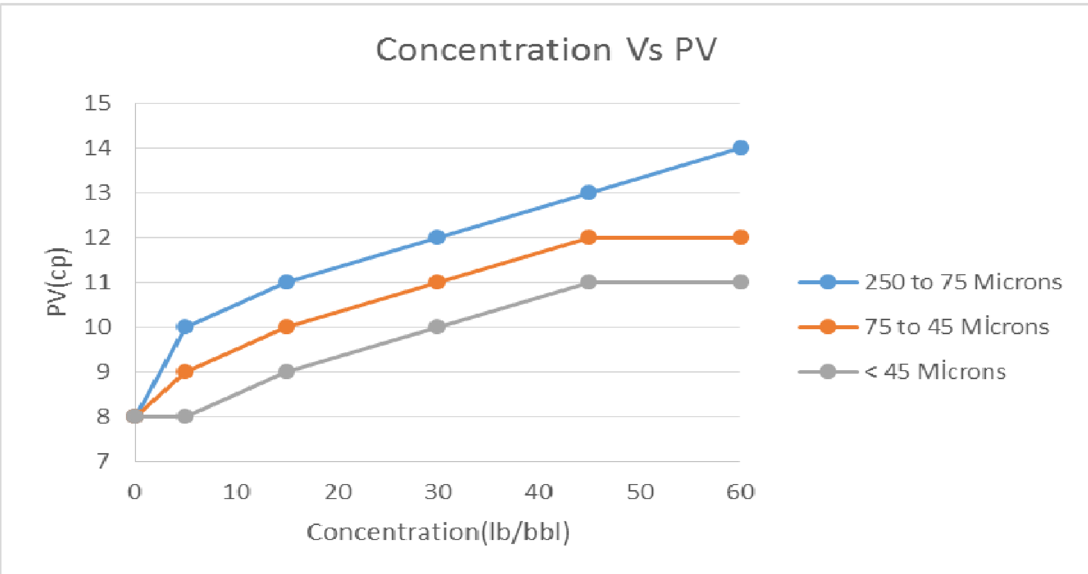

Figure 36 Effect of CaCO3 Concentration on PV for Different Particle Sizes

As shown from Figures 37 to 39, yield point (YP) does not show sensitivity to concentration of $CaCO_3$ for any size. YP values for sizes less than 45 micron and size 75 to 45 micron show a decrement for increasing concentrations but for size

250 to 75 micron, YP remains nearly constant except zero concentration of $CaCO_3$. YP decreases suddenly from 0 lb/bbl concentration to 5 lb/bbl concentration of $CaCO_3$. It can be explained as the consumption of XCD polymer by $CaCO_3$ particles.

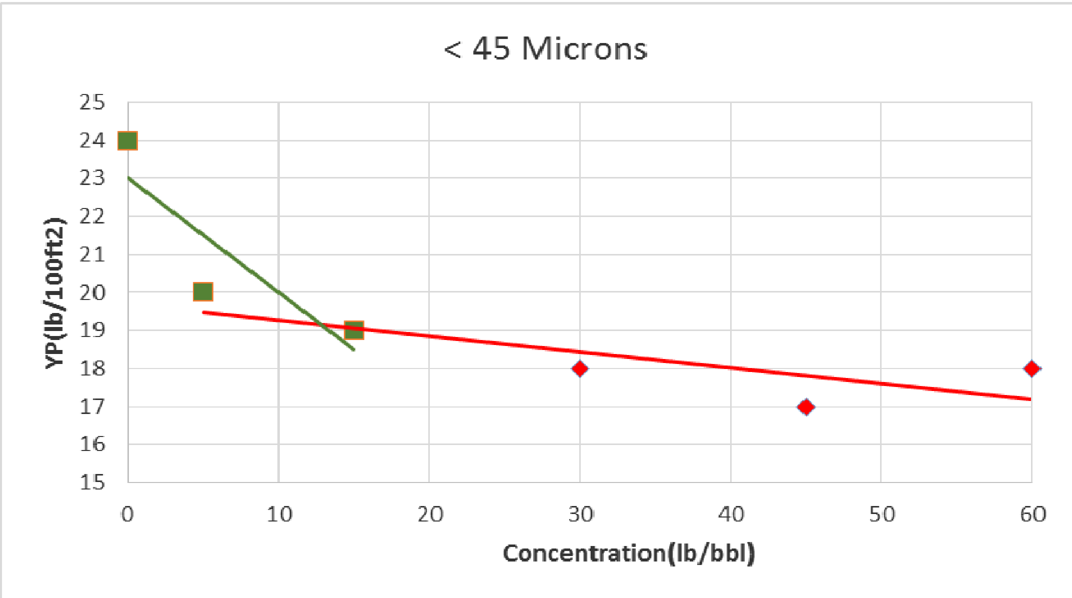

Figure 37 Effect of CaCO3 Concentration on YP (<45 μm)

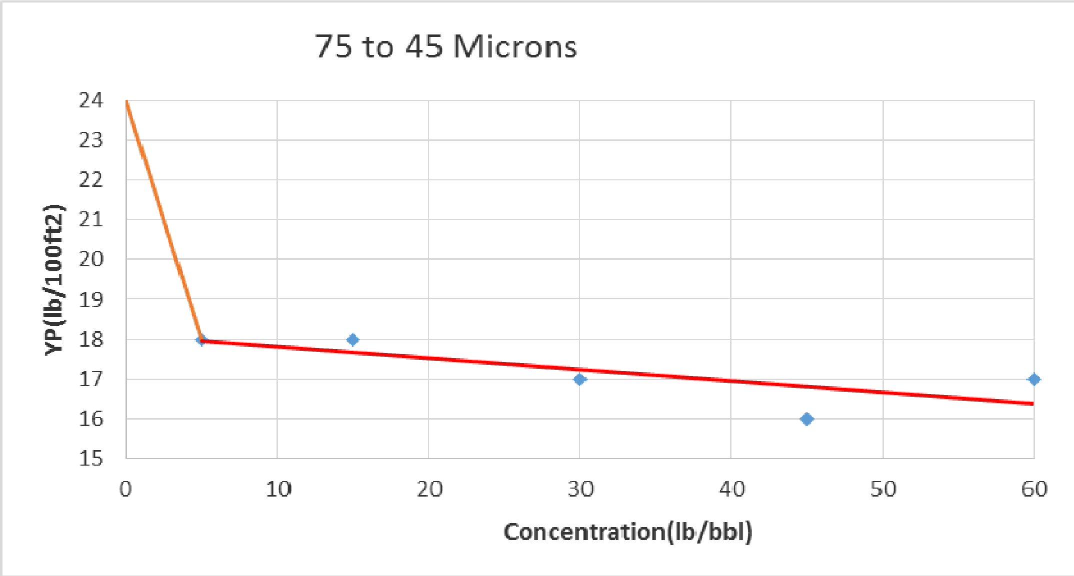

Figure 38 Effect of CaCO3 Concentration on YP (75-45 µm)

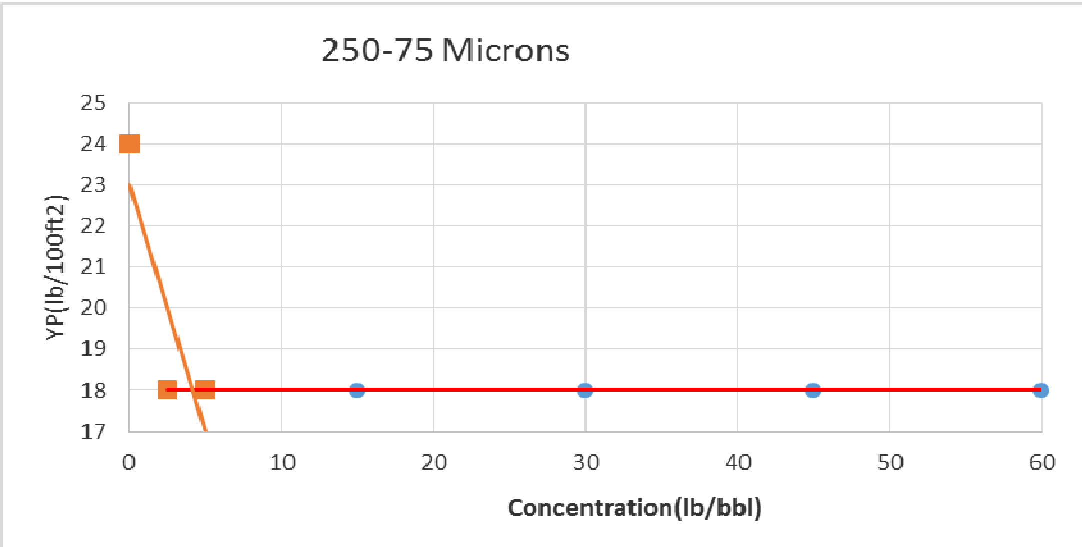

Figure 39 Effect of CaCO3 Concentration on YP (250-75 µm)

These Figures 37,38 and 39 have two parts as seen , first part is the sharp decrease between 0lb/bbl and 5lb/bbl and the second part is the slight decrease between 5lb/bbl and other concentrations.

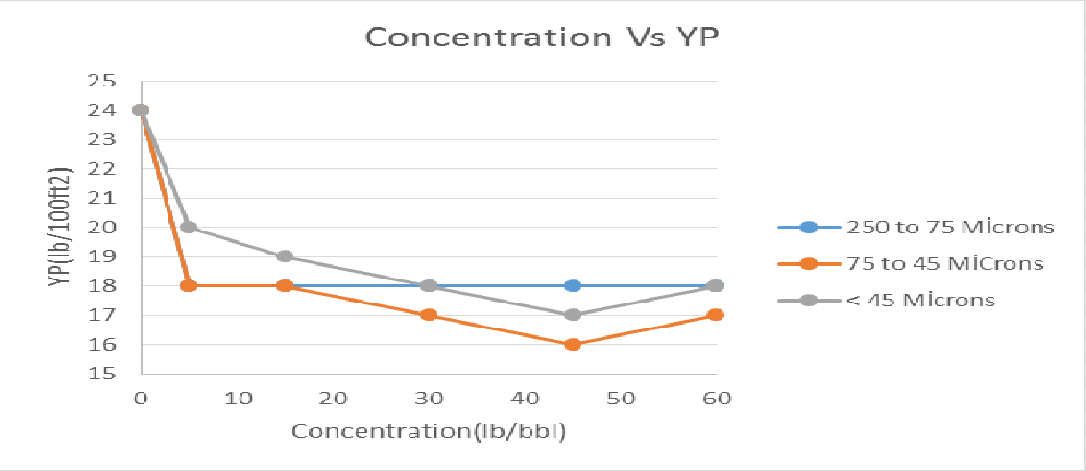

Figure 40 Effect of CaCO3 Concentration on YP for Different Particle Sizes

As shown from Figure 40, YP does not consistently changes with the particle size of $CaCO_3$.

5.2.2. Effect of Concentration and Particle Size of $CaCO_3$ on n_a and K_a

As seen in Figures 41 to 43; Flow behavior index in annulus (n_a) shows a decreasing tendency as the concentration of $CaCO_3$ increases for all sizes. This means that the fluid becomes more shear thinning with increasing concentration of $CaCO_3$.

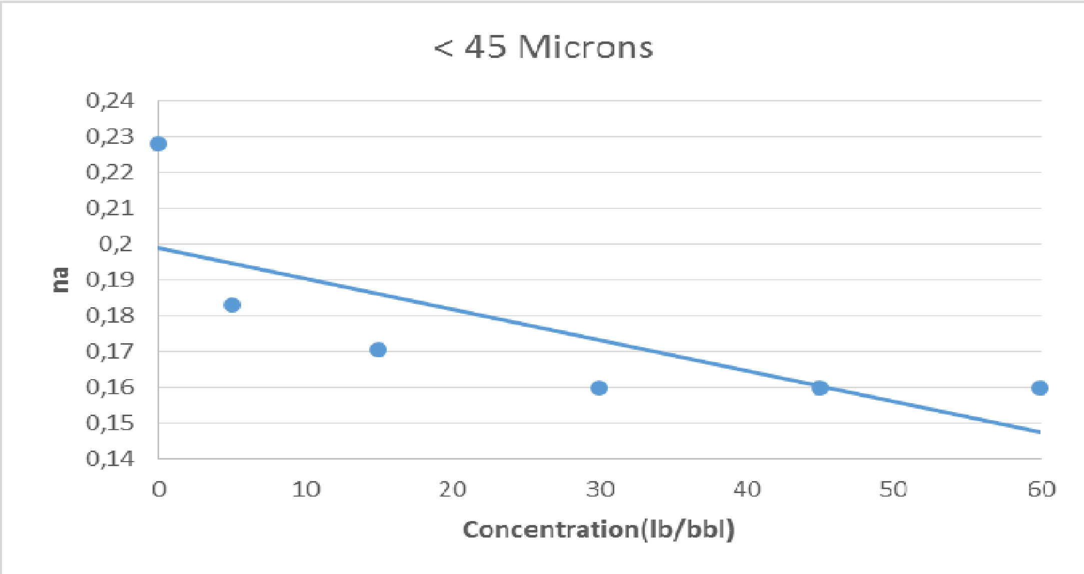

Figure 41 Effect of CaCO3 Concentration on na (<45 µm)

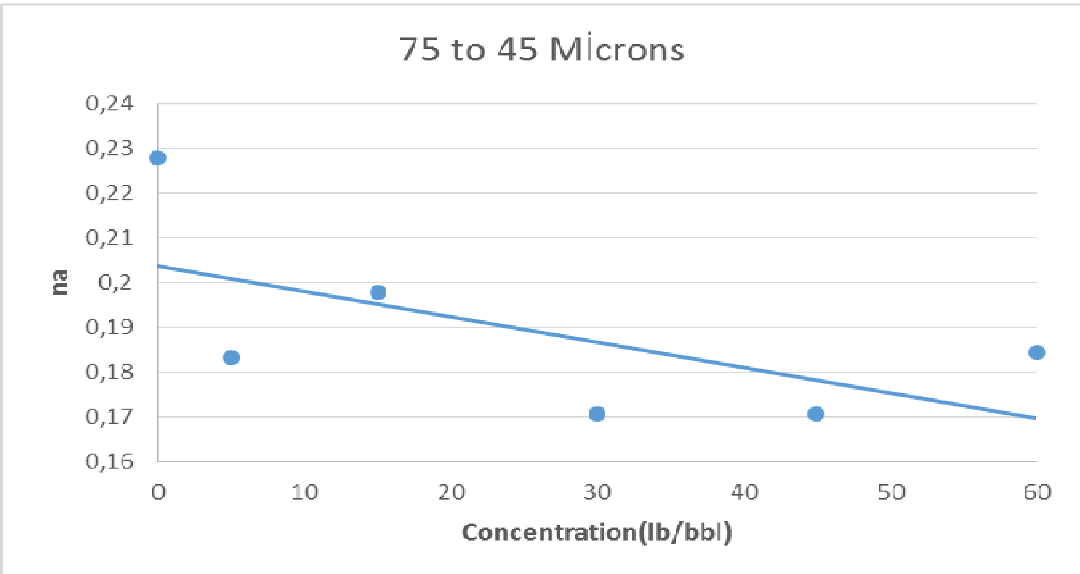

Figure 42 Effect of CaCO3 Concentration on na (75-45 µm)

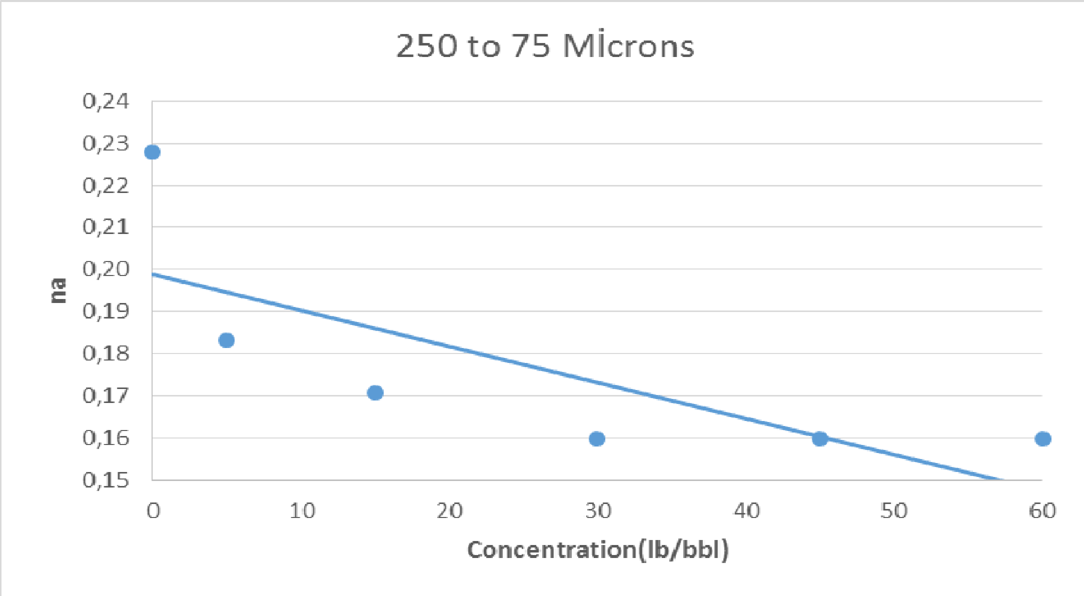

Figure 43 Effect of CaCO3 Concentration on na (250-75 µm)

As shown from Figure 44, n_a does not consistently changes with the particle size of $CaCO_3$.

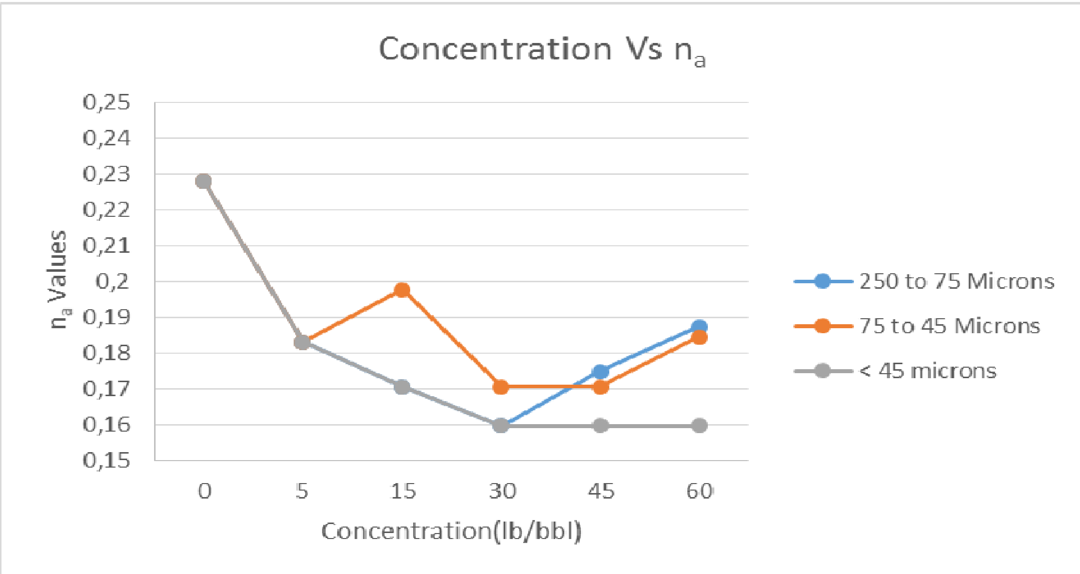

Figure 44 Effect of CaCO3 Concentration on na for Different Particle Sizes

From Figures 45 to 47, the consistency index in annulus (K_a) shows a perfect inverse proportion with "n_a" as the mathematical manner proves. K_a increases with increasing concentration of $CaCO_3$ in consistent with the plastic viscosity due increasing mechanical friction between solid particles as a function $CaCO_3$ concentration in DIFs.

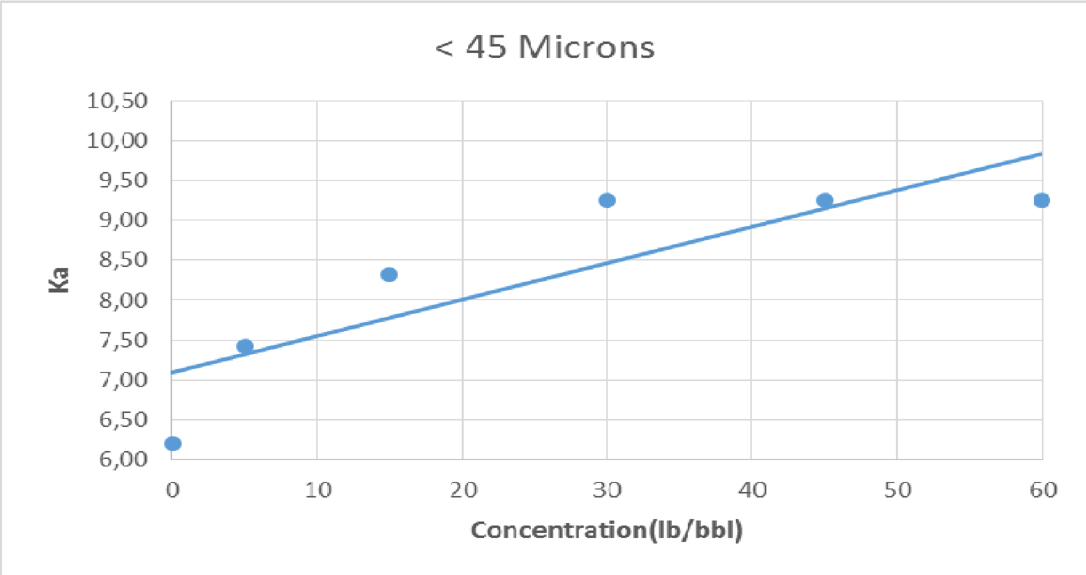

Figure 45 Effect of CaCO3 Concentration on Ka (<45 µm)

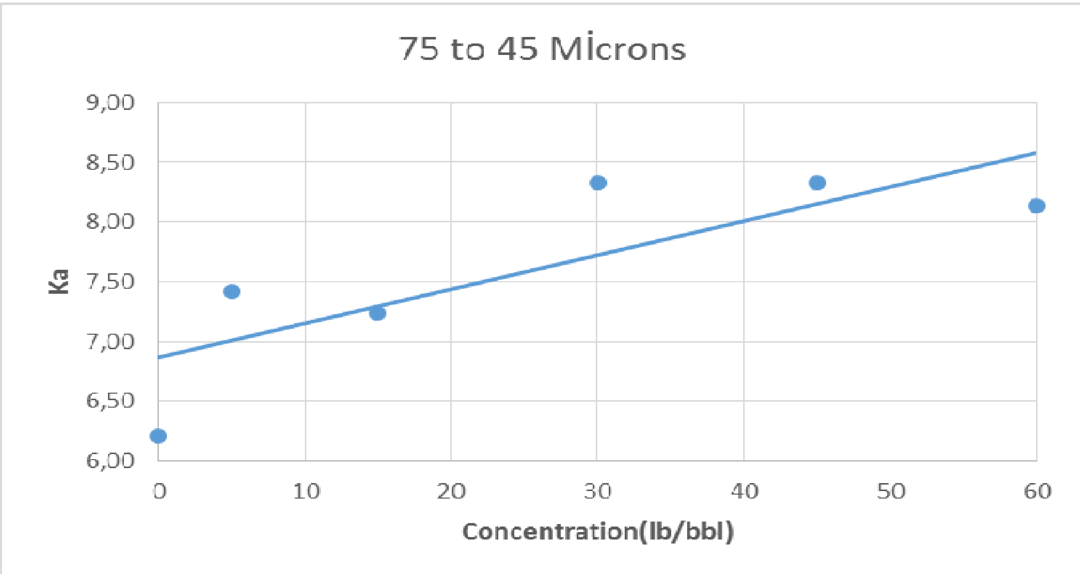

Figure 46 Effect of CaCO3 Concentration on Ka (75-45 µm)

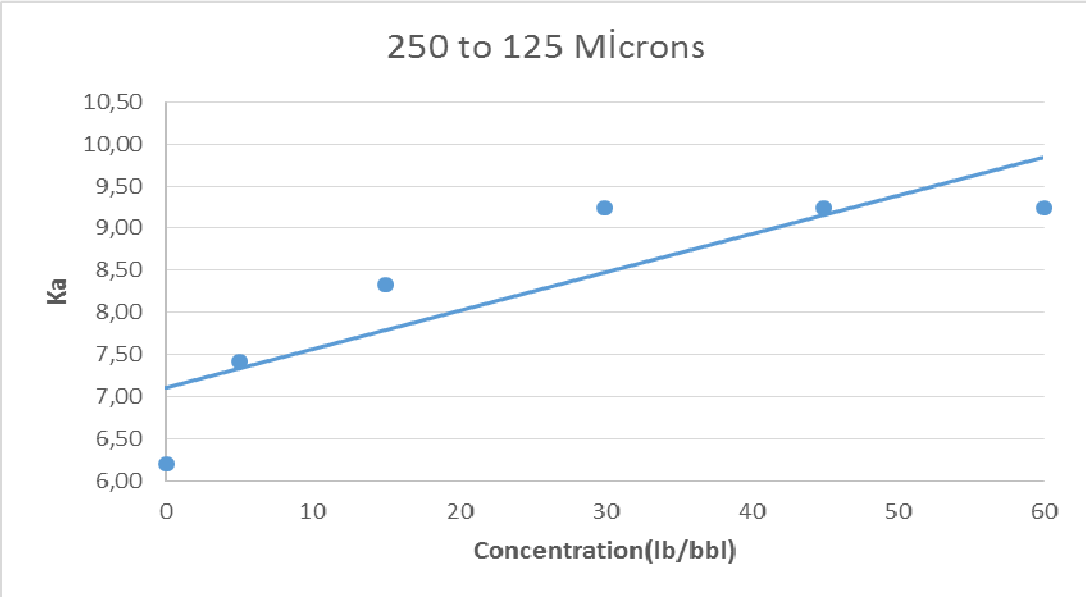

Figure 47 Effect of CaCO3 Concentration on Ka (250-75 µm)

As shown from Figure 48, K_a does not consistently changes with the particle size of $CaCO_3$

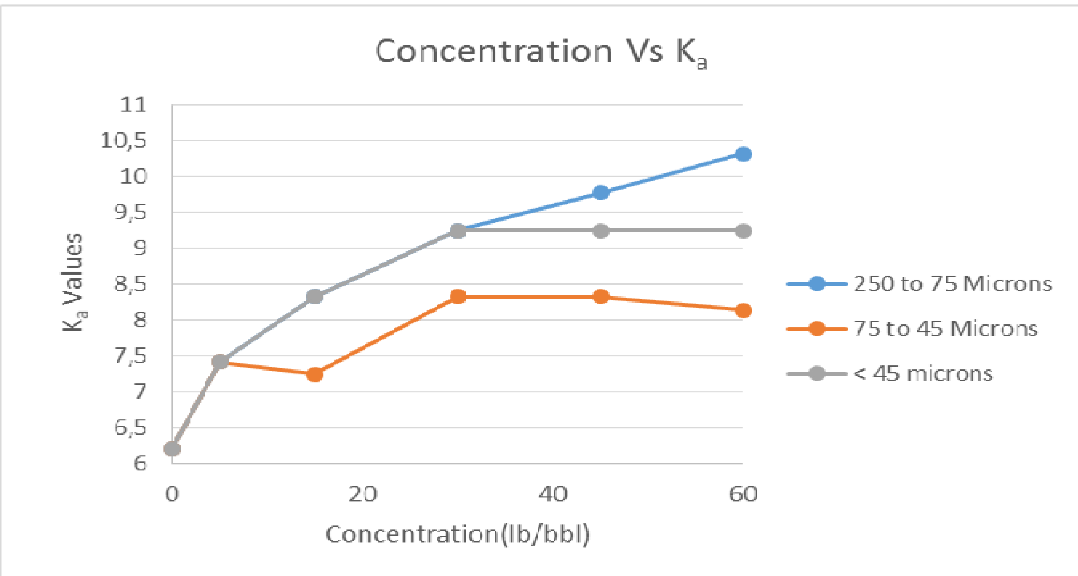

Figure 48 Effect of CaCO3 Concentration on na for Different Particle Sizes

5.2.3 Effect of Concentration and Particle Size of $CaCO_3$ on n_p and K_p

Figures 49 to 51 illustrates the increment of flow behavior index in pipe flow (n_p) as the concentration of $CaCO_3$ increases. This indicates that increasing concentration of $CaCO_3$ makes the fluid more Newtonian at high shear rates.

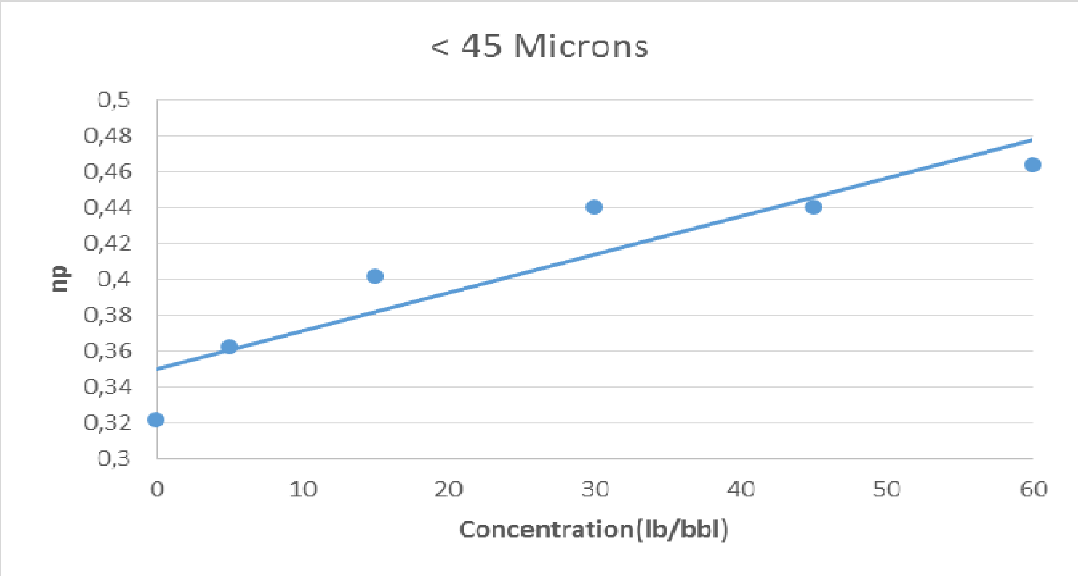

Figure 49 Effect of CaCO3 Concentration on np (<45 µm)

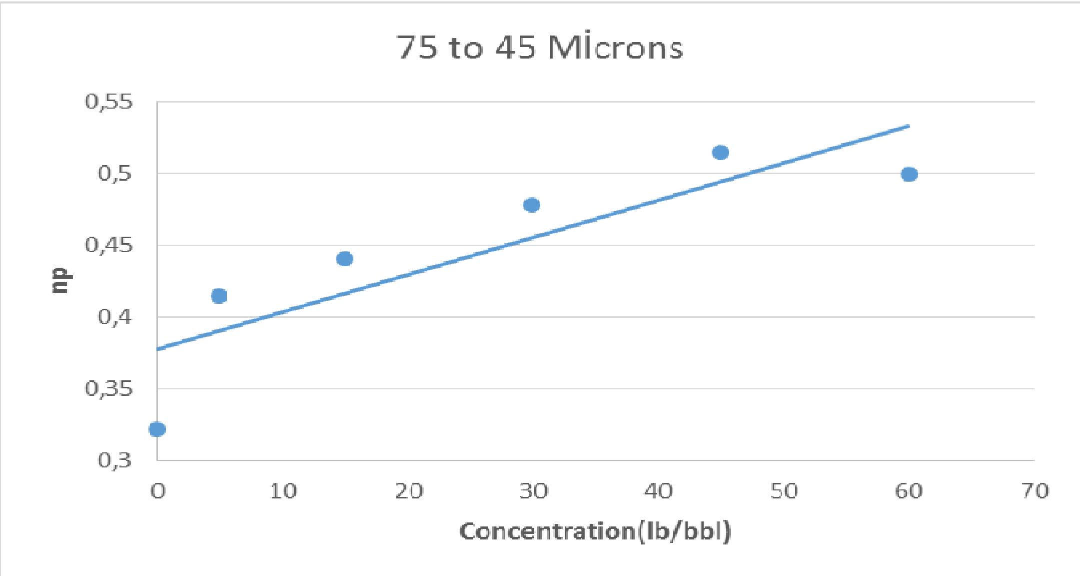

Figure 50 Effect of CaCO3 Concentration on np (75-45 µm)

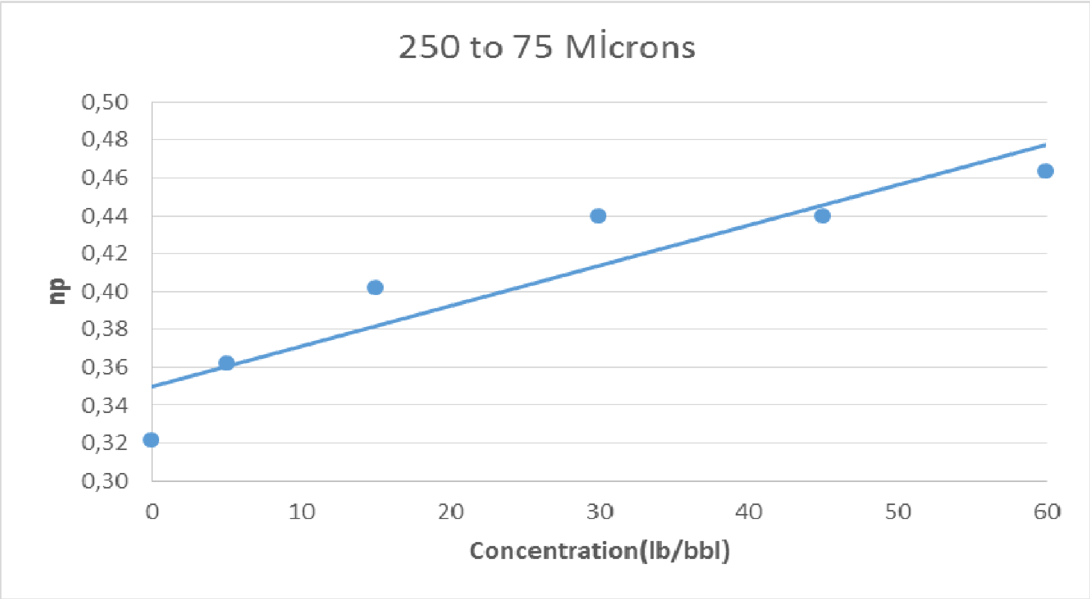

Figure 51Effect of CaCO3 Concentration on np (250-75 µm)

As shown from Figure 52, n_p decreases with incresing particle size of $CaCO_3$. The smaller particle sizes of of $CaCO_3$ makes the fluid more shear thinning.

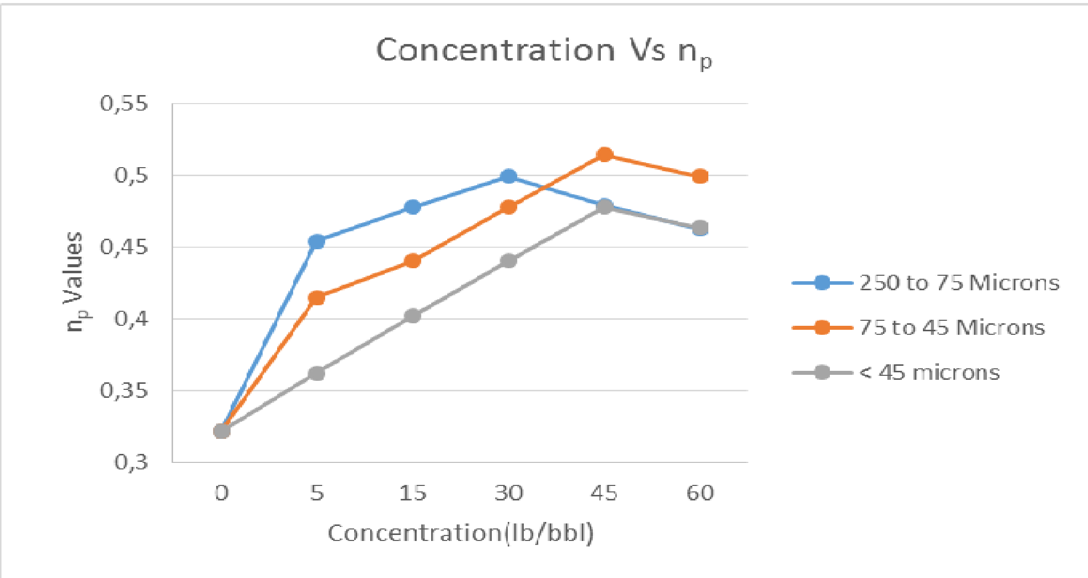

Figure 52 Effect of CaCO3 Concentration on np for Different Particle Sizes

In Figures 53 to 55 same behavior of consistency index in pipe flow (K_p) can be seen for three different sizes. As the concentration of $CaCO_3$ increases, the K_p value decreases with an inverse proportion to "n_p".

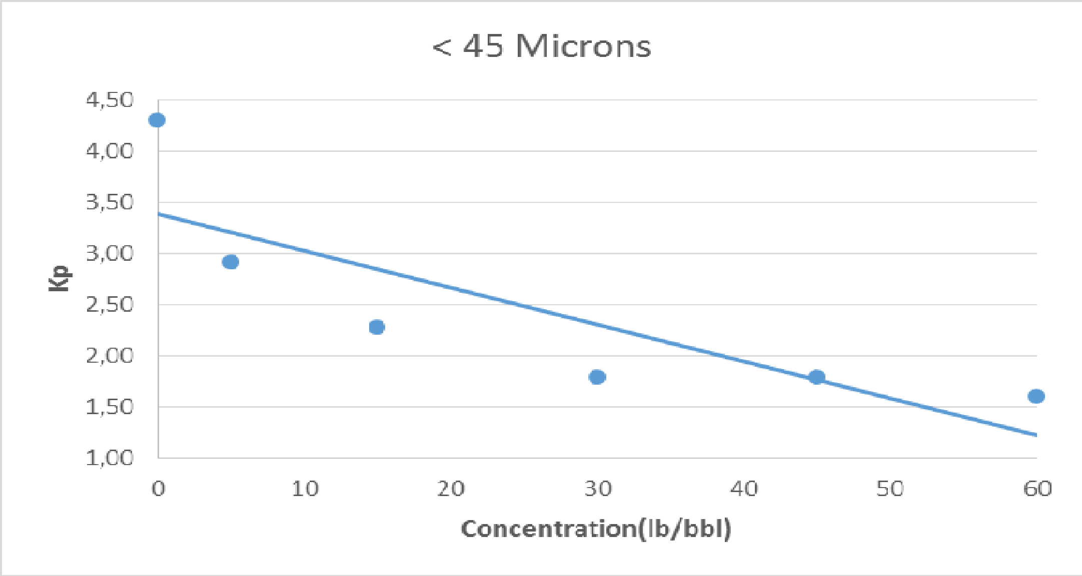

Figure 53 Effect of CaCO3 Concentration on Kp (<45 µm)

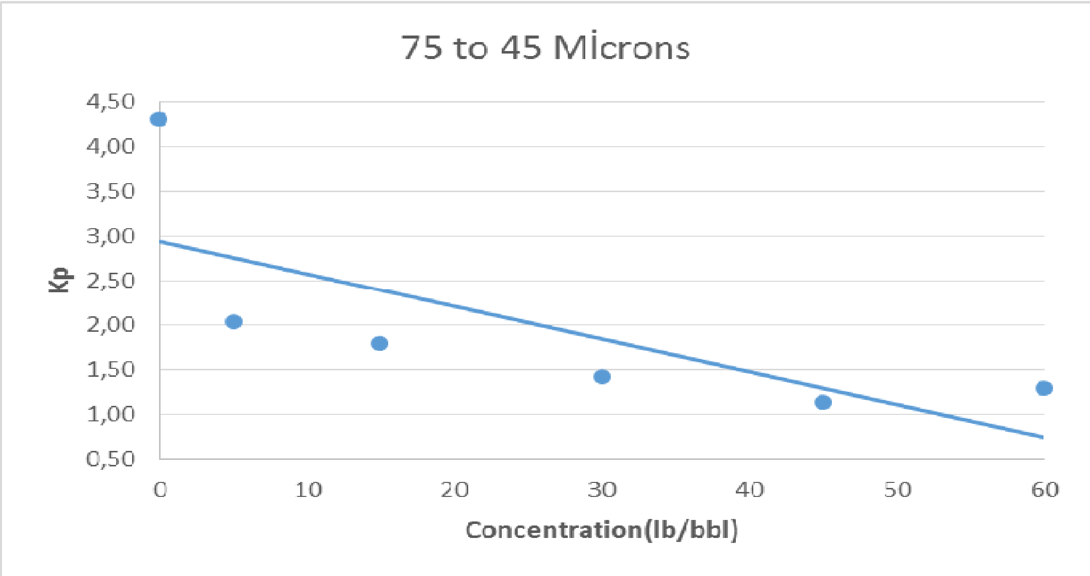

Figure 54 Effect of CaCO3 Concentration on Kp (75-45 µm)

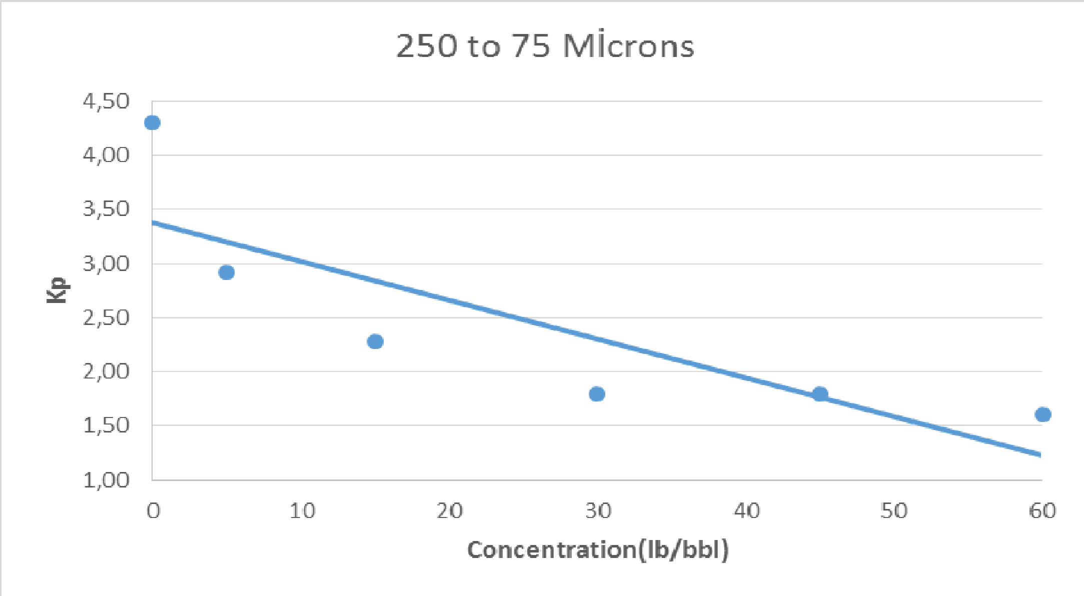

Figure 55 Effect of CaCO3 Concentration on Kp (250-75 µm)

As shown from Figure 56, K_p increases with incresing particle size of $CaCO_3$ for all concentrations of $CaCO_3$.

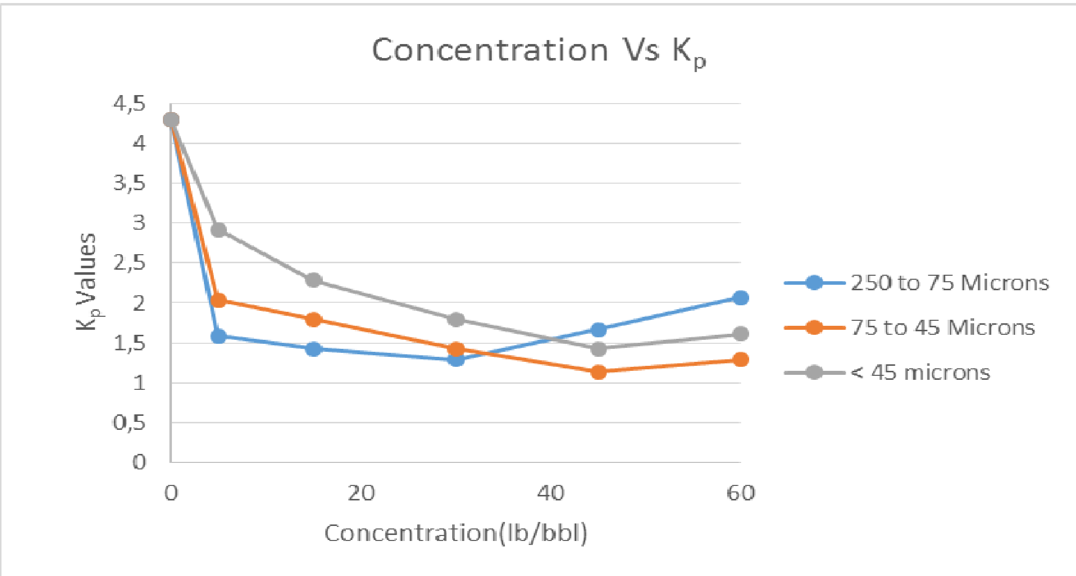

Figure 56 Effect of CaCO3 Concentration on Kp for Different Particle Sizes

5.2.4 Effect of Concentration and Particle Size of $CaCO_3$ on τ_y, m and k

Figures 57 to 59 show that the low-shear-rate yield point (τ_y) of DIF increases with increasing $CaCO_3$ concentration for all $CaCO_3$ sizes. This increasing tendency of the low-shear-rate yield point with $CaCO_3$ concentration is completely opposite to decreasing or the less sensitive nearly independent behavior of the high shear rate Bingham plastic YP. Dependency of the low-shear-rate yield point on $CaCO_3$ concentration disappears at 30 lb/bbl and becomes nearly constant at higher concentrations the $CaCO_3$ sizes less than 75µ. Consistent increase in τ_y with $CaCO_3$ concentration for particle sizes greater than 75µ.

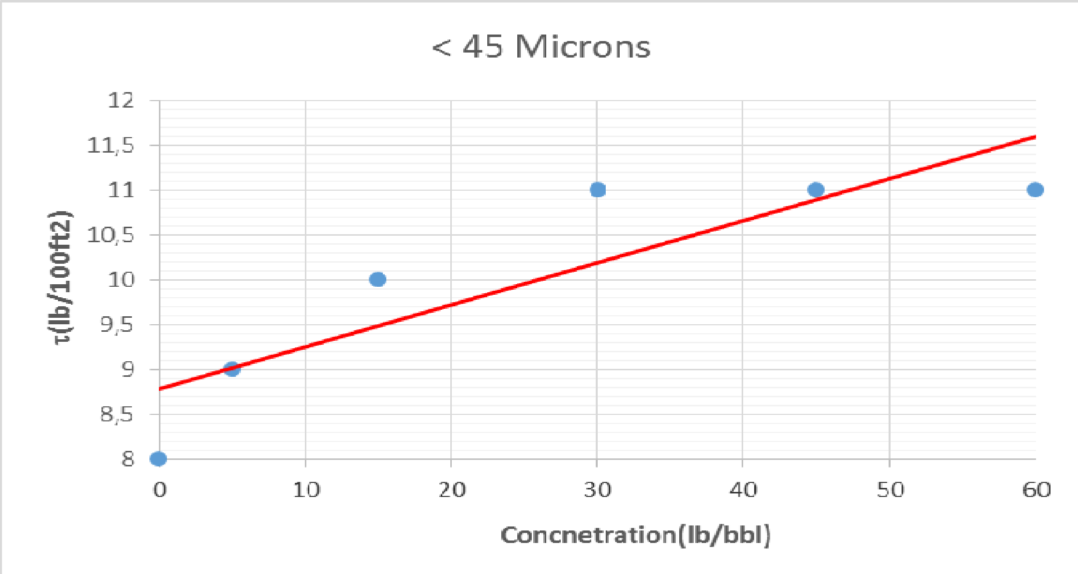

Figure 57 Effect of CaCO3 Concentration on □y (<45 µm)

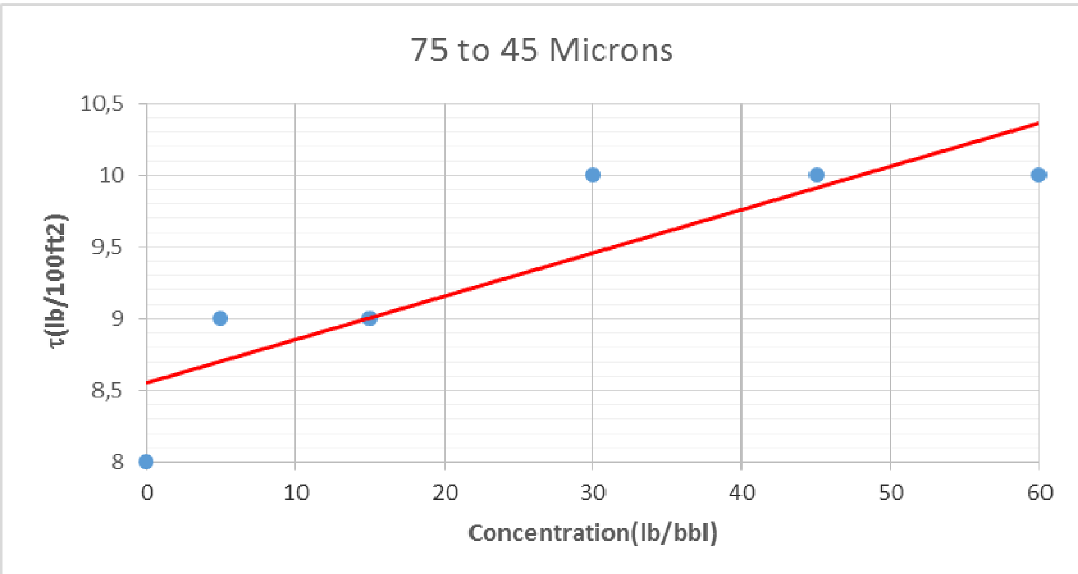

Figure 58 Effect of CaCO3 Concentration on □y (75-45 µm)

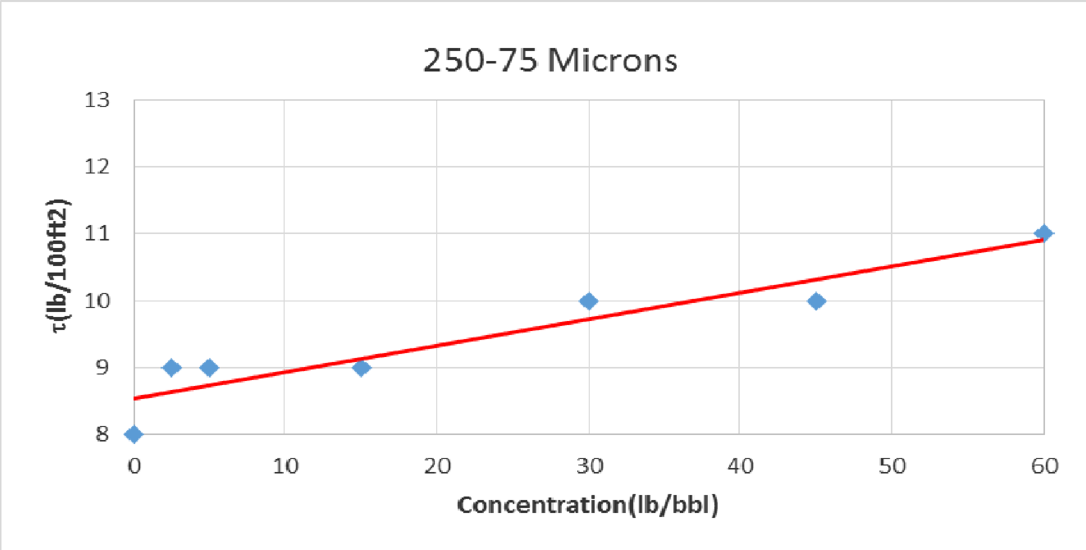

Figure 59 Effect of CaCO3 Concentration on y (250-75 µm)

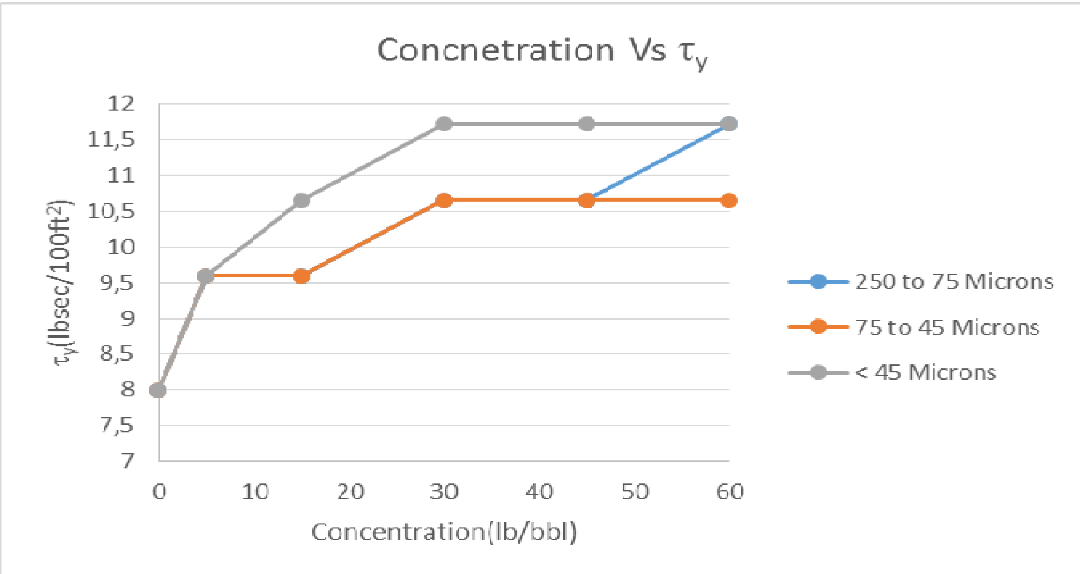

Figure 60 . Effect of CaCO3 Concentration on τy for Different Particle Sizes

As shown from Figure 60, τ_y increases with decresing particle size of $CaCO_3$ for all concentrations of $CaCO_3$.

As seen from Figures 61 to 63 the flow behavior index (m) of DIF generally increases as the concentration of $CaCO_3$ increases.

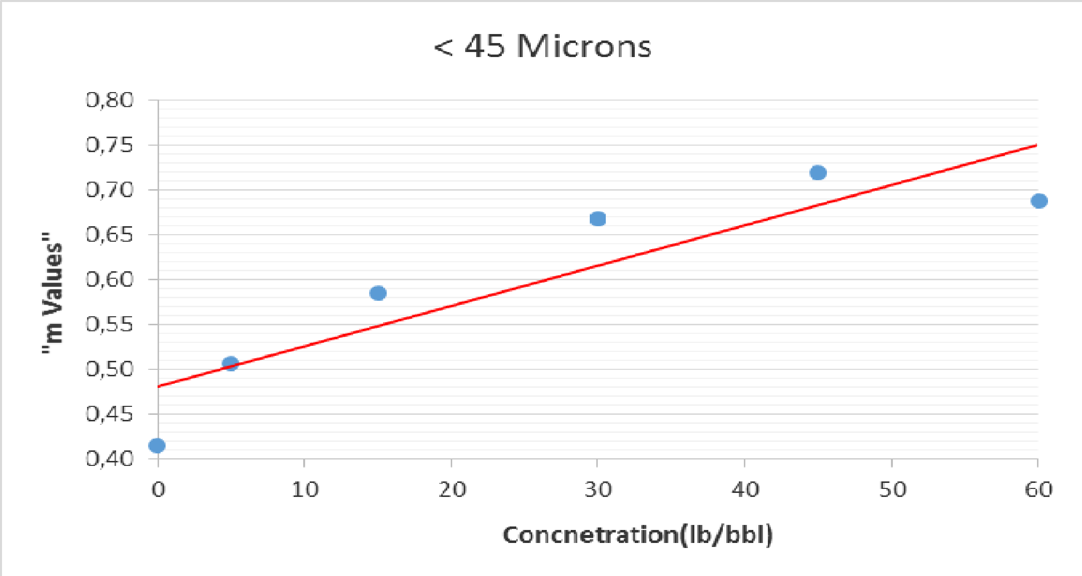

Figure 61 Effect of CaCO3 Concentration on m (<45 µm)

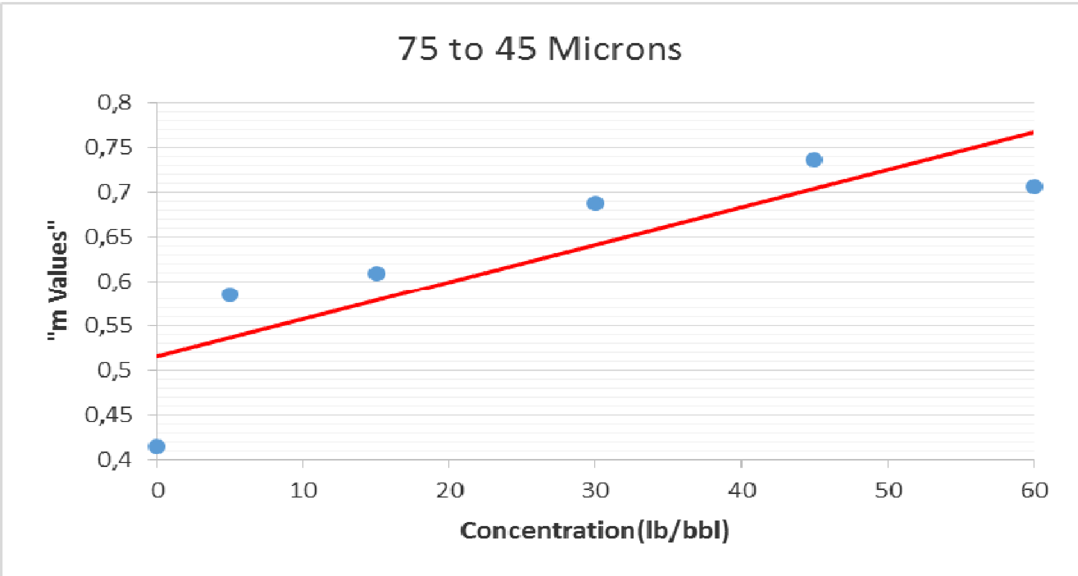

Figure 62 Effect of CaCO3 Concentration on m (75-45 µm)

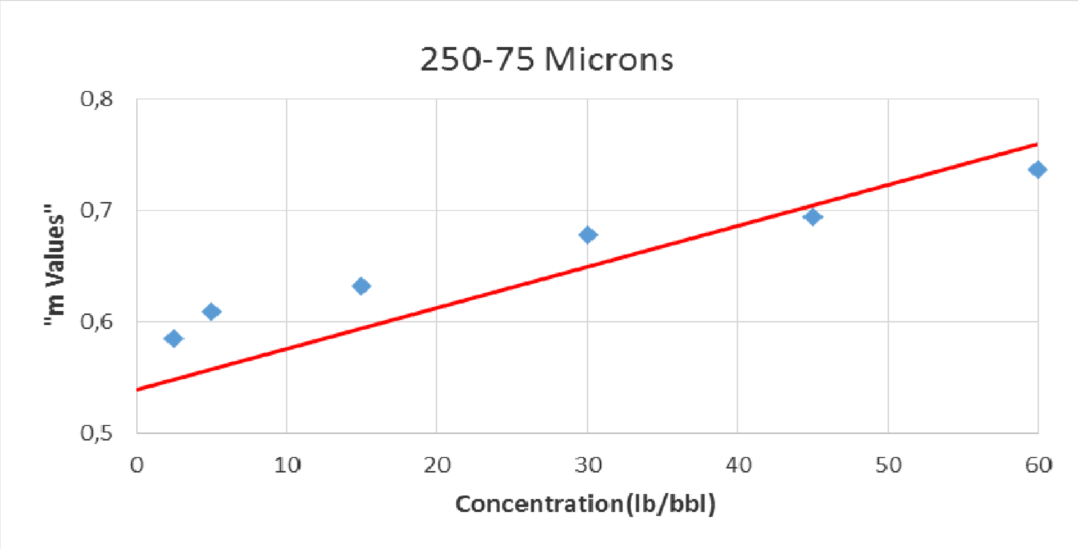

Figure 63 Effect of CaCO3 Concentration on m (250-75 µm)

As shown from Figure 64, m decreases with decresing particle size of $CaCO_3$ for all concentrations of $CaCO_3$.

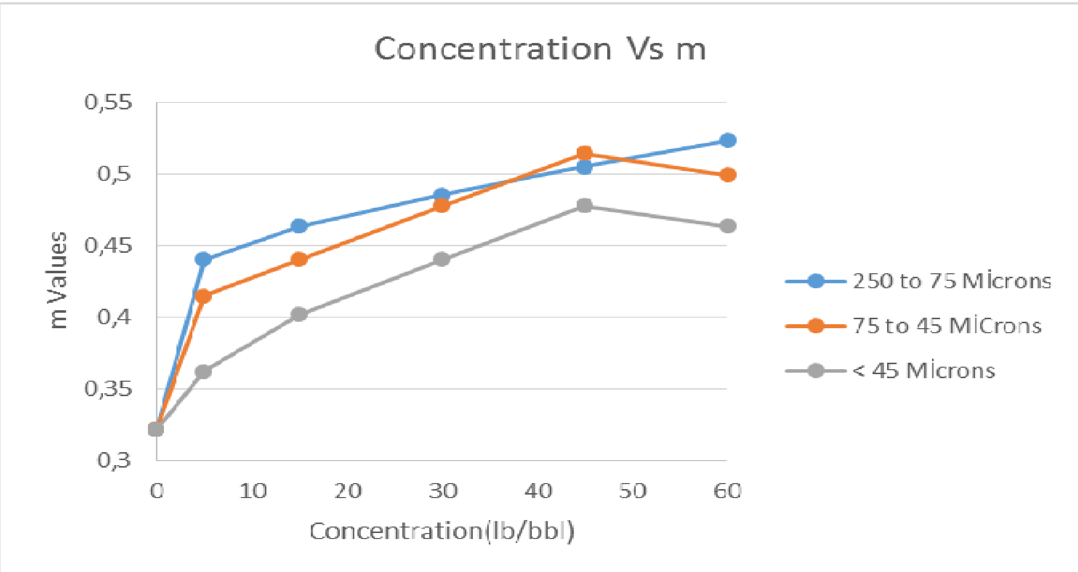

Figure 64 Effect of CaCO3 Concentration on □y for Different Particle Sizes

As seen from Figures 65 to 67 the consistency index (k) of DIF generally decrease as the concentration of $CaCO_3$ increases. For $CaCO_3$ sizes less than 75µ "k" does not further change with $CaCO_3$ concentration above 30 lbb/bbl. However, there is consistent proportionality between "k" and $CaCO_3$ concentration for fluids containing $CaCO_3$ particles in sizes greater than 75µ.

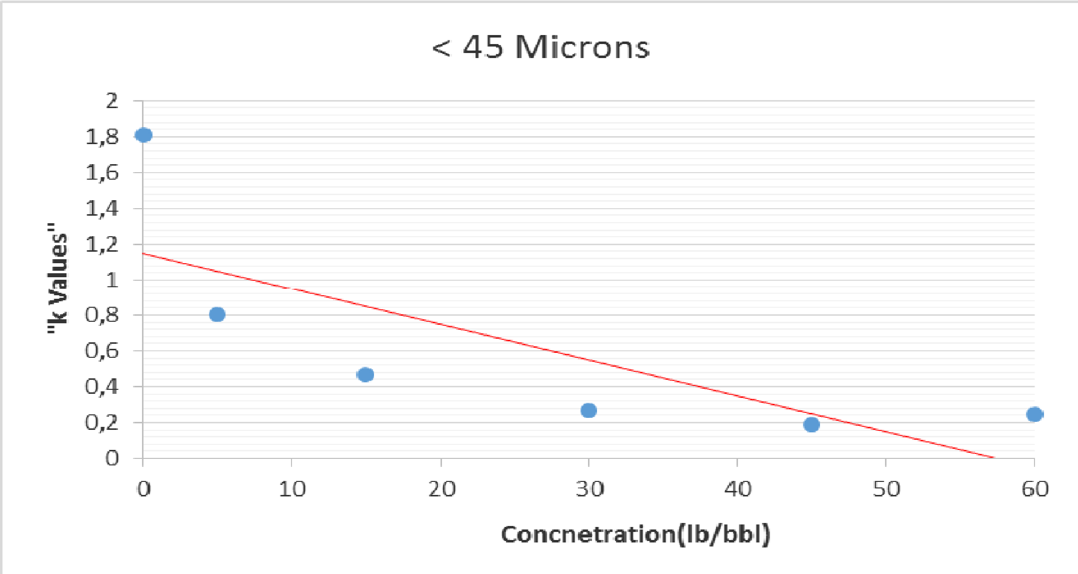

Figure 65 Effect of CaCO3 Concentration on k (<45 µm)

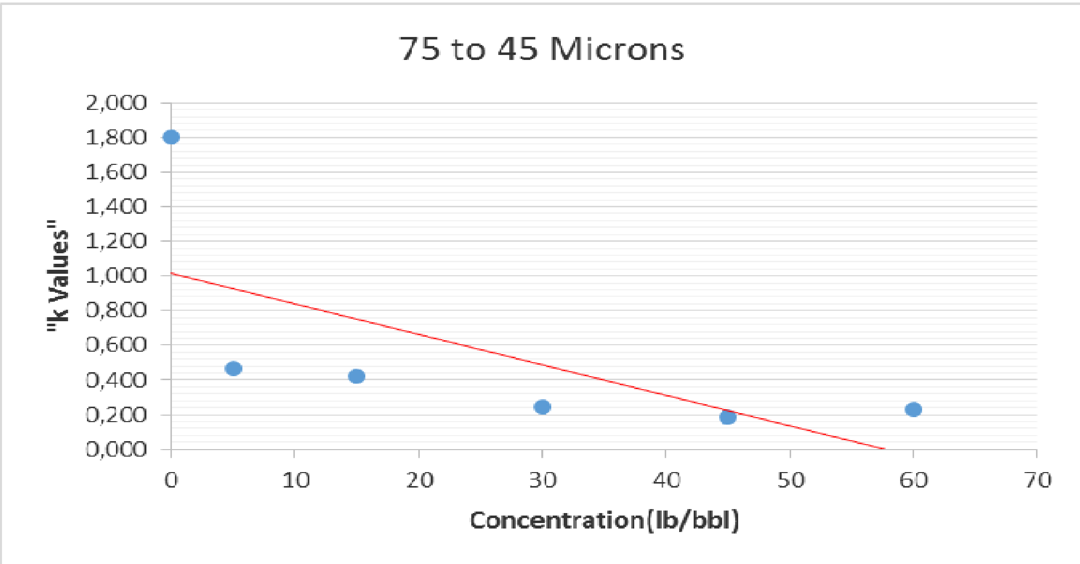

Figure 66 Effect of CaCO3 Concentration on k (75-45 µm)

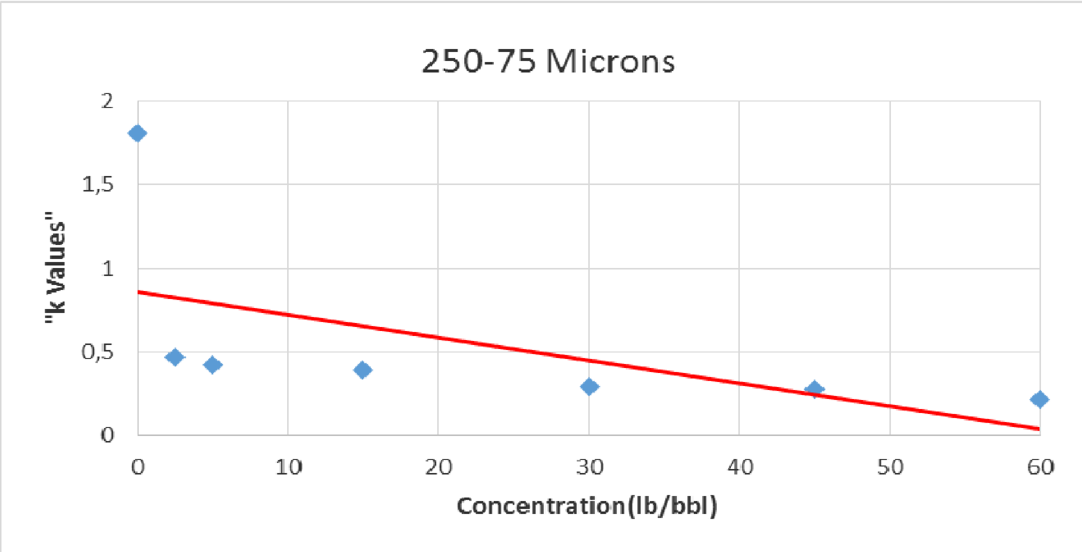

Figure 67 Effect of $CaCO3$ Concentration on k (250-75 µm)

As shown from Figure 68, k increeases with decresing particle size of $CaCO_3$ for all concentrations of $CaCO_3$.

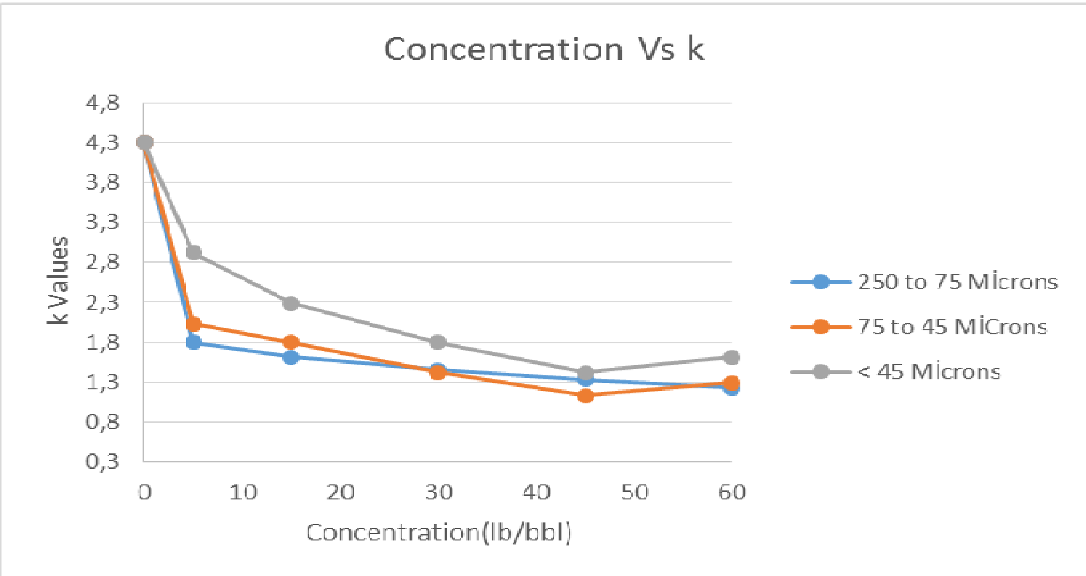

Figure 68 Effect of $CaCO3$ Concentration on k for Different Particle Sizes

5.3. Effect of $CaCO_3$ Concentration and Particle Size on Fluid Loss

Fom Figure 69 to 71 it is obviously seen that as the concentration of $CaCO_3$ increases, the fluid loss of DIFs decreases. The graphs devided into two parts; the first part describes how the addition of small amount of $CaCO_3$ affects the fluid loss.

When no $CaCO_3$ is added, particles needed to form the main skeloton of filter cake are not available. Therefoe, the spurt loss occurs for $CaCO_3$ free (0 lb/bbl) DIF. In the second part between 5 lb/bbl of $CaCO_3$ to 60 lb/bbl of $CaCO_3$, fluid loss consistently decreases with increasing $CaCO_3$ concentration for all particle sizes.

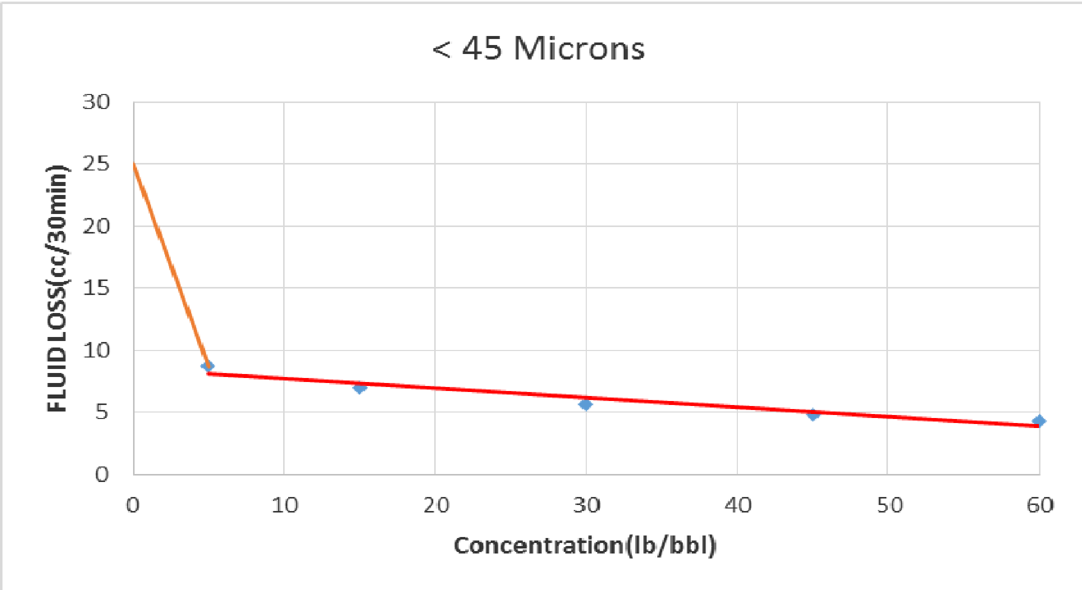

Figure 69 Effect of CaCO3 Concentration on Fluid Loss (<45 µm)

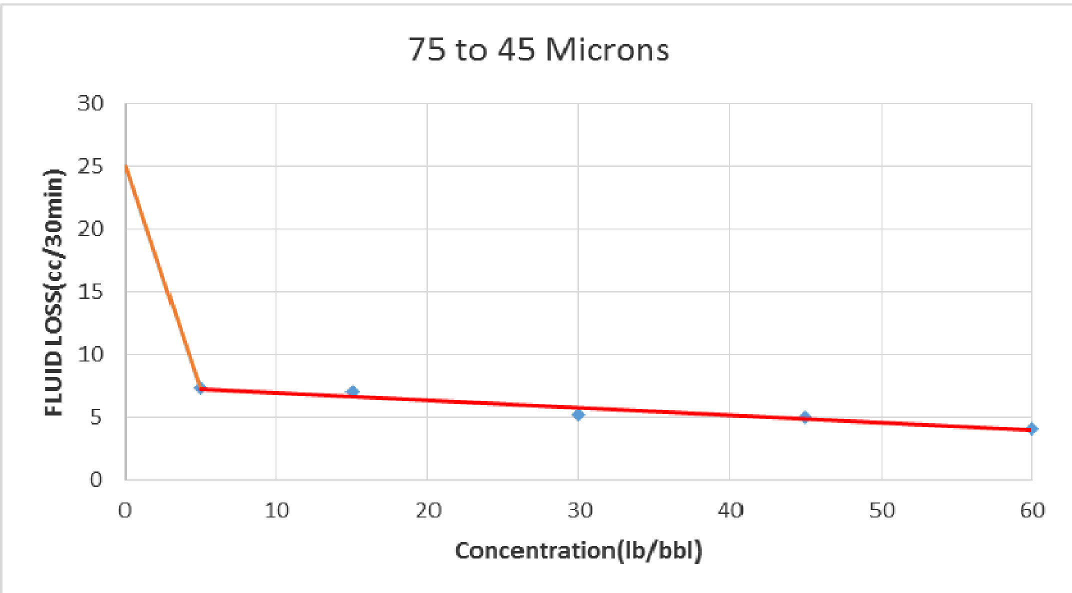

Figure 70 Effect of CaCO3 Concentration on Fluid Loss (75-45 µm)

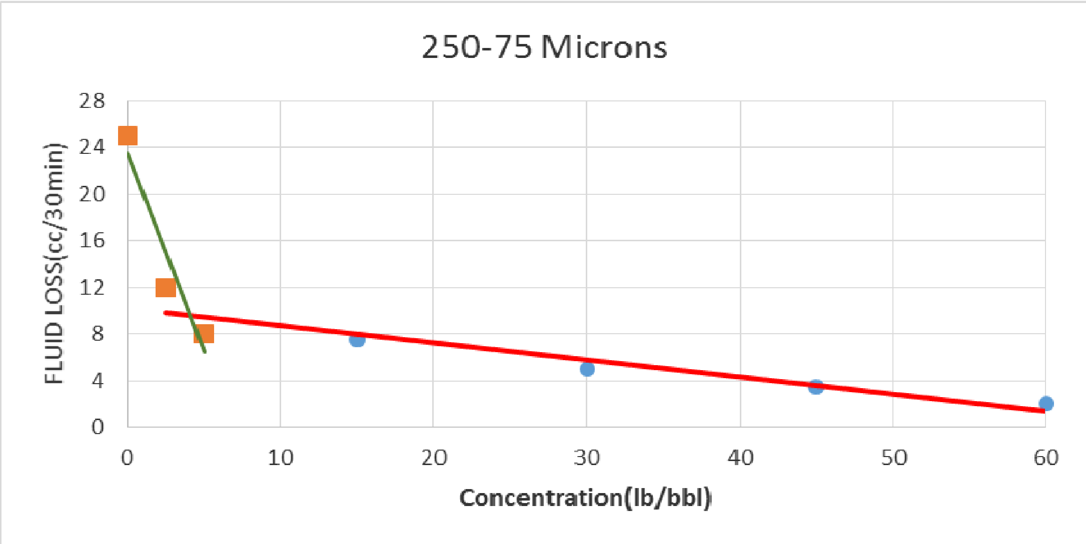

Figure 71 Effect of CaCO3 Concentration on Fluid Loss (250-75 µm)

These Figures 69,70 and 71 have two parts as seen , first part is the sharp decrease between 0lb/bbl and 5lb/bbl and the second part is the slight decrease between 5lb/bbl and other concentrations.

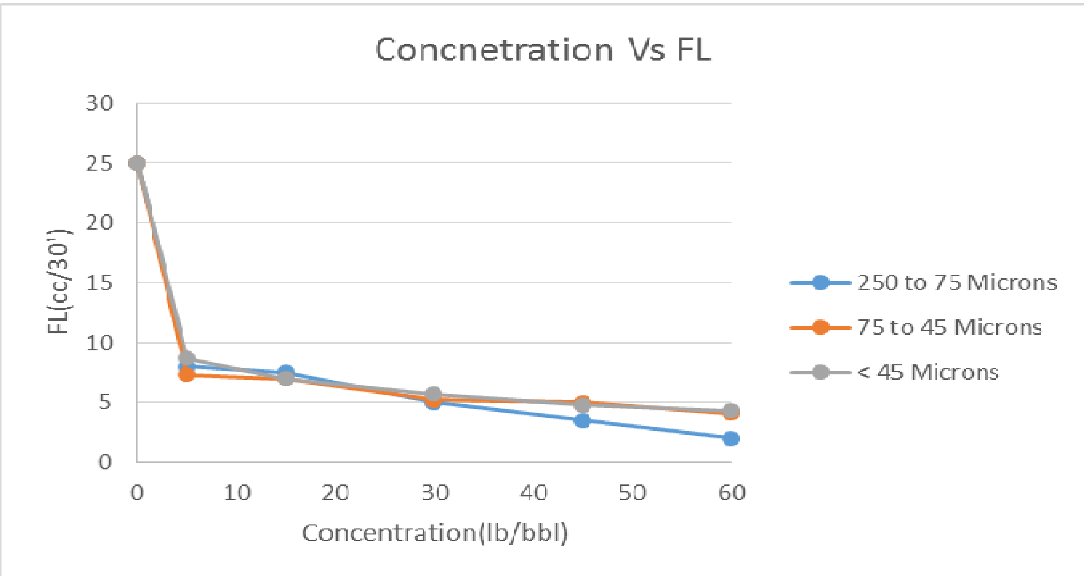

Figure 72 Effect of CaCO3 Concentration on FL for Different Particle Sizes

Figure 72 has two parts in each graph as seen , first part is the sharp decrease between 0lb/bbl and 5lb/bbl and the second part is the slight decrease between 5lb/bbl and other concentrations

CHAPTER 6

CONCLUSIONS

During this study, performance of $CaCO_3$ is tested as a bridging material for DIFs in polymer base mud. Different sizes and concentrations of $CaCO_3$ are tested for several tests. The experiments were carried out in GEOS Central Laboratory. The results are analyzed and the following conclusions can be drawn:

- Drill-in fluids tested here exhibit the yield-pseudo plastic behavior which is characterized non-linear relationship between the shear stress and the shear rate above the low shear rate yield point (τ_y).

- The Herschel Buckley Model accurately describes the yield-pseudo plastic rheology of the DIFs in a range of shear rate from 5.11 to 1022 sec^{-1}compared to the Bingham plastic and power law models.

- Plastic viscosity (PV) of DIFs increases proportionally with concentration for all sizes of $CaCO_3$ due to increasing mechanical friction between solid particles as a function $CaCO_3$ concentration.

- The Bingham plastic yield point (YP) gives consistent decrease with addition of small amount of $CaCO_3$ but after 5 lb/bbl it does not show sensitivity to concentration of $CaCO_3$ for any size. This behavior becomes more pronounced for $CaCO_3$ sizes greater than 75μ.
- Flow behavior index in annulus (n_a) shows a decreasing tendency as the concentration of $CaCO_3$ increases for all sizes making the fluid more shear thinning.

- Consistency index in annulus (K_a) increases with increasing concentration of $CaCO_3$ in consistent with the plastic viscosity due increasing mechanical friction between solid particles as a function $CaCO_3$ concentration in DIFs.

- Flow behavior index in pipe flow (n_p) increases as the concentration of $CaCO_3$ increases making the fluid more Newtonian at high shear rates.

- Consistency index in pipe flow (K_p) decreases with the increasing $CaCO_3$ concentration.

- The low-shear-rate yield point (τ_y) of DIF increases with increasing $CaCO_3$ concentration for all $CaCO_3$ sizes.

- Dependency of the low-shear-rate yield point on $CaCO_3$ concentration disappears at 30 lb/bbl and becomes nearly constant at higher concentrations the $CaCO_3$ sizes less than 75μ.

- The Herschel-Bulkley flow behavior index (m) generally increases as the concentration of $CaCO_3$ increases. For $CaCO_3$ sizes less than 75μ "n" does not further change with $CaCO_3$ concentration above 30 lbb/bbl.

- The Herschel-Bulkley consistency index (k) decreases with the concentration of $CaCO_3$.

- Fluids without $CaCO_3$ concentration increases, the fluid loss of DIFs decreases.
- Spurt loss occurs due to the lack of bridging materials when no $CaCO_3$ is added. Therefore addition of small amount of $CaCO_3$ leads to significant reduction in fluid loss contributing to the formation of filter cake.

CHAPTER 7

RECOMMENDATIONS

This study is a well experimented stage to see the effect of particle size and concentration of $CaCO_3$ used in DIF's and the relationship between the size and concentration of $CaCO_3$ in other properties of DIF like fluid Loss. Although all of the experiments run and results obtained with this study, further studies are highly recommended for better understanding the effect of size and concentration of $CaCO_3$.

- Different sizes of $CaCO_3$ like nano-particle sized $CaCO_3$ can be used to see the different effects on DIF.

- Different microfiber celluloses and viscosity agents can be used to see the new rheological parameters to compare the effects of polymers.

- Different types of fluids, like synthetic drilling fluids, can be tested.

- Tests should be run in different temperatures and pressure differentials to compare the temperature and pressure effects.

REFERENCES

Abdou, M.I. and El-Sayed Ahmed H. (2011). "Effect of Particle Size of Bentonite on "Rheological Behavior of the Drilling Mud" *Petroleum Science and Technology*, 29:2220–2233.

Abrams, A. (1977). "Mud Design to Minimize Rock Impairment due to Particle Invasion," *Journal Petroleum Technology.*

Adachi, J., Bailey, L., Houwen, O.H., Meeten, G.H. and Way, P.W., Schlemmer, R.P. (2004). *Depleted Zone Drilling: Reducing Mud Losses Into Fractures, IADC/SPE 87224*. IADC/SPE Drilling Conference, Dallas, Texas, U.S.A.

American Petroleum Institute. (1997). "*Recommended Practice Standard Procedure for Field Testing Water-based Drilling Fluids*," 2nd Ed.

ASTM E175-82 .(1995). "Standard Terminology of Microscopy," *American Society for Testing and Materials*, West Conshohocken, PA.

Baker Huges Drilling Fluids Manual (1998). *Baker Fluid Facts.*

Bourgoyne Jr, A., Millheim, K., Chenevert, M. and Young Jr, F. (2003). Applied Drilling Engineering, *SPE Textbook Series*, Vol. 2, SPE, Richardson, Texas.

Bugbee, J. M. (1953). *Lost Circulation-A Major Problem in Exploration and Development.* Southwestern District, Division of Production, Forth Worth, Texas.

Cargnel, R.D. and Luzardo, J.P. (1999). *Particle Size Distribution Selection of*

$CaCO_3$ in Drill-In Fluids: Theory and Applications, SPE 53937. SPE Latin American and Caribbean Petroleum Engineering Conference, Caracas, Venezuela.

Chowdhury,D., Skalle, P., Rahman, M.M. (2009). *Prediction of Stand Pipe Pressure using Conveintional Approach*.

Dick, M.A., Heinz, T.J., Svoboda, C.F., Aston, M. (2000, 23-24 February). *Optimizing the Selection of Bridging Particles for Reservoir Drilling Fluids*, *SPE 58793.* 2000 SPE International Sypmposium on Formation Damage, Lafayette, Louisiana.

Fann Instrument Company. (2015). *Model 35 Viscometer Instruction Manual.*

GEOS Drilling Fluids Inc. (2015). *Product Data Sheet, GeoCarb*.

Gücüyener, I.H. (2010). *Drilling Hydraulics*, lecture notes at METU.

Gücüyener, I.H. (2010). *Drilling Fluids Engineering,* lecture notes at METU.

Gueven, N., Hemphill, D. J., and Carney, L. L. (1988). *Comparative Rheology of Water-Base Drilling Fluids with Various Clays*. Richardson, TX: Society of Petroleum Engineers.

Gockel, J.F., Gockel C.E., and Brinemann, M. (1987, 15–18 March). *Lost Circulation: A Solution Based on the Problem, SPE/IADC 16082.* SPE/IADC Drilling Conference, New Orleans, L.A.

De Lloyd, D. (2000). Chemistry Department, the University of The West Indies, St. Augustine campus, The Republic of Trinidad and Tobago.

Rheology of Drilling Muds. (n.d.). Retrieved March, 2015 from http://rishibabuadari.tripod.com/MudRheology/Rheology.htm

Particle Size Conversion Table. (2015). In *Chemicals - Technical Library.* Retrieved

April, 2015from http://www.sigmaaldrich.com/chemistry/stockroomreagents/learning-center/technical-library/particle-size-conversion.html

Hand N., Kowbel K., Maikranz S., Nouris R. (1998, 13 July). Drill-in Fluid Reduces Formation Damage, Increases Production Rates. *Oil & Gas Journal.*

Islam A. (2008). *Drilling Fluid Rheology Note*, lecture note at IPT, NTNU, Trondheim.

Lapeyrouse N.J. (2002). *Formulas and Calculations for Drilling*, Production and Workover, Second Edition**.**

M-I Drilling Fluids. L.C. (1998). *Drilling Fluids Engineering Manual.*

Nayberg T. M. And Petty B. R. (1986, 10-12 February). *Laboratory Study of Lost Circulation Materials for Use in both Oil-Base and Water-Base Drilling Muds*. IDAC/SPE 14723.

Pilehvari; Nyshadham, V. R. (2002, 20-21 February). *Effect of Material Type and Size Distribution on Performance of Loss/Seepage Control Material*, *SPE 73791.* SPE International Symposium and Exhibition on Formation Damage Control Lafayette. Louisiana.

Schafer, D.M., Loeppke, G.E., Glowka, D.A. and Scott, D.D. (1992, February 18-21). *An Evaluation of Flowmeters for the Detection of Kicks and Lost Circulation During Drilling*. In Sandia National Laboratories, and Wright, E.K. Ktech Corp. IADC/SPE 1992 Drilling Conference, New Orleans, Louisianna.

Nidaş A.Ş. (2010). *Product Sheet*

OFITE Instruments. (2009). *OFITE API Filter Press Instruction Manual.*

OFITE Instruments. (2009). *OFITE Metal Mud Balance Instruction Manual.*

Rojas, J.C., Bern, P.A., Fitzgerald, B.L., Modi, S., Bezant, P.N. (1998, 3 -6 March). *Minimizing Down Hole Mud Losses IADC/SPE 39398.* 1888 IADC/SPE

Drilling Conference, Dallas, Texas,.

Rosato, M.J. and Supriono, A. (2002, April 9-10). *Use of a Crosslinked Polymer Fluid-Loss Control Agent to Aid Well Cleanouts SPE 74845.* SPE/ICOTA Coiled Tubing Conference, Houston, Texas.

Sharma, U., Suri, A., and Mukul, M. (2004). *Strategies for sizing particles in drilling and completion fluid.* SPE J. 9:13–23.

Fluid Loss. (2015). In *Schlumberger.* Retrieved February, 2015 from http://www.glossary.oilfield.slb.com/en/Terms/f/fluid_loss.aspx

Stephens, M. (1995). M-I Drilling Fluids L.L.C.

Sterling Multimixer Model #983 Instruction Manual. (2003).

Verret, R., Robinson, B., Cowan J., Fader, P., Looney, M. (2000, 23-24 February). *Use of Micronized Cellulose Fibers to Protect Producing Formations SPE 58794* SPE International Symposium on Formation Damage Control, Lafayette, Louisiana.

AZO Materials. (2015). Particle Size - US Sieve Series and Tyler Mesh Size Equivalents. In *Azo-Materials.* Retrieved January from http://www.azom.com/details.asp?AticleID=1417

APPENDIX A

Measured and Calculated Shear Stresses-Shear Rates Data for Bingham Plastic Model for Less Than 45 Micron Size

Table 4 5 lb/bbl Concentration Data

SR (1/s)	**SS (lb/100ft2)**	**SS_c (lb/100ft^2)**	**γ(1/s)**	**τ_m (lb/100ft^2)**	**τ_c (lb/100ft^2)**	**%Error**
1022,22	38,38	23,64	1022,22	38,38	23,64	38,41
511,11	29,85	16,62	511,11	29,85	16,62	44,33
340,66	24,52	14,27	340,66	24,52	14,27	41,78
170,33	20,25	11,93	170,33	20,25	11,93	41,08
10,22	11,73	9,73	10,22	11,73	9,73	16,98
5,11	10,66	9,66	5,11	10,66	9,66	9,34
Less Than 45 Micron Size/ 5lb/bbl Concentration		**YP(lb/100ft2)**	**PV(lbsec/100ft2)**	**PV(cp)**	**AVERAGE**	**STDDEV**
		9,59	0,01	7,02	31,99	**14,90**

Table 5 15 lb/bbl Concentration Data

SR (1/s)	**SS (lb/100ft2)**	**SS_c (lb/100ft^2)**	**γ(1/s)**	**τ_m (lb/100ft^2)**	**τ_c (lb/100ft^2)**	**%Error**
1022,22	39,44	26,24	1022,22	39,44	26,24	33,46
511,11	29,85	18,45	511,11	29,85	18,45	38,18
340,66	25,58	15,85	340,66	25,58	15,85	38,03
170,33	21,32	13,26	170,33	21,32	13,26	37,82
10,22	12,79	10,82	10,22	12,79	10,82	15,45
5,11	11,73	10,74	5,11	11,73	10,74	8,43
Less Than 45 Micron Size/ 15lb/bbl Concentration		**YP(lb/100ft2)**	**PV(lbsec/100ft2)**	**PV(cp)**	**AVERAGE**	**STDDEV**
		10,66	0,02	7,79	28,56	**13,19**

Table 6 30 lb/bbl Concentration Data

SR (1/s)	**SS (lb/100ft2)**	**SS_c (lb/100ft^2)**	**γ(1/s)**	**τ_m (lb/100ft^2)**	**τ_c (lb/100ft^2)**	**%Error**
1022,22	40,51	28,79	1022,22	40,51	28,79	28,93
511,11	29,85	20,26	511,11	29,85	20,26	32,13
340,66	26,65	17,41	340,66	26,65	17,41	34,66
170,33	22,39	14,57	170,33	22,39	14,57	34,92
10,22	13,86	11,90	10,22	13,86	11,90	14,15
5,11	12,79	11,81	5,11	12,79	11,81	7,67
Less Than 45 Micron Size/ 30lb/bbl Concentration		**YP(lb/100ft2)**	**PV(lbsec/100ft2)**	**PV(cp)**	**AVERAGE**	**STDDEV**
		11,73	0,02	8,53	25,41	**11,62**

Table 7 45 lb/bbl Concentration Data

SR (1/s)	SS (lb/100ft2)	SS_c (lb/100ft^2)	γ(1/s)	τ_m (lb/100ft^2)	τ_c (lb/100ft^2)	%Error
1022,22	41,57	28,81	1022,22	41,57	28,81	30,70
511,11	29,85	20,27	511,11	29,85	20,27	32,10
340,66	26,65	17,42	340,66	26,65	17,42	34,64
170,33	22,39	14,57	170,33	22,39	14,57	34,90
10,22	13,86	11,90	10,22	13,86	11,90	14,15
5,11	12,79	11,81	5,11	12,79	11,81	7,67
Less Than 45 Micron Size/ 45lb/bbl Concentration		**YP(lb/100ft2)**	**PV(lbsec/100ft2)**	**PV(cp)**	**AVERAGE**	**STDDEV**
		11,73	0,02	8,54	25,69	**11,74**

Table 8 60 lb/bbl Concentration Data

SR (1/s)	SS (lb/100ft2)	SS_c (lb/100ft^2)	γ(1/s)	τ_m (lb/100ft^2)	τ_c (lb/100ft^2)	%Error
1022,22	42,64	28,85	1022,22	42,64	28,85	32,34
511,11	30,91	20,29	511,11	30,91	20,29	34,37
340,66	26,65	17,43	340,66	26,65	17,43	34,59
170,33	22,39	14,58	170,33	22,39	14,58	34,87
10,22	13,86	11,90	10,22	13,86	11,90	14,15
5,11	12,79	11,81	5,11	12,79	11,81	7,66
Less Than 45 Micron Size/ 60lb/bbl Concentration		**YP(lb/100ft2)**	**PV(lbsec/100ft2)**	**PV(cp)**	**AVERAGE**	**STDDEV**
		11,73	0,02	8,56	26,33	**12,16**

APPENDIX B

Measured and Calculated Shear Stresses-Shear Rates Data for Power Law Model for Less Than 45 Micron Size

Table 9 5 lb/bbl Concentration Data

SR (1/s)	**SS (lb/100ft2)**	**SS_c (lb/100ft^2)**	**γ(1/s)**	**τ_m (lb/100ft^2)**	**τ_c (lb/100ft^2)**	**%Error**
1022,22	38,38	28,78	1022,22	38,38	28,78	25,01
511,11	29,85	20,26	511,11	29,85	20,26	32,14
340,66	24,52	16,49	340,66	24,52	16,49	32,73
170,33	20,25	11,61	170,33	20,25	11,61	42,69
10,22	11,73	2,79	10,22	11,73	2,79	76,20
5,11	10,66	1,96	5,11	10,66	1,96	81,57
Less Than 45 Micron Size/ 5 lb/bbl Concentration		**YP(lb/100ft2)**	**PV(lbsec/100ft2)**	**PV(cp)**	**AVERAGE**	**STDDEV**
		4,7523	0,0259	13,2349	**48,38969513**	**24,34467402**

Table 10 15 lb/bbl Concentration Data

SR (1/s)	**SS (lb/100ft2)**	**SS_c (lb/100ft^2)**	**γ(1/s)**	**τ_m (lb/100ft^2)**	**τ_c (lb/100ft^2)**	**%Error**
1022,22	39,44	26,24	1022,22	39,44	26,24	33,46
511,11	29,85	18,45	511,11	29,85	18,45	38,18
340,66	25,58	15,85	340,66	25,58	15,85	38,03
170,33	21,32	13,26	170,33	21,32	13,26	37,82
10,22	12,79	10,82	10,22	12,79	10,82	15,45
5,11	11,73	10,74	5,11	11,73	10,74	8,43
Less Than 45 Micron Size/ 15 lb/bbl Concentration		**YP(lb/100ft2)**	**PV(lbsec/100ft2)**	**PV(cp)**	**AVERAGE**	**STDDEV**
		3,57	0,03	13,64	**28,56**	**13,19**

Table 11 30 lb/bbl Concentration Data

SR (1/s)	**SS (lb/100ft2)**	**SS_c (lb/100ft^2)**	**γ(1/s)**	**τ_m (lb/100ft^2)**	**τ_c (lb/100ft^2)**	**%Error**
1022,22	40,51	28,78	1022,22	40,51	28,78	28,96
511,11	29,85	18,12	511,11	29,85	18,12	39,28
340,66	26,65	13,83	340,66	26,65	13,83	48,11
170,33	22,39	8,71	170,33	22,39	8,71	61,10
10,22	13,86	1,33	10,22	13,86	1,33	90,38
5,11	12,79	0,84	5,11	12,79	0,84	93,44
Less Than 45 Micron Size/ 30 lb/bbl Concentration		**YP(lb/100ft2)**	**PV(lbsec/100ft2)**	**PV(cp)**	**AVERAGE**	**STDSAP**
		2,57	0,03	13,95	**60,21**	**26,74**

Table 12 45 lb/bbl Concentration Data

SR (1/s)	SS (lb/100ft2)	SS_c (lb/100ft^2)	γ(1/s)	τ_m (lb/100ft^2)	τ_c (lb/100ft^2)	%Error
1022,22	41,57	29,84	1022,22	41,57	29,84	28,21
511,11	29,85	18,12	511,11	29,85	18,12	39,28
340,66	26,65	13,54	340,66	26,65	13,54	49,21
170,33	22,39	8,22	170,33	22,39	8,22	63,28
10,22	13,86	1,09	10,22	13,86	1,09	92,16
5,11	12,79	0,66	5,11	12,79	0,66	94,84
Less Than 45 Micron Size/ 45 lb/bbl Concentration		**YP(lb/100ft2)**	**PV(lbsec/100ft2)**	**PV(cp)**	**AVERAGE**	**STDDEV**
		2,11	0,03	14,61	**61,16**	**27,60**

Table 13 60 lb/bbl Concentration Data

SR (1/s)	SS (lb/100ft2)	SS_c (lb/100ft^2)	γ(1/s)	τ_m (lb/100ft^2)	τ_c (lb/100ft^2)	%Error
1022,22	42,64	30,91	1022,22	42,64	30,91	27,51
511,11	30,91	19,19	511,11	30,91	19,19	37,92
340,66	26,65	14,52	340,66	26,65	14,52	45,52
170,33	22,39	9,01	170,33	22,39	9,01	59,73
10,22	13,86	1,30	10,22	13,86	1,30	90,60
5,11	12,79	0,81	5,11	12,79	0,81	93,68
Less Than 45 Micron Size/ 60 lb/bbl Concentration		**YP(lb/100ft2)**	**PV(lbsec/100ft2)**	**PV(cp)**	**AVERAGE**	**STDDEV**
		2,52	0,03	15,02	**59,16**	**27,64**

APPENDIX C

Measured and Calculated Shear Stresses-Shear Rates Data for Yield Power Law Model for Less Than 45 Micron Size

Table 14 5 lb/bbl Concentration Data

SR (1/s)	SS (lb/100ft2)	SS_c (lb/100ft^2)	γ(1/s)	τ_m (lb/100ft^2)	τ_c (lb/100ft^2)	%Error
1022,22	38,38	38,37	1022,22	38,38	38,37	0,01
511,11	29,85	29,85	511,11	29,85	29,85	0,01
340,66	24,52	26,09	340,66	24,52	26,09	6,40
170,33	20,25	21,20	170,33	20,25	21,20	4,68
10,22	11,73	12,38	10,22	11,73	12,38	5,62
5,11	10,66	11,56	5,11	10,66	11,56	8,43
Less Than 45 Micron Size/ 5 lb/bbl Concentration		**YP(lb/100ft2)**	**PV(lbsec/100ft2)**	**PV(cp)**	**AVERAGE**	**STDDEV**
		14,34	0,025	13,24	4,19	**3,46**

Table 15 15 lb/bbl Concentration Data

SR (1/s)	SS (lb/100ft2)	SS_c (lb/100ft^2)	γ(1/s)	τ_m (lb/100ft^2)	τ_c (lb/100ft^2)	%Error
1022,22	39,44	39,44	1022,22	39,44	38,37	2,71
511,11	29,85	29,85	511,11	29,85	29,85	0,01
340,66	25,58	25,80	340,66	25,58	26,09	1,96
170,33	21,32	20,75	170,33	21,32	21,20	0,55
10,22	12,79	12,61	10,22	12,79	12,38	3,18
5,11	11,73	11,96	5,11	11,73	11,56	1,43
Less Than 45 Micron Size/ 15 lb/bbl Concentration		**YP(lb/100ft2)**	**PV(lbsec/100ft2)**	**PV(cp)**	**AVERAGE**	**STDDEV**
		14,23	0,03	13,64	1,64	**1,23**

Table 16 30 lb/bbl Concentration Data

SR (1/s)	SS (lb/100ft2)	SS_c (lb/100ft^2)	γ(1/s)	τ_m (lb/100ft^2)	τ_c (lb/100ft^2)	%Error
1022,22	40,51	40,50	1022,22	40,51	40,50	0,01
511,11	29,85	29,85	511,11	29,85	29,85	0,01
340,66	26,65	25,55	340,66	26,65	25,55	4,11
170,33	22,39	20,43	170,33	22,39	20,43	8,72
10,22	13,86	13,06	10,22	13,86	13,06	5,76
5,11	12,79	12,57	5,11	12,79	12,57	1,77
Less Than 45 Micron Size/ 30 lb/bbl Concentration		**YP(lb/100ft2)**	**PV(lbsec/100ft2)**	**PV(cp)**	**AVERAGE**	**STDDEV**
		14,29	0,03	13,95	3,40	**3,47**

Table 17 45 lb/bbl Concentration Data

SR (1/s)	SS (lb/100ft2)	SS_c (lb/100ft^2)	γ(1/s)	τ_m (lb/100ft^2)	τ_c (lb/100ft^2)	%Error
1022,22	41,57	41,57	1022,22	41,57	41,57	0,01
511,11	29,85	29,85	511,11	29,85	29,85	0,01
340,66	26,65	25,26	340,66	26,65	25,26	5,21
170,33	22,39	19,95	170,33	22,39	19,95	10,90
10,22	13,86	12,81	10,22	13,86	12,81	7,55
5,11	12,79	12,39	5,11	12,79	12,39	3,18
Less Than 45 Micron Size/ 45 lb/bbl Concentration		**YP(lb/100ft2)**	**PV(lbsec/100ft2)**	**PV(cp)**	**AVERAGE**	**STDDEV**
		14,29	0,03	13,95	4,47	**4,31**

Table 18 60 lb/bbl Concentration Data

SR (1/s)	SS (lb/100ft2)	SS_c (lb/100ft^2)	γ(1/s)	τ_m (lb/100ft^2)	τ_c (lb/100ft^2)	%Error
1022,22	42,64	42,64	1022,22	42,64	42,64	0,01
511,11	30,91	30,92	511,11	30,91	30,92	0,01
340,66	26,65	26,24	340,66	26,65	26,24	1,52
170,33	22,39	20,74	170,33	22,39	20,74	7,35
10,22	13,86	13,03	10,22	13,86	13,03	5,99
5,11	12,79	12,53	5,11	12,79	12,53	2,01
Less Than 45 Micron Size/ 60 lb/bbl Concentration		**YP(lb/100ft2)**	**PV(lbsec/100ft2)**	**PV(cp)**	**AVERAGE**	**STDDEV**
		14,25	0,03	15,02	2,81	**3,12**

APPENDIX D

Measured and Calculated Shear Stresses-Shear Rates Data for Bingham Plastic Model for 75 to 45 Micron Size

Table 19 5 lb/bbl Concentration Data

SR (1/s)	**SS (lb/100ft2)**	**SS$_c$ (lb/100ft^2)**	**□□□□□γ(1/s)**	**τ_m (lb/100ft^2)**	**τ_c (lb/100ft^2)**	**%Error**
1022,22	38,376	23,52	1022,22	38,38	23,52	38,72
511,11	28,782	16,56	511,11	28,78	16,56	42,48
340,66	23,452	14,23	340,66	23,45	14,23	39,31
170,33	20,254	11,91	170,33	20,25	11,91	41,18
10,22	11,726	9,73	10,22	11,73	9,73	16,99
5,11	10,66	9,66	5,11	10,66	9,66	9,35
75 to 45 Micron Size/		**YP(lb/100Fft2)**	**PV(lbsec/100ft2)**	**PV(cp)**	**AVERAGE**	**STDDEV**
5 lb/bbl Concentration		9,59	0,014	6,95	31,34	14,34

Table 20 15 lb/bbl Concentration Data

SR (1/s)	**SS (lb/100ft2)**	**SS$_c$ (lb/100ft^2)**	**γ(1/s)**	**τ_m (lb/100ft^2)**	**τ_c (lb/100ft^2)**	**%Error**
1022,22	40,51	23,24	1022,22	40,51	23,24	42,64
511,11	29,85	16,42	511,11	29,85	16,42	45,00
340,66	25,58	14,14	340,66	25,58	14,14	44,73
170,33	21,32	11,87	170,33	21,32	11,87	44,34
10,22	11,73	9,73	10,22	11,73	9,73	17,02
5,11	10,66	9,66	5,11	10,66	9,66	9,36
75 to 45 Micron Size/		**YP(lb/100Fft2)**	**PV(lbsec/100ft2)**	**PV(cp)**	**AVERAGE**	**STDDEV**
15 lb/bbl Concentration		9,594	0,013	6,796	33,847	16,205

Table 21 30 lb/bbl Concentration Data

SR (1/s)	**SS (lb/100ft2)**	**SS$_c$ (lb/100ft^2)**	**γ(1/s)**	**τ_m (lb/100ft^2)**	**τ_c (lb/100ft^2)**	**%Error**
1022,22	41,57	26,01	1022,22	41,57	26,01	37,43
511,11	29,85	18,34	511,11	29,85	18,34	38,57
340,66	26,65	15,78	340,66	26,65	15,78	40,80
170,33	21,32	13,22	170,33	21,32	13,22	38,00
10,22	12,79	10,81	10,22	12,79	10,81	15,47
5,11	11,73	10,74	5,11	11,73	10,74	8,44
75 to 45 Micron Size/		**YP(lb/100Fft2)**	**PV(lbsec/100ft2)**	**PV(cp)**	**AVERAGE**	**STDDEV**
30 lb/bbl Concentration		10,660	0,015	7,665	29,783	14,037

Table 22 45 lb/bbl Concentration Data

SR (1/s)	SS (lb/100ft2)	SS_c (lb/100ft^2)	γ(1/s)	τ_m (lb/100ft^2)	τ_c (lb/100ft^2)	%Error
1022,22	42,64	25,91	1022,22	42,64	25,91	39,25
511,11	29,85	18,28	511,11	29,85	18,28	38,75
340,66	26,65	15,74	340,66	26,65	15,74	40,94
170,33	21,32	13,20	170,33	21,32	13,20	38,08
10,22	12,79	10,81	10,22	12,79	10,81	15,48
5,11	11,73	10,74	5,11	11,73	10,74	8,44
75 to 45 Micron Size/ 45 lb/bbl Concentration		**YP(lb/100Fft2)**	**PV(lbsec/100ft2)**	**PV(cp)**	**AVERAGE**	**STDDEV**
		10,660	0,015	7,614	30,155	14,301

Table 23 60 lb/bbl Concentration Data

SR (1/s)	SS (lb/100ft2)	SS_c (lb/100ft^2)	γ(1/s)	τ_m (lb/100ft^2)	τ_c (lb/100ft^2)	%Error
1022,22	43,71	25,74	1022,22	43,71	25,74	41,10
511,11	30,91	18,20	511,11	30,91	18,20	41,12
340,66	27,72	15,69	340,66	27,72	15,69	43,40
170,33	22,39	13,17	170,33	22,39	13,17	41,15
10,22	12,79	10,81	10,22	12,79	10,81	15,49
5,11	11,73	10,74	5,11	11,73	10,74	8,45
75 to 45 Micron Size/ 60 lb/bbl Concentration		**YP(lb/100Fft2)**	**PV(lbsec/100ft2)**	**PV(cp)**	**AVERAGE**	**STDDEV**
		10,660	0,015	7,563	31,785	15,536

APPENDIX E

Measured and Calculated Shear Stresses-Shear Rates Data for Power Law Model for 75 to 45 Micron Size

Table 24 5 lb/bbl Concentration Data

SR (1/s)	SS (lb/100ft2)	SS_c (lb/100ft^2)	γ(1/s)	τ_m (lb/100ft^2)	τ_c (lb/100ft^2)	%Error
1022,22	38,38	28,78	1022,22	38,38	28,78	25,01
511,11	28,78	19,19	511,11	28,78	19,19	33,32
340,66	23,45	15,14	340,66	23,45	15,14	35,45
170,33	20,25	10,09	170,33	20,25	10,09	50,16
10,22	11,73	1,95	10,22	11,73	1,95	83,38
5,11	10,66	1,30	5,11	10,66	1,30	87,81
75 to 45 Micron Size/ 5 lb/bbl Concentration		YP(lb/100Fft2)	PV(lbsec/100ft2)	PV(cp)	AVERAGE	STDDEV
		3,571	0,027	13,644	52,522	26,907

Table 25 15 lb/bbl Concentration Data

SR (1/s)	SS (lb/100ft2)	SS_c (lb/100ft^2)	γ(1/s)	τ_m (lb/100ft^2)	τ_c (lb/100ft^2)	%Error
1022,22	40,51	30,91	1022,22	40,51	30,91	23,69
511,11	29,85	20,26	511,11	29,85	20,26	32,13
340,66	25,58	15,82	340,66	25,58	15,82	38,17
170,33	21,32	10,37	170,33	21,32	10,37	51,38
10,22	11,73	1,86	10,22	11,73	1,86	84,10
5,11	10,66	1,22	5,11	10,66	1,22	88,54
75 to 45 Micron Size/ 15 lb/bbl Concentration		YP(lb/100Fft2)	PV(lbsec/100ft2)	PV(cp)	AVERAGE	STDDEV
		3,483	0,029	14,768	53,002	27,373

Table 26 30 lb/bbl Concentration Data

SR (1/s)	SS (lb/100ft2)	SScalculated	γ(1/s)	τ_m (lb/100ft^2)	τ_c (lb/100ft^2)	%Error
1022,22	41,57	30,91	1022,22	41,57	30,91	25,65060259
511,11	29,85	19,19	511,11	29,85	19,19	35,70476996
340,66	26,65	14,52	340,66	26,65	14,52	45,52009656
170,33	21,32	9,01	170,33	21,32	9,01	57,71940717
10,22	12,79	1,30	10,22	12,79	1,30	89,81916823
5,11	11,73	0,81	5,11	11,73	0,81	93,10448754
75 to 45 Micron Size/ 30 lb/bbl Concentration		YP(lb/100Fft2)	PV(lbsec/100ft2)	PV(cp)	AV	STDSAP
		2,5228	0,0294	15,0234	50,8828089	24,7920095

Table 27 45 lb/bbl Concentration Data

SR (1/s)	SS (lb/100ft2)	SS_c (lb/100ft^2)	γ(1/s)	τ_m (lb/100ft^2)	τ_c (lb/100ft^2)	%Error
1022,22	42,64	31,98	1022,22	42,64	31,98	25,01
511,11	29,85	19,19	511,11	29,85	19,19	35,70
340,66	26,65	14,23	340,66	26,65	14,23	46,59
170,33	21,32	8,54	170,33	21,32	8,54	59,93
10,22	12,79	1,08	10,22	12,79	1,08	91,59
5,11	11,73	0,65	5,11	11,73	0,65	94,49
75 to 45 Micron Size/ 45 lb/bbl Concentration		**YP(lb/100Fft2)**	**PV(lbsec/100ft2)**	**PV(cp)**	**AVERAGE**	**STDDEV**
		2,078	0,031	15,688	58,887	28,896

Table 28 60 lb/bbl Concentration Data

SR (1/s)	SS (lb/100ft2)	SS_c (lb/100ft^2)	γ(1/s)	τ_m (lb/100ft^2)	τ_c (lb/100ft^2)	%Error
1022,22	43,71	33,04	1022,22	43,71	33,04	24,40
511,11	30,91	20,26	511,11	30,91	20,26	34,47
340,66	27,72	15,21	340,66	27,72	15,21	45,11
170,33	22,39	9,33	170,33	22,39	9,33	58,34
10,22	12,79	1,28	10,22	12,79	1,28	89,99
5,11	11,73	0,78	5,11	11,73	0,78	93,31
75 to 45 Micron Size/ 60 lb/bbl Concentration		**YP(lb/100Fft2)**	**PV(lbsec/100ft2)**	**PV(cp)**	**AVERAGE**	**STDDEV**
		2,485	0,032	16,148	57,603	28,698

APPENDIX F

Measured and Calculated Shear Stresses-Shear Rates Data for Yield Power Law Model for 75 to 45 Micron Size

Table 29 5 lb/bbl Concentration Data

SR (1/s)	SS (lb/100ft2)	SS_c (lb/100ft^2)	γ(1/s)	τ_m (lb/100ft^2)	τ_c (lb/100ft^2)	%Error
1022,22	38,38	38,37	1022,22	38,38	38,37	0,01
511,11	28,78	28,78	511,11	28,78	28,78	0,01
340,66	23,45	24,73	340,66	23,45	24,73	5,46
170,33	20,25	19,69	170,33	20,25	19,69	2,79
10,22	11,73	11,54	10,22	11,73	11,54	1,56
5,11	10,66	10,89	5,11	10,66	10,89	2,19
75 to 45 Micron Size/ 5 lb/bbl Concentration		**YP(lb/100ft2)**	**PV(lbsec/100ft2)**	**PV(cp)**	**AVERAGE**	**STDDEV**
		13,165	0,027	13,644	2,003	2,037

Table 30 15 lb/bbl Concentration Data

SR (1/s)	SS (lb/100ft2)	SS_c (lb/100ft^2)	γ(1/s)	τ_m (lb/100ft^2)	τ_c (lb/100ft^2)	%Error
1022,22	40,51	40,50	1022,22	40,51	40,50	0,01
511,11	29,85	29,85	511,11	29,85	29,85	0,01
340,66	25,58	25,41	340,66	25,58	25,41	0,67
170,33	21,32	19,96	170,33	21,32	19,96	6,38
10,22	11,73	11,46	10,22	11,73	11,46	2,28
5,11	10,66	10,82	5,11	10,66	10,82	1,46
75 to 45 Micron Size/ 15 lb/bbl Concentration		**YP(lb/100ft2)**	**PV(lbsec/100ft2)**	**PV(cp)**	**AVERAGE**	**STDDEV**
		13,077	0,029	14,768	1,802	2,408

Table 31 30 lb/bbl Concentration Data

SR (1/s)	SS (lb/100ft2)	SS_c (lb/100ft^2)	γ(1/s)	τ_m (lb/100ft^2)	τ_c (lb/100ft^2)	%Error
1022,22	41,57	41,57	1022,22	41,57	41,57	0,01
511,11	29,85	29,85	511,11	29,85	29,85	0,01
340,66	26,65	25,18	340,66	26,65	25,18	5,52
170,33	21,32	19,67	170,33	21,32	19,67	7,72
10,22	12,79	11,96	10,22	12,79	11,96	6,49
5,11	11,73	11,47	5,11	11,73	11,47	2,20
75 to 45 Micron Size/ 30 lb/bbl Concentration		**YP(lb/100ft2)**	**PV(lbsec/100ft2)**	**PV(cp)**	**AVERAGE**	**STDDEV**
		13,183	0,029	15,023	3,657	3,368

Table 32 45 lb/bbl Concentration Data

SR (1/s)	SS (lb/100ft2)	SS_c (lb/100ft^2)	γ(1/s)	τ_m (lb/100ft^2)	τ_c (lb/100ft^2)	%Error
1022,22	42,64	42,64	1022,22	42,64	42,64	0,01
511,11	29,85	29,85	511,11	29,85	29,85	0,01
340,66	26,65	24,89	340,66	26,65	24,89	6,59
170,33	21,32	19,20	170,33	21,32	19,20	9,93
10,22	12,79	11,74	10,22	12,79	11,74	8,26
5,11	11,73	11,31	5,11	11,73	11,31	3,59
75 to 45 Micron Size/ 45 lb/bbl Concentration		**YP(lb/100ft2)**	**PV(lbsec/100ft2)**	**PV(cp)**	**AVERAGE**	**STDDEV**
		12,738	0,031	15,688	4,731	4,214

Table 33 60 lb/bbl Concentration Data

SR (1/s)	SS (lb/100ft2)	SS_c (lb/100ft^2)	γ(1/s)	τ_m (lb/100ft^2)	τ_c (lb/100ft^2)	%Error
1022,22	43,71	43,70	1022,22	43,71	43,70	0,01
511,11	30,91	30,92	511,11	30,91	30,92	0,01
340,66	27,72	25,87	340,66	27,72	25,87	6,65
170,33	22,39	19,99	170,33	22,39	19,99	10,72
10,22	12,79	11,94	10,22	12,79	11,94	6,66
5,11	11,73	11,44	5,11	11,73	11,44	2,40
75 to 45 Micron Size/ 60 lb/bbl Concentration		**YP(lb/100ft2)**	**PV(lbsec/100ft2)**	**PV(cp)**	**AVERAGE**	**STDDEV**
		13,145	0,032	16,148	4,407	4,304

APPENDIX G

Measured and Calculated Shear Stresses-Shear Rates Data for Bingham Plastic Model for 250 to 75 Micron Size

Table 34 5 lb/bbl Concentration Data

SR (1/s)	SS (lb/100ft2)	SS_c (lb/100ft^2)	γ(1/s)	τ_m (lb/100ft^2)	τ_c (lb/100ft^2)	%Error
1022,22	39,44	23,38	1022,22	39,44	23,38	40,71
511,11	28,78	16,49	511,11	28,78	16,49	42,71
340,66	24,52	14,19	340,66	24,52	14,19	42,12
170,33	20,25	11,89	170,33	20,25	11,89	41,29
10,22	11,73	9,73	10,22	11,73	9,73	17,01
5,11	10,66	9,66	5,11	10,66	9,66	9,35
250 to 75 Micron Size/ 5 lb/bbl Concentration		**YP(lb/100ft2)**	**PV(lbsec/100ft2)**	**PV(cp)**	**AVERAGE**	**STDDEV**
		9,594	0,014	6,899	32,198	14,945

Table 35 15 lb/bbl Concentration Data

SR (1/s)	SS (lb/100ft2)	SS_c (lb/100ft^2)	γ(1/s)	τ_m (lb/100ft^2)	τ_c (lb/100ft^2)	%Error
1022,22	41,57	24,98	1022,22	41,57	24,98	39,91
511,11	29,85	17,29	511,11	29,85	17,29	42,08
340,66	25,58	14,72	340,66	25,58	14,72	42,45
170,33	21,32	12,16	170,33	21,32	12,16	42,97
10,22	12,79	9,75	10,22	12,79	9,75	23,80
5,11	11,73	9,67	5,11	11,73	9,67	17,53
250 to 75 Micron Size/ 15 lb/bbl Concentration		**YP(lb/100ft2)**	**PV(lbsec/100ft2)**	**PV(cp)**	**AVERAGE**	**STDDEV**
		9,594	0,015	7,716	34,789	11,170

Table 36 30 lb/bbl Concentration Data

SR (1/s)	SS (lb/100ft2)	SS_c (lb/100ft^2)	γ(1/s)	τ_m (lb/100ft^2)	τ_c (lb/100ft^2)	%Error
1022,22	43,71	27,62	1022,22	43,71	27,62	36,80
511,11	30,91	19,14	511,11	30,91	19,14	38,08
340,66	27,72	16,31	340,66	27,72	16,31	41,14
170,33	22,39	13,49	170,33	22,39	13,49	39,75
10,22	13,86	10,83	10,22	13,86	10,83	21,85
5,11	12,79	10,74	5,11	12,79	10,74	16,00
250 to 75 Micron Size/ 30 lb/bbl Concentration		**YP(lb/100ft2)**	**PV(lbsec/100ft2)**	**PV(cp)**	**AVERAGE**	**STDDEV**
		10,660	0,017	8,483	32,272	10,603

Table 37 45 lb/bbl Concentration Data

SR (1/s)	SS (lb/100ft2)	SS_c (lb/100ft^2)	γ(1/s)	τ_m (lb/100ft^2)	τ_c (lb/100ft^2)	%Error
1022,22	49,04	28,66	1022,22	49,04	28,66	41,55
511,11	35,18	19,66	511,11	35,18	19,66	44,11
340,66	31,98	16,66	340,66	31,98	16,66	47,91
170,33	25,58	13,66	170,33	25,58	13,66	46,61
10,22	14,92	10,84	10,22	14,92	10,84	27,37
5,11	13,86	10,75	5,11	13,86	10,75	22,43
250 to 75 Micron Size/ 45 lb/bbl Concentration		**YP(lb/100ft2)**	**PV(lbsec/100ft2)**	**PV(cp)**	**AVERAGE**	**STDDEV**
		10,660	0,018	8,994	38,326	10,743

Table 38 60 lb/bbl Concentration Data

SR (1/s)	SS (lb/100ft2)	SS_c (lb/100ft^2)	γ(1/s)	τ_m (lb/100ft^2)	τ_c (lb/100ft^2)	%Error
1022,22	54,37	30,85	1022,22	54,37	30,85	43,25
511,11	39,44	21,29	511,11	39,44	21,29	46,03
340,66	35,18	18,10	340,66	35,18	18,10	48,55
170,33	28,78	14,91	170,33	28,78	14,91	48,19
10,22	15,99	11,92	10,22	15,99	11,92	25,47
5,11	14,92	11,82	5,11	14,92	11,82	20,79
250 to 75 Micron Size/ 60 lb/bbl Concentration		**YP(lb/100ft2)**	**PV(lbsec/100ft2)**	**PV(cp)**	**AVERAGE**	**STDDEV**
		11,726	0,019	9,556	38,713	12,307

APPENDIX H

Measured and Calculated Shear Stresses-Shear Rates Data for Power Law Model for 250 to 75 Micron Size

Table 39 15 lb/bbl Concentration Data

SR (1/s)	SS (lb/100ft2)	SS$_c$ (lb/100ft^2)	γ(1/s)	τ_m (lb/100ft^2)	τ_c (lb/100ft^2)	%Error
1022,22	39,44	30,91	1022,22	39,44	30,91	21,63
511,11	28,78	20,26	511,11	28,78	20,26	29,62
340,66	24,52	15,82	340,66	24,52	15,82	35,49
170,33	20,25	10,37	170,33	20,25	10,37	48,82
10,22	11,73	1,86	10,22	11,73	1,86	84,10
5,11	10,66	1,22	5,11	10,66	1,22	88,54
250 to 75 Micron Size/ 5 lb/bbl Concentration		**YP(lb/100ft2)**	**PV(lbsec/100ft2)**	**PV(cp)**	**AVERAGE**	**STDDEV**
		3,483	0,029	14,768	51,365	28,526

SR (1/s)	SS (lb/100ft2)	SS$_c$ (lb/100ft^2)	γ(1/s)	τ_m (lb/100ft^2)	τ_c (lb/100ft^2)	%Error
1022,22	41,57	33,04	1022,22	41,57	33,04	20,52
511,11	29,85	21,32	511,11	29,85	21,32	28,56
340,66	25,58	16,50	340,66	25,58	16,50	35,50
170,33	21,32	10,65	170,33	21,32	10,65	50,05
10,22	12,79	1,80	10,22	12,79	1,80	85,93
5,11	11,73	1,16	5,11	11,73	1,16	90,10
250 to 75 Micron Size/ 15 lb/bbl Concentration		**YP(lb/100ft2)**	**PV(lbsec/100ft2)**	**PV(cp)**	**AVERAGE**	**STDDEV**
		3,410	0,031	15,892	51,778	29,727

SR (1/s)	SS (lb/100ft2)	SS$_c$ (lb/100ft^2)	γ(1/s)	τ_m (lb/100ft^2)	τ_c (lb/100ft^2)	%Error
1022,22	43,71	34,11	1022,22	43,71	34,11	21,96
511,11	30,91	21,32	511,11	30,91	21,32	31,02
340,66	27,72	16,20	340,66	27,72	16,20	41,56
170,33	22,39	10,13	170,33	22,39	10,13	54,77
10,22	13,86	1,50	10,22	13,86	1,50	89,14
5,11	12,79	0,94	5,11	12,79	0,94	92,65
250 to 75 Micron Size/ 30 lb/bbl Concentration		**YP(lb/100ft2)**	**PV(lbsec/100ft2)**	**PV(cp)**	**AVERAGE**	**STDDEV**
		2,908	0,032	16,556	55,183	29,765

SR (1/s)	SS (lb/100ft2)	SS_c (lb/100ft^2)	γ(1/s)	τ_m (lb/100ft^2)	τ_c (lb/100ft^2)	%Error
1022,220	49,036	36,239	1022,220	49,036	36,239	26,097
511,110	35,178	22,389	511,110	35,178	22,389	36,354
340,660	31,980	16,890	340,660	31,980	16,890	47,185
170,330	25,584	10,435	170,330	25,584	10,435	59,213
10,220	14,924	1,478	10,220	14,924	1,478	90,097
5,110	13,858	0,913	5,110	13,858	0,913	93,411
250 to 75 Micron Size/ 45 lb/bbl Concentration		**YP(lb/100ft2)**	**PV(lbsec/100ft2)**	**PV(cp)**	**AVERAGE**	**STDDEV**
		2,886	0,035	17,630	**58,726**	**27,878**

SR (1/s)	SS (lb/100ft2)	SS_c (lb/100ft^2)	γ(1/s)	τ_m (lb/100ft^2)	τ_c (lb/100ft^2)	%Error
1022,220	54,366	37,305	1022,220	54,366	37,305	31,382
511,110	39,442	22,390	511,110	39,442	22,390	43,234
340,660	35,178	16,606	340,660	35,178	16,606	52,794
170,330	28,782	9,967	170,330	28,782	9,967	65,372
10,220	15,990	1,255	10,220	15,990	1,255	92,152
5,110	14,924	0,753	5,110	14,924	0,753	94,953
250 to 75 Micron Size/ 60 lb/bbl Concentration		**YP(lb/100ft2)**	**PV(lbsec/100ft2)**	**PV(cp)**	**AVERAGE**	**STDDEV**
		2,424	0,036	18,294	**63,314**	**25,963**

APPENDIX I

Measured and Calculated Shear Stresses-Shear Rates Data for Yield Power Law Model for 250 to 75 Micron Size

Table 40 5 lb/bbl Concentration Data

SR (1/s)	SS (lb/100ft2)	SS_c (lb/100ft^2)	γ (1/s)	τ_m (lb/100ft^2)	τ_c (lb/100ft^2)	%Error
1022,22	40,51	40,50	1022,22	40,51	40,50	0,01
511,11	29,85	29,85	511,11	29,85	29,85	0,01
340,66	25,58	25,41	340,66	25,58	25,41	0,67
170,33	20,25	19,96	170,33	20,25	19,96	1,45
10,22	11,73	11,46	10,22	11,73	11,46	2,28
5,11	10,66	10,82	5,11	10,66	10,82	1,46
250 to 75 Micron Size/ 5 lb/bbl Concentration		**YP(lb/100ft2)**	**PV(lbsec/100ft2)**	**PV(cp)**	**AVERAGE**	**STDDEV**
		13,077	0,029	14,768	0,981	0,908

Table 41 15 lb/bbl Concentration Data

SR (1/s)	SS (lb/100ft2)	SS_c (lb/100ft^2)	γ (1/s)	τ_m (lb/100ft^2)	τ_c (lb/100ft^2)	%Error
1022,22	42,64	42,64	1022,22	42,64	42,64	0,01
511,11	30,91	30,92	511,11	30,91	30,92	0,01
340,66	26,65	26,09	340,66	26,65	26,09	2,08
170,33	21,32	20,24	170,33	21,32	20,24	5,05
10,22	11,73	11,39	10,22	11,73	11,39	2,83
5,11	10,66	10,76	5,11	10,66	10,76	0,90
250 to 75 Micron Size/ 15 lb/bbl Concentration		**YP(lb/100ft2)**	**PV(lbsec/100ft2)**	**PV(cp)**	**AVERAGE**	**STDDEV**
		13,003	0,031	15,892	1,814	1,948

Table 42 30 lb/bbl Concentration Data

SR (1/s)	SS (lb/100ft2)	SS_c (lb/100ft^2)	γ (1/s)	τ_m (lb/100ft^2)	τ_c (lb/100ft^2)	%Error
1022,220	44,772	44,768	1022,220	44,772	44,768	0,010
511,110	31,980	31,983	511,110	31,980	31,983	0,010
340,660	26,650	26,858	340,660	26,650	26,858	0,779
170,330	21,320	20,786	170,330	21,320	20,786	2,504
10,220	12,792	12,165	10,220	12,792	12,165	4,904
5,110	11,726	11,601	5,110	11,726	11,601	1,069
250 to 75 Micron Size/ 30 lb/bbl Concentration		**YP(lb/100ft2)**	**PV(lbsec/100ft2)**	**PV(cp)**	**AVERAGE**	**STDDEV**
		13,568	0,032	16,556	1,546	1,883

Table 43 45 lb/bbl Concentration Data

SR (1/s)	SS (lb/100ft2)	SS_c (lb/100ft^2)	γ (1/s)	τ_m (lb/100ft^2)	τ_c (lb/100ft^2)	%Error
1022,220	46,904	46,899	1022,220	46,904	46,899	0,010
511,110	33,046	33,049	511,110	33,046	33,049	0,010
340,660	28,782	27,550	340,660	28,782	27,550	4,280
170,330	23,452	21,095	170,330	23,452	21,095	10,050
10,220	12,792	12,138	10,220	12,792	12,138	5,114
5,110	11,726	11,573	5,110	11,726	11,573	1,304
250 to 75 Micron Size/ 45 lb/bbl Concentration		**YP(lb/100ft2)**	**PV(lbsec/100ft2)**	**PV(cp)**	**AVERAGE**	**STDDEV**
		13,526	0,035	17,630	3,461	3,880

Table 44 60 lb/bbl Concentration Data

SR (1/s)	SS (lb/100ft2)	SS_c (lb/100ft^2)	γ(1/s)	τ_m (lb/100ft^2)	τ_c (lb/100ft^2)	%Error
1022,220	49,036	49,031	1022,220	49,036	49,031	0,010
511,110	34,112	34,116	511,110	34,112	34,116	0,010
340,660	29,848	28,332	340,660	29,848	28,332	5,078
170,330	25,584	21,693	170,330	25,584	21,693	15,210
10,220	13,858	12,981	10,220	13,858	12,981	6,329
5,110	12,792	12,479	5,110	12,792	12,479	2,445
250 to 75 Micron Size/ 60 lb/bbl Concentration		**YP(lb/100ft2)**	**PV(lbsec/100ft2)**	**PV(cp)**	**AVERAGE**	**STDDEV**
		14,150	0,036	18,294	4,847	5,695

APPENDIX J

Rheological Properties as a Function of $CaCO_3$ Concentration and Particle Size

Table 45 Effect of $CaCO_3$ Concentration and Size on PV and YP

CONCENTRATION	Size	PV	YP
0	<45 µm	8	24
5	<45 µm	8	20
15	<45 µm	9	19
30	<45 µm	10	18
45	<45 µm	11	17
60	<45 µm	11	18
CONCENTRATION	Size	PV	YP
0	75-45 µm	8	24
5	75-45 µm	9	18
15	75-45 µm	10	18
30	75-45 µm	11	17
45	75-45 µm	12	16
60	75-45 µm	12	17
CONCENTRATION	Size	PV	YP
0	250-75µm	8	24
5	250-75µm	10	18
15	250-75µm	11	18
30	250-75µm	12	18
45	250-75µm	13	18
60	250-75µm	14	18

Table 46 . Effect of $CaCO_3$ Concentration and Size on n_a and K_a

CONCENTRATION	Size	n_a	K_a
0	<45 µm	0,2278	6,2040
5	<45 µm	0,1831	7,4153
15	<45 µm	0,1706	8,3258
30	<45 µm	0,1597	9,2459
45	<45 µm	0,1597	9,2459
60	<45 µm	0,1597	9,2459
CONCENTRATION	Size	n_a	K_a
0	75-45 µm	0,2278	6,2040
5	75-45 µm	0,1831	7,4153
15	75-45 µm	0,1978	7,2402
30	75-45 µm	0,1706	8,3258
45	75-45 µm	0,1706	8,3258
60	75-45 µm	0,1845	8,1387
CONCENTRATION	Size	n_a	K_a
0	250-75 µm	0,2278	6,2040
5	250-75 µm	0,1831	7,4153
15	250-75 µm	0,1706	8,3258
30	250-75 µm	0,1597	9,2459
45	250-75 µm	0,1597	9,2459
60	250-75 µm	0,1597	9,2459

Table 47 Effect of $CaCO_3$ Concentration and Size on n_p and K_p

CONCENTRATION	Size	n_p	K_p
0	<45 µm	0,3217	4,3027
5	<45 µm	0,3624	2,9224
15	<45 µm	0,4019	2,2842
30	<45 µm	0,4403	1,7972
45	<45 µm	0,4403	1,7972
60	<45 µm	0,4637	1,6090
CONCENTRATION	Size	n_p	K_p
0	75-45 µm	0,3217	4,3027
5	75-45 µm	0,4148	2,0320
15	75-45 µm	0,4403	1,7972
30	75-45 µm	0,4778	1,4228
45	75-45 µm	0,5143	1,1331
60	75-45 µm	0,4993	1,2886
CONCENTRATION	Size	n_p	K_p
0	250-75 µm	0,3217	4,3027
5	250-75 µm	0,3624	2,9224
15	250-75 µm	0,4019	2,2842
30	250-75 µm	0,4403	1,7972
45	250-75 µm	0,4403	1,7972
60	250-75 µm	0,4637	1,6090

Table 48 Effect of $CaCO_3$ Concentration and Size on m , k and τy

CONCENTRATION	Size	m	k	τ_y
0	<45 µm	0,3217	4,30268	8
5	<45 µm	0,3624	2,92237	9
15	<45 µm	0,4019	2,28422	10
30	<45 µm	0,4403	1,79719	11
45	<45 µm	0,4778	1,42284	11
60	<45 µm	0,4637	1,60903	11
CONCENTRATION	Size	m	k	τy
0	75-45 µm	0,3217	4,30268	8
5	75-45 µm	0,4148	2,03198	9
15	75-45 µm	0,4403	1,79719	9
30	75-45 µm	0,4778	1,42284	10
45	75-45 µm	0,5143	1,13315	10
60	75-45 µm	0,4993	1,28865	10
CONCENTRATION	Size	m	k	τy
0	250-75 µm	0,3217	4,30268	8
5	250-75 µm	0,4403	1,79719	9
15	250-75 µm	0,4637	1,60903	9
30	250-75 µm	0,4851	1,45594	10
45	250-75 µm	0,5049	1,32974	10
60	250-75 µm	0,5233	1,22447	11

APPENDIX K

Fluid Loss Data As a Function of Concentration and Particle Size of $CaCO_3$

Table 49 Fluid Loss Data of Concentrations- and Particle Size of $CaCO_3$

CONCENTRATION	Size	FL (cc/30 min.)
0	<45 µm	25,0
5	<45 µm	8,7
15	<45 µm	7,0
30	<45 µm	5,7
45	<45 µm	4,8
60	<45 µm	4,3
0	75-45 µm	25,0
5	75-45 µm	7,3
15	75-45 µm	7,0
30	75-45 µm	5,2
45	75-45 µm	5,0
60	75-45 µm	4,1
0	250-75µm	25,0
5	250-75µm	8,0
15	250-75µm	7,5
30	250-75µm	5,0
45	250-75µm	3,5
60	250-75µm	2,0